

Year 2 Report on NASA Grant NNX16AC79G

Participating Scientist in Residence for the Venus Climate Orbiter/Akatsuki

INVESTIGATION OF THE VENUS WEATHER

From Venus Climate Orbiter (VCO) / Akatsuki Data

Sanjay S. Limaye

Principal Investigator

R.A. Pertzborn

Co-Investigator

Space Science and Engineering Center

University of Wisconsin

1225 West Dayton Street

Madison, Wisconsin 53706, USA

30 September 2017

1. Introduction

The Akatsuki orbiter began systematic collection of Venus observations in April 2016 following a successful orbit insertion on 7 December 2015 followed by a checkout period. All four imaging cameras have returned useful data and, the radio science experiment has conducted many radio occultations using the JAXA and Indian Deep Space Network facilities. The fifth camera on the Akatsuki orbiter (Lightning and Airglow Camera) has also been successfully operated during specific observing periods on the dark side of Venus.

For the purpose of the investigation of weather on Venus, the four imaging cameras provide the primary data, with the radio occultation profiles providing supplementary information on the thermal structure of the atmosphere for weather events near the occultation locations. These data are being archived by JAXA and also are being delivered to the NASA Planetary Data System.

Following modifications to the software previously developed to access the Akatsuki data, preliminary tests were conducted to verify the camera focal lengths and boresight alignment in accordance with the available spacecraft pointing information and ephemeris.

The progress made in Year two of this investigation is described below.

2. Akatsuki Data

The Akatsuki orbiter hosts four imaging cameras – UVI, IR1, IR2 and LIR, each one tailored for specific wavelength range. Thus, the UVI with two filters (283 and 365 nm) observes Venus at the ultraviolet to learn about the distribution and movements of the contrasts caused by SO₂ and other unknown absorbers. The IR1 camera, images Venus at near infra-red on the day and night side of the planet at 0.97, 1.01 μm to probe the surface topography and the low level clouds. The IR2 camera images Venus at 2.02 μm on the day side to probe the Venus cloud deck at a wavelength where carbon dioxide (the main constituent of the Venus atmosphere) has an absorption band, thereby indicating cloud altitude differences and on the night side at 1.74, 2.26 and 2.32 μm to investigate the mid-cloud layer of Venus. Finally, the LIR camera obtains cloud top temperature differences globally. Figure 1 shows some examples of the images.

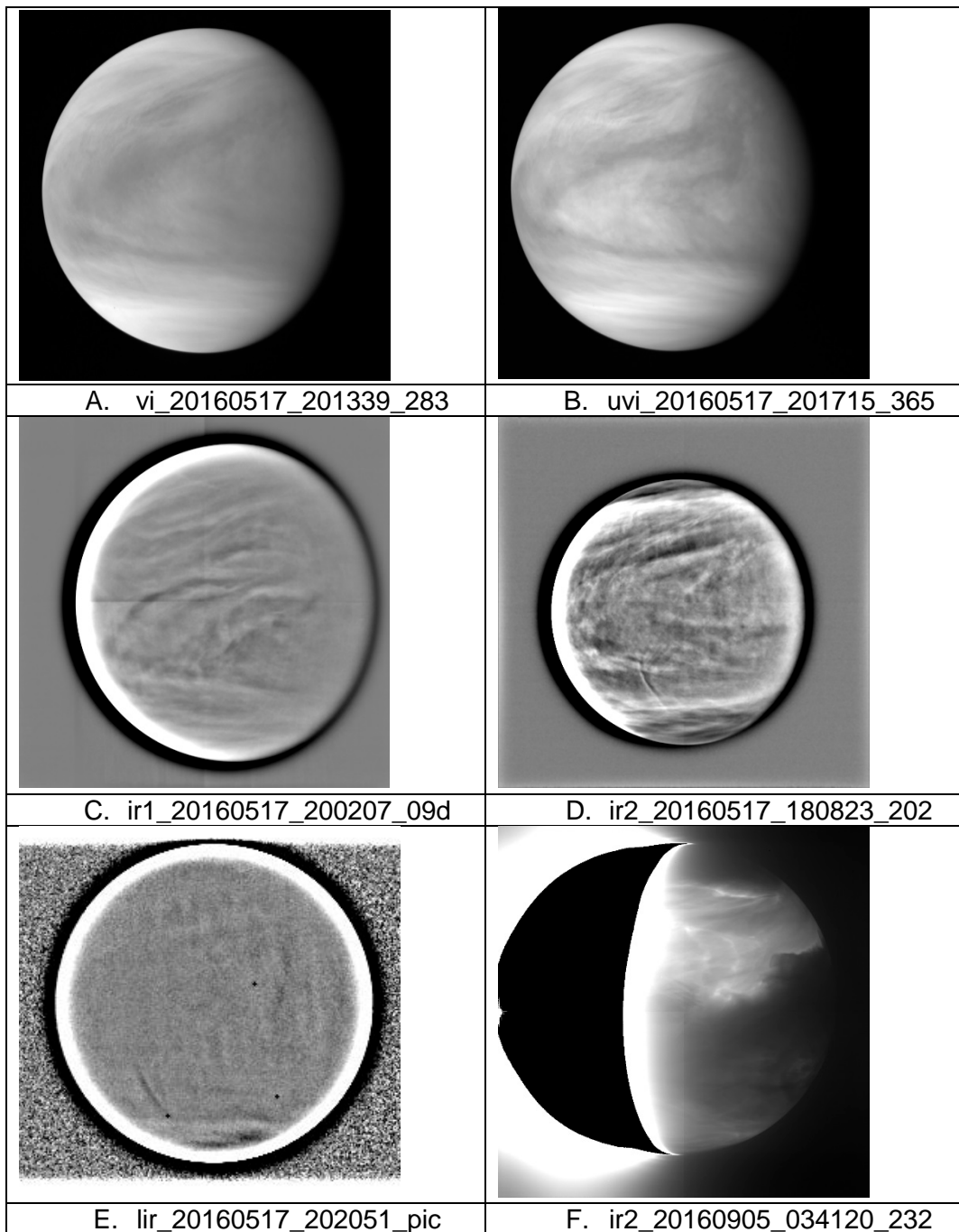


Figure 1. A selection of images taken from Akatsuki cameras. The date, time and filter are noted below each image. Day side images (A through E) were taken on 17 May 2016 while F is a night side image (IR2 camera) taken on 5 September 2016. Images A and B are from the UVI camera at 20:13:39 (283 nm) and 20:17:15 UT. Image C is taken from IR1 camera (0.9 μm) on the same day at 20:02:07 UT while image D is from the IR2 camera (2.02 μm) acquired at 18:08:23 UT. Images C and D are shown in high-pass filtered versions to bring out detail. Image E is from the LIR (8-12 μm) camera taken at 20:20:51 UT. The night side image (F) is taken through the 2.32 μm filter. At 2.26 and 1.74 μm , Venus appears similar.

Several new phenomenon were observed in the nightside images of Venus acquired by the IR 2 camera, such as the classical “mushroom” organization, analogous to formations routinely observed in terrestrial water vapor images from geosynchronous weather satellites, which have been shown to be mesoscale cyclonic and anticyclonic circulations (Houghton & Suomi, 1978; Martín et al., 1999), frontal boundaries, and stationary gravity waves that appear to be triggered by topography. The cloud features seen in all camera data enable determination of cloud motions and an equatorial jet has been detected from the night side measurements. A paper of which I am a co-author, has been published in Nature Geoscience (Horinouchi et al., 2017).

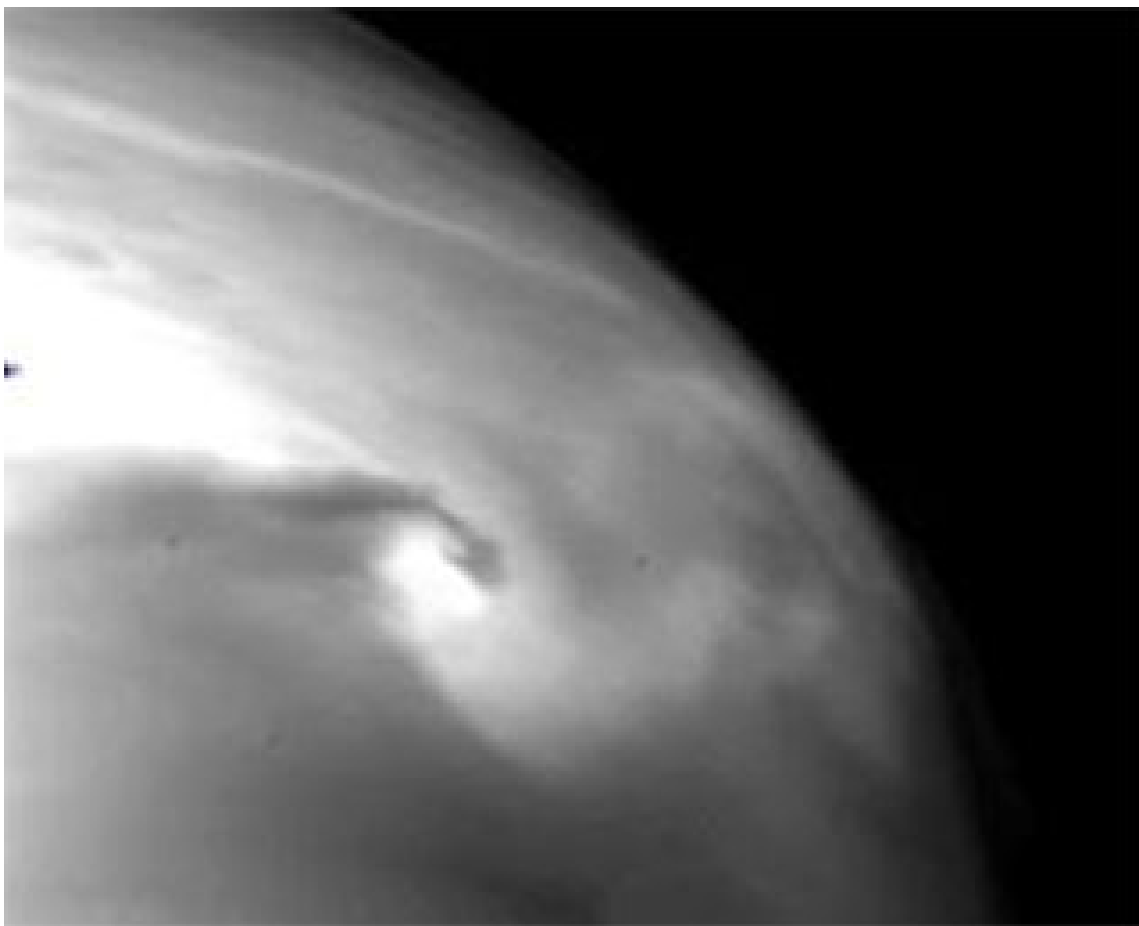


Figure 2. A “mushroom” feature was noticed in images from the IR2 camera taken on 7 May 2016 at 1.74, 2.26 and 2.32 μm . A search for similar formations revealed that a similar feature was observed in a similar location two orbits earlier, on 25 April 2016. This shape is seen commonly in water vapor channel images of Earth from weather satellites and the “mushroom” shape has been shown to be a result of a pair of anti-cyclonic and cyclonic circulations. The detection of such meso scale vortices on Venus is striking, raising questions about the creation of vorticity and the departures from the zonal nature of the atmospheric circulation on a slowly rotating planet.

2.1 Investigations

One of the primary tools for detecting weather on Venus is the morphology of the clouds, both on the day in reflected sunlight images and night side when the images are acquired in the near infrared radiation region (1 – 3 μm), that is emitted by the surface and the lower atmosphere below the cloud bottom (~ 47 km) from IR1 and IR2 cameras. These features appear as silhouettes due to differential absorption by the clouds and hazes above the emission levels. However, the cause of these contrasts both on the day and night sides of the planet are still unknown. This led to two separate investigations, one exploring the possibility of microorganisms contributing to the absorption and contrasts in the clouds and the other one focusing on cloud morphology at different wavelengths on the day and night side and new phenomenon detected in the images. These investigations led to submission of two papers and one being prepared for publication at present.

2.1.1 Absorption of incident solar energy by the clouds

It has been known for some time that sulfur dioxide gas is present in the Venus atmosphere at many levels as well as above the clouds. The two UVI camera filters were chosen such that one of the wavelengths is in one of the absorption bands for sulfur dioxide (283 nm) while the other one (365 nm) is at the peak of cloud cover contrast magnitude, thereby enabling investigation of the presence of other absorbers of sunlight which still remain unknown (Esposito et al., 1983). Since at least two absorbers were postulated from the spectral dependence of albedo of Venus and the global cloud contrasts (Pollack, 1980; Travis, 1975), and sulfur dioxide being identified as one of the absorbers, much of the discussion in the literature has focused on the other “unknown” absorber. However, a new assessment of the available information suggests that there may be more than one absorber (Jessup and Limaye, 2017) and the possibility of some microorganisms contributing to the absorption on the day side as well as contrasts cannot be ruled out. This possibility has been explored further with colleagues with an astrobiology background and a paper titled “**Venus' Spectral Signatures and the Potential for Life in the Clouds**” by Limaye et al. has been submitted to *Astrobiology Journal*.

2.1.2 Cloud Morphology at different wavelengths from day and night images from Akatsuki cameras

In images acquired routinely by the earth weather satellites, Earth clouds show very similar morphology at all wavelengths from visible to thermal infrared. One exception is the water vapor band images which depict the “dry” regions of the low and mid atmosphere more distinctly than images acquired at other wavelengths (Figure 1).

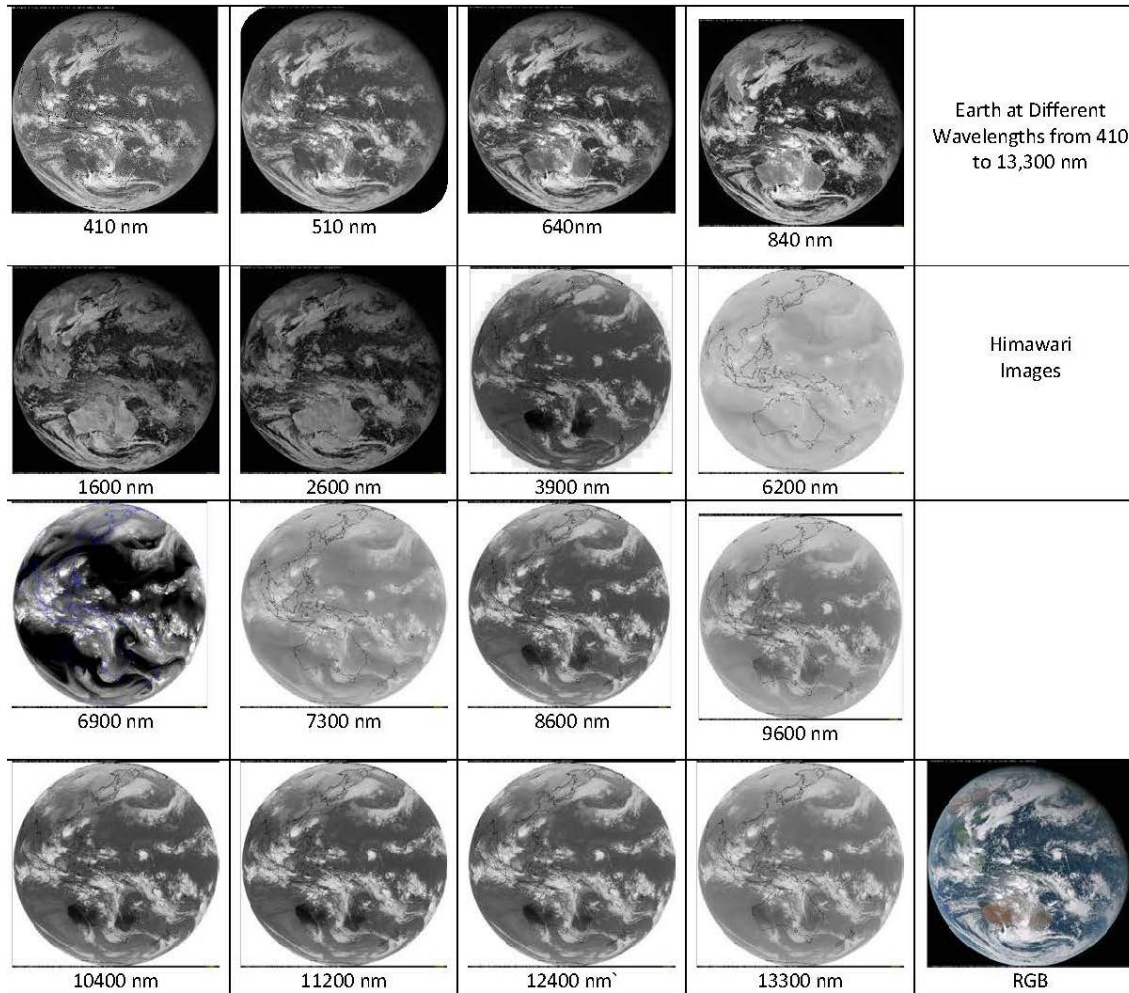


Figure 1. Earth images acquired by the Himawari weather satellite at different wavelengths showing the similarity of the cloud morphology.

In contrast, Venus appears remarkably different over the same wavelength range (Figure 2). This difference is due to the different composition of the Venus clouds at the atmosphere they evolve in and also the thickness atmosphere. The difference in the appearance of the Venus cloud features at different wavelengths highlight the complex

chemical, physical and perhaps biological processes that determine the cloud structure. The morphology of the Venus cloud features observed by Akatsuki cameras has been described in a paper submitted to the Akatsuki Special issue of Earth, Planets and Space.

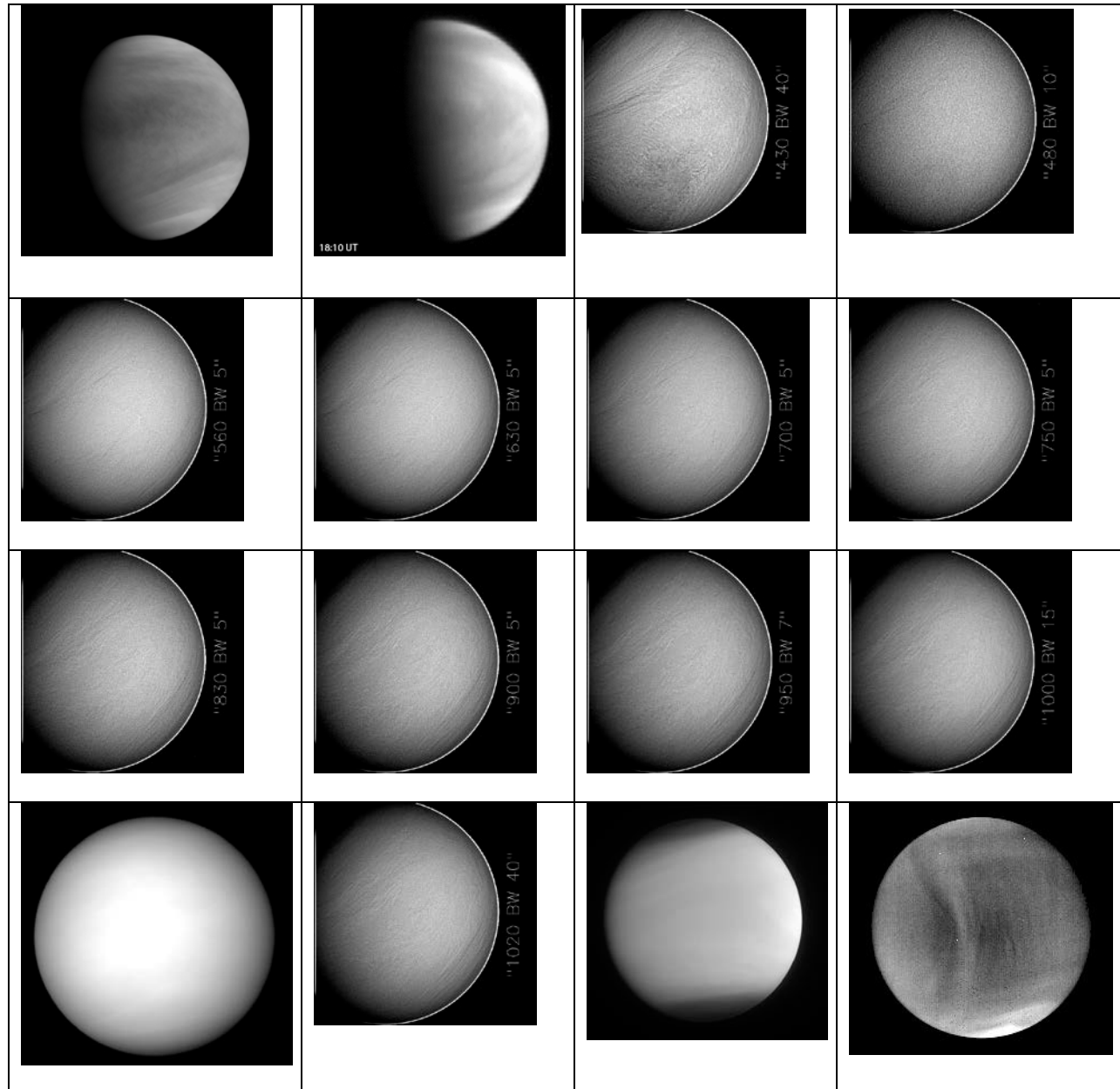


Figure 2. Venus at different wavelengths imaged by Akatsuki and MESSENGER cameras. Top row – (left to right) 283 nm, 365 nm (UVI Akatsuki), 430 nm, and 480 nm (MESSENGER –MDIS/WA). Second row – 560, 630, 700 and 750 nm (MDIS-WA). Third row- 830, 900, 950 and 1000 nm (MDIS-WA). Bottom row – 900 nm (IR1) 1020 nm (MDIS-WA), 2020 nm (IR2) and 10-14 μ m (LIR). All MESSENGER images have been high pass filtered to bring out the very low contrast features.

2.1.3 Meso-scale vortex circulations in the IR2 images of Venus

The “mushroom” feature shown in Figure 2 was also observed two orbits earlier on 25 April 2016 and later in August. As indicated earlier, the morphology of the Venus features is very similar to such features seen in water vapor imagery. Unfortunately the data coverage from Akatsuki IR2 camera did not capture time sequences on the days when the features were discovered, and the time difference between the three filters in which the features are generally seen (Figure 3) is too short for any detection of vorticity within the features. A search for similar features in the same wavelength region (1.74 – 2.32 μm) revealed a few instances, but once again, time sequences as high resolution were not available. One key finding is that the features are found upstream of elevated topographic regions. A manuscript is being prepared documenting these findings and will be submitted for publication.

3. Akatsuki Venus International Conference

The Akatsuki project will host an international conference on Venus with support from the Fujihara Foundation, Japan as the 74th Fujihara Seminar: "Akatsuki" Novel Development of Venus Science during September 11-14, 2018 in Niseko, Hokkaido, Japan. An organizing team has been formed of which I am a member.



Science Organizing committee: Takehiko Satoh (Akatsuki, ISAS/JAXA) Masato Nakamura (Akatsuki, ISAS/JAXA) Yoshiyuki Hayashi (Theory/Modeling, CPS/Kobe Univ.) Yoshihisa Matsuda (Modeling) Kevin McGouldrick (NASA PS) Sanjay Limaye (NASA PS) Colin Wilson (Modeling) Thomas Widemann (Ground-based) Agustin Sánchez-Lavega (Cloud tracking) Martha Gilmore (Surface) Ludmila Zasova (Russian mission, IKI). URL: <https://www.cps-jp.org/~akatsuki/pub/venus2018/>

4. Akatsuki Science Working Team Meetings

There were three Akatsuki Science Working Team meetings held during 2017, in January 2017, April 2017, and July 2017 at ISAS/JAXA in Sagamihara, Japan. I participated in all three meetings and provided progress reports. The 7th meeting will be held during November 9-11, 2017.

5. PUBLICATIONS and Presentations

The following papers were published during this reporting period:

1. Horinouchi, T., Murakami, S.-Ya, Satoh, T., Peralta, J., Ogohara, K., Kouyama, T., Imamura, T., Kashimura, H., **Limaye, S. S.**, McGouldrick, K., et al. (2017a). Equatorial jet in the lower to middle cloud layer of Venus revealed by Akatsuki. *Nature Geoscience*, advance online publication. doi:10.1038/ngeo3016
2. T. Imamura, H. Ando, S. Tellmann, M. Pätzold, B. Häusler, T. M. Sato, Katsuyuki Noguchi, Yoshifumi Futaana, Janusz Oschlisniok, S. Limaye, R.K. Choudhary, Y. Murata, H. Takeuchi, C. Hirose, T. Ichikawa, T. Toda, A. Tomiki, T. Abe, Z. Yamamoto, H. Noda, T. Iwata, S. Murakami, T. Satoh, T. Fukuhara, K. Ogohara, K. Sugiyama, H. Kashimura, S. Ohtsuki, S. Takagi, Y. Yamamoto, N. Hirata, G. L. Hashimoto, M. Yamada, M. Suzuki, I. Nobuaki, T. Hayashiyama, Y. J. Lee, M. Nakamura, 2017. Initial performance of the radio occultation experiment 1 in the Venus orbiter mission Akatsuki, accepted for publication, *Earth, Planets and Space*. To appear in the Akatsuki special issue, late 2017.
3. Limaye, S. S., Lebonnois, S., Mahieux, A., Pätzold, M., Bougher, S., Bruinsma, S., et al. (2017). The thermal structure of the Venus atmosphere: Intercomparison of Venus Express and ground based observations of vertical temperature and density profiles☆. *Icarus*, 294, 124-155. Vandaele, A. C., Korabiev, O.; Belyaev, D.; Chamberlain, S.; Evdokimova, D.; Encrenaz, Th.; Esposito, L., Jessup, K. L., Lefèvre, F., **Limaye, S.**, et al. (2017a). Sulfur dioxide in the Venus atmosphere: I. Vertical distribution and variability. *Icarus*, 295, 16-33.
4. Vandaele, A. C., Korabiev, O., Belyaev, D., Chamberlain, S., Evdokimova, D., Encrenaz, Th., Esposito, L., Jessup, K. L., Lefèvre, F., **Limaye, S.**, et al. (2017b). Sulfur dioxide in the Venus Atmosphere: II. Spatial and temporal variability. *Icarus*, 295, 1-15.

PAPERS UNDER REVIEW:

The following papers were submitted during the current reporting period for publication and are currently undergoing Peer Review:

1. S.S. Limaye, S. Watanabe, A. Yamazaki, M. Yamada, T. Satoh, T. M. Sato, M. Nakamura, M. Taguchi, T. Fukuhara, T. Imamura, T. Kouyama, Y. J. Lee, T. Horinouchi, J. Peralta, N. Iwagami, G.L. Hashimoto, S Takagi, S. Ohtsuki, S. Murakami, Y. Yamamoto, K.

Ogohara, H. Ando, K. Sugiyama, N. Ishii, T. Abe, C. Hirose, M. Suzuki, N. Hirata, E. F. Young, **Venus Looks Different at Different Wavelengths: Morphology of the Global Day and Night Cloud Cover at Different Wavelengths from Akatsuki Cameras**, *Submitted to Earth, Planets and Space*.

2. Limaye, S.S., R. Mogul, A.H. Ansari, G.P. Słowik, D.J. Smith, and P. Vaishampayan, **Venus' Spectral Signatures and the Potential for Life in the Clouds**. *Submitted to Astrobiology*.
3. Limaye, S.S., D. Grassi, A. Mahieux, A. Miglioriono, S. Tellmann, and D. Titov, Venus atmospheric thermal structure and radiative balance. *Submitted to Space Science Reviews. To be included as Chapter 4 of Venus III (C. Russell, Chief Editor)*.

CONFERENCE PRESENTATIONS

1. Bullock, M., S.S. Limaye, D.H. Grinspoon, and M.J. Way, The Effect of Bond Albedo on Venus' Atmospheric and Surface Temperatures. American Geophysical Union 2017 Fall meeting, New Orleans, 8-12 December 2017
2. Gero, J., S. Limaye, P. Fry, Y. J. Lee, G. Petty, J. Taylor, S. Warwick, An airborne spectrophotometer for investigating solar absorption on Venus, 14th VEXAG Meeting, Applied Physics Laboratory/Johns Hopkins University, Laurel, MD, 14-16 November 2017.
3. Jessup, K-L., R. Carlson, S. Perez-Hoyos, N. Ignatiev, Y-J. Lee, S. Limaye, F. P., Mills, L. Zasova, Motivations and Priorities for a Detailed In-situ Investigation of the Spatial and Temporal Variability of Venus' UV absorber, 8th Solar System Symposium, Space Research Institute (IKI), Moscow, Russia, 9-13 October 2017.
4. Jessup, K-L., R. Carlson, S. Perez-Hoyos, Y-J. Lee, F. P., Mills, S. Limaye, N. Ignatiev, L. Zasova, Motivations for a Detailed In-situ Investigation of the Spatial and Temporal Variability of Venus UV absorber, 14th VEXAG Meeting, Applied Physics Laboratory/Johns Hopkins University, Laurel, MD, 14-16 November 2017.
5. Limaye, S. S.; Jessup, K. L., Questions About Venus and Measurements Needed to Address Them from Future Missions to Venus, Lunar and Planetary Science Conference, the Woodlands, Texas, March 2017.
6. Limaye, S.; Słowik, G.; Ansari, A.; Smith, D.; Mogul, R.; Vaishampayan, P., Short wavelength albedo, contrasts and micro-organisms on Venus, European Geophysical Union, Vienna, Austria, April 2017.
7. Limaye, S.S., T. Satoh, T. Horinouchi, J. Peralta and T. Imamura, Mesoscale vortices on Venus, Japan Geophysical Union Meeting, Chiba, Japan, May 2017.
8. Limaye, S.S., and the Akatsuki team, Venus looks different at different wavelengths, Venera-D Modeling Workshop, Space Research Institute (IKI), Moscow, Russia, 5-7 October 2017
9. Limaye, S.S., T. Satoh, T. Horinouchi, J. Peralta and T. Imamura, Meso-scale circulations on Venus, 8th Solar System Symposium, Space Research Institute (IKI), Moscow, Russia, 9-13 October 2017.
10. Limaye, S.S., R. Mogul, A. Yamagishi, A. Ansari, D.J. Smith, G. Slowik, P. Vaishampayan, Y.J. Lee, 14th VEXAG Meeting, Applied Physics Laboratory/Johns Hopkins University, Laurel, MD, 14-16 November 2017.

6. Outreach and Communications

The Akatsuki Mission provides an unprecedented opportunity to utilize international missions for outreach and communications in the absence of any NASA missions to Venus in recent history by continuing the efforts and programs previously developed in conjunction with the European Space Agency's (ESA) Venus Express Mission's (VEX) which ended in 2014. The unusual opportunity to have an almost continuous collection of new data allows for sustained public communication and citizen scientist efforts focused on the earth's nearest and most comparable planetary neighbor within this solar system. The continued investigation of the Venusian atmosphere and its weather in particular has become of critical interest to the scientific community as well as the general public, as it provides a relatively accessible, natural planetary laboratory with the potential to greatly enhance our understanding of the earth's own atmosphere and more recently, an opportunity to explore the potential for past or present life within the Venusian clouds. Along with the successful leveraging of ongoing partnerships, programs and activities, the Akatsuki communication initiative continues our team's efforts to effectively communicate the critical scientific significance of Venus and its dynamic, potentially life supporting atmosphere.

Accomplishments

In the past year, the Akatsuki communications and citizen science initiative has maintained a continuous effort to represent the research performed under this grant in a comparative planetology context to some extent. Highlights to date include, i) development and re-launch of a dedicated web presence (venus.wisc.edu) that will be updated with Akatsuki Mission news and events, ii) planning for the adaptation of an applet to enable tracking of winds on Venus using new Akatsuki data, iii) support of hands on activities to introduce Gifted and Talented Middle/ School Students (UW-Madison PACE Program) to learn about the processes of research using the Venus winds applet, and iv) Visiting Scientist presentations at schools and other presentations at special events and activities locally and internationally. These are described below.

6.1 Workshop for Students

[Preparatory Academic Campus Experience \(PACE\) - UW Madison](#)

This program gives current 5th through 8th grade students an opportunity to explore their current interests and passions with like-minded peers in a college setting. Students will spend one week taking one accelerated course designed specifically for middle school advanced learners on the UW-Madison campus. This program is designed to engage, intellectually challenge, and inspire young minds.



6.2 Visiting Scientist talks at schools

Dr. Limaye visited three schools in Poland through an on-going informal collaboration with the Regional Teacher Training Center in Skierniewice, Poland (facilitated by Mrs. A. E. Dąbrowska, Teacher consultant of Science Subjects and European Education). The Science Coordinator at this center has arranged many school visits and also conducts on-line programs for science teachers in which Dr. Limaye continues to participate. This collaboration has also been responsible for some new directions in research in the area of the unknown absorbers of incident solar radiation in the Venus clouds.

Talks given in May 2017 at the following schools:

1. Zespół Szkół im. Księdza Stanisława Konarskiego" in Skierniewice
Colloquia Classica, May 17th, 2017 | Skierniewice, Poland

<http://www.klasykskierniewice.pl/index.php/wydarzenia/334-spotkanie-colloquia-classica>



Dr. Sanjay S. Limaye visited students at school "Zespół Szkół im. Księdza Stanisława Konarskiego" in Skierniewice, Poland to discuss Venus, the solar system, and space exploration.

2. Zespół Szkół nr 1, w Kole, 62-600 Koło ul. Poniatowskiego 22, Poland
Tel: (63) 26-16-771 <http://www.zs1kolo.szkolnastrona.pl/index.php?c=article&id=997>
Host: Michał Kazmierczak, School Complex No. 1, Kolo

This was a repeat visit, the first one being during 2016.

Profesor astronomii z USA odwiedził naszą szkołę

Wyjątkowa wizyta: naszą szkołę odwiedził profesor Sanjay Limaye z Uniwersytetu Wisconsin w Stanach Zjednoczonych. Wizyta znanego astronoma związana jest z piątą rocznicą działalności szkolnego Klubu Młodych Odkrywców „Kolska Wyspa” oraz licznymi projektami, które realizuje nasza placówka.

Uczniowie szkoły i członkowie Klubu Młodych Odkrywców od lat biorą udział w ciekawych i niezwykłych projektach rozwijających ich zainteresowania, a związanych m. in. z badaniem kosmosu. Zainteresowania klubu obejmują również takie dziedziny jak: fizyka, astronomia, geografia, chemia, biologia, matematyka, mechatronika i informatyka. Warto dodać, że to właśnie w tej szkole realizowano w ramach zajęć lekcyjnych nauczanie mechatroniki z elementami robotyki, które dziś kontynuowane jest z uczniami należącymi do Klubu Młodych Odkrywców. W realizacji swoich projektów uczniowie na co dzień współpracują z Centrum Nauki Kopernik w Warszawie, ABM Space z Torunia, a nawet NASA – Amerykańską Agencją Kosmiczną.

Podczas wizyty w szkole profesor poprowadził wykład w jęz. angielskim na temat budowy planet skalistych w Układzie Słonecznym oraz przeprowadził warsztaty dla uczniów biorących udział w dwóch projektach:

1. EarthKAM – widok Ziemi z Międzynarodowej Stacji Kosmicznej przy współpracy z Sally Ride Science i NASA,
2. REMY-ESERO z mechatroniki dotyczący kierowania łazikiem marsjańskim na kraterze i wykonywania badań pomiarowych na jego powierzchni zorganizowanym przez biuro ESERO w CNK Kopernik w Warszawie oraz ABM Space z Torunia.

Podczas zajęć warsztatowych uczniowie zaprezentowali swoje osiągnięcia w budowie i programowaniu robotów, wymieniali się spostrzeżeniami oraz wysłuchali wskazówek naukowca dotyczących dalszej pracy. Była to już druga wizyta tego światowej sławy badacza kosmosu w szkole przy ul. Poniatowskiego w Kole, który spotka się z młodymi naukowcami na zaproszenie opiekuna klubu, nauczyciela fizyki i informatyki p. Michała Kazimierczaka.

Galeria



- a. Szkoła Mojego Dziecka, miesięcznik dla rodziców, Gimnazjum nr 3 im. Ignacego Krasickiego, w Skierniewicach

<http://www.gim3-skierniewice.pl/aktualnosci/12-aktualnosci/864-wyklady-dr-snajaya-limaye>



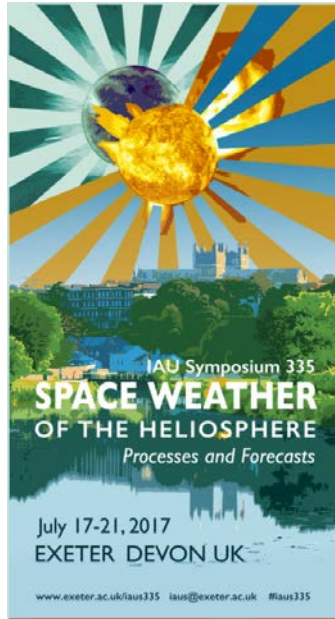
"May 16, 2017. Our middle school hosted Dr. Sanjay Limaye of the University of Wisconsin-Madison in the United States. His research interests include solar systems with Venus, Mars, Jupiter, Saturn, Uranus, and global warming and climate change. Dr. Limaye gave lectures in English to our junior high school students. The first was about India, the country where Dr. Limaye came from. He told his students about contemporary India, society, culture and nature. The second lecture was devoted to the planet Venus and its comparison to Earth. Maybe, at some time, one of the students will be a participant in the Venus mission?"

We hope this was not the last visit of Dr. Limaye at our school.

- Agnieszka Jelonek-Krupińska", Host Teacher

6.3 Public Lectures

Dr. Limaye was invited to give a public lecture as part of the outreach activities for the IAU Symposium on Space Weather of the Heliosphere held in Exeter, UK during 17-21 July. An audience of approximately 300 persons of all ages filled the auditorium for this lecture ("Venus – An exoplanet next door" which followed immediately after a lecture by Dr. Lucie Green on the workings of the Sun.



"Venus – an Exoplanet next door"

Tuesday, July 18, Exeter, Streatham campus, Northcott Theatre, following the lecture above – please [book here](#) or share it on [Facebook](#).

Public lecture by Dr Sanjay S. Limaye, University of Wisconsin, Madison, USA

In 1761 Lomonosov observed the transit of Venus as it crossed the Sun's disc, making the first observed discovery about another planet – that our nearest solar system neighbor had an atmosphere. This technique has led to the discovery of thousands of planets around other stars. Nearly two hundred years later in 1962, the Mariner 2 spacecraft successfully flew past Venus and made the major discovery that the planet's surface was extremely hot. Since then Venus has been explored by atmospheric entry probes, landers, balloons and orbiters in addition to



being observed by spacecraft on their way to other destinations. We have discovered that the cloud covered planet which takes longer to rotate about itself than to orbit the Sun is still shrouded in mystery. If we cannot understand our closest planetary neighbor, how can we really appreciate with confidence the mysteries of other exoplanets beyond our own solar system?

Sanjay Limaye is a planetary scientist at the Space Science and Engineering Center at the University of Wisconsin-Madison.

6.4 Planned Future Activities (December 2017 through December 2018)

Planned activities include: 1) Ongoing website updates, 2) addition of new Akatsuki data to enhance the Venus winds applet, 3) Participation in the UW-Madison PACE program for Middle School students, and 4) submission of a UW-Madison Baldwin proposal to create a research course credit opportunity for the Madison Area Technical College's STEM Center (targeting minority and low income students) using the Venus Wind Tracking applet.

References

- Esposito, L. W., Knollenberg, R. G., Marov, M. Y., Toon, O. B., & Turco, R. P. (1983). The clouds and hazes of Venus. In D. M. Hunten (Ed.), *Venus*. Arizona: University of Arizona Press.
- Horinouchi, T., Murakami, S., Satoh, T., Peralta, J., Ogohara, K., Kouyama, T., et al. (2017). Equatorial jet in the lower to middle cloud layer of Venus revealed by Akatsuki. *ArXiv e-prints*, 1709. Retrieved from <http://adsabs.harvard.edu/abs/2017arXiv170902216H>
- Houghton, D. D., & Suomi, V. E. (1978). Information content of satellite images. *Bulletin of the American Meteorological Society*, 59(12), 1614-1617.
- Martín, F., Elizaga, F., & Riosalido, R. (1999). The mushroom configuration in water vapour imagery and operational applications. *Meteorological Applications*, 6(2), 143-154. doi:10.1017/S1350482799001085
- Pollack, J. B. (1980). Distribution and source of the UV absorption in Venus' atmosphere. *J. Geophys. Res.*, 85, 8141-8150.
- Travis, L. D. (1975). On the origin of ultraviolet contrasts on Venus. *Journal of Atmospheric Sciences*, 32, 1190-1200.

Appendix 1

Preprints of papers

1. Copy of “Venus Looks Different at Different Wavelengths: Morphology of the Global Day and Night Cloud Cover at Different Wavelengths from Akatsuki Cameras” submitted to Earth, Planets and Space.
2. Copy of “**Venus' Spectral Signatures and the Potential for Life in the Clouds**” submitted to Astrobiology.

Earth, Planets and Space

Venus Looks Different at Different Wavelengths: Morphology of the Global Day and Night Cloud Cover at Different Wavelengths from Akatsuki Cameras

--Manuscript Draft--

Manuscript Number:	EPSP-D-17-00201R1	
Full Title:	Venus Looks Different at Different Wavelengths: Morphology of the Global Day and Night Cloud Cover at Different Wavelengths from Akatsuki Cameras	
Article Type:	Full paper	
Section/Category:	Planetary science	
Funding Information:	National Aeronautics and Space Administration (NNX16AC79G)	Dr. Sanjay Limaye
	JSPS (JP16H02231)	Dr Masato Nakamura
	JSPS KAKENHI (16H05738)	Dr Takehiko Satoh
	JSPA KAKENHI (JP16H02231)	Dr Takeshi Imamura
	JSPS KAKENHI (JP16H02231)	Dr Takeshi Horinouchi
Abstract:	<p>Since insertion into orbit around Venus on December 7, 2015, Akatsuki orbiter has returned unprecedented global images of Venus from its four imaging cameras at ultraviolet (283 and 365 nm), near infrared (1 to 2.3 μm) and at thermal infrared (8-12 μm) showing the dynamic morphology of its day and night time cloud cover nearly continuously. Past orbiting or fly-by missions to Venus did not provide such long-term global, wide spectral range or frequency of observations. The day side cloud cover imaged at the ultraviolet wavelengths shows morphologies similar to what was observed from Mariner 10, Pioneer Venus, Galileo, Venus Express and MESSENGER, but the day time images at 0.9 and 2.02 μm also reveal some interesting features which bear similarity to the ultraviolet images. The night time images at 1.74, 2.26 and 2.32 μm and at 8-12μm reveal features not seen before and show new details on the night side structure and ribbon like narrow width, long scale waves, frontal boundaries and even small vortices. Some features seen previously, such as Circum-Equatorial Belts (CEBs) and occasional brightenings at ultraviolet (seen in Venus Express observations) of the cloud cover at ultraviolet have not been seen so far. Evidence for the hemispheric vortex organization of the global circulation can be seen at all wavelengths on day and night side.</p> <p>The cloud morphologies provide some clues to the processes occurring in the atmosphere and are thus a key diagnostic tool when quantitative dynamical analysis is not feasible due to lack of sufficient information.</p>	
Corresponding Author:	Sanjay Limaye, Ph.D. University of Wisconsin Superior Madison, Wisconsin UNITED STATES	
Corresponding Author Secondary Information:		
Corresponding Author's Institution:	University of Wisconsin Superior	
Corresponding Author's Secondary Institution:		
First Author:	Sanjay Limaye, Ph.D.	
First Author Secondary Information:		
Order of Authors:	Sanjay Limaye, Ph.D.	
	Shigeto Watanabe	

	Atsushi Yamazaki
	Manabu Yamada
	Takehiko Satoh
	Takao M Sato
	Masato Nakamura
	Makoto Taguchi
	Tetsuya Fukuhara
	Takeshi Imamura
	Toru Kouyama
	Yeon Joo Lee
	Takeshi Horinouchi
	Javier Peralta
	Naomoto Iwagami
	George L. Hashimoto
	Seiko Takagi
	Shoko Ohtsuki
	Shin-ya Murakami
	Yukio Yamamoto
	Kazunori Ogohara
	Hiroki Ando
	Ko-ichiro Sugiyama
	Nobuaki Ishii
	Takumi Abe
	Chikako Hirose
	Makoto Suzuki
	Naru Hirata
	Eliot F. Young
	Adriana C Ocampo, Ph.D.
Order of Authors Secondary Information:	
Response to Reviewers:	<p>Response to Reviewers on the Incomplete Submission:</p> <ol style="list-style-type: none"> 1.The ambiguity in the e-mail address of the corresponding author has been corrected. 2.The author list entered on-line has been reconciled with the main text and includes addition of one author. There was a spelling error in one name, one name was omitted on-line. One name cited by the reviewer as incorrect (Kashiwanoha Kashiwa) was not found in the main text as a co-author. 3.The Ethics Declaration (Not applicable) has been added in the main text. 4.Each co-author's role/contribution has been noted.

Response to Reviewers on the Incomplete Submission:

1. The ambiguity in the e-mail address of the corresponding author has been corrected.
2. The author list entered on-line has been reconciled with the main text and includes addition of one author. There was a spelling error in one name, one name was omitted on-line.

One name cited by the reviewer as incorrect (Kashiwanoha Kashiwa) was not found in the main text as a co-author.

3. The Ethics Declaration (Not applicable) has been added in the main text.
4. Each co-author's role/contribution has been noted.

[Click here to view linked References](#)

- 1
 - 2
 - 3
 - 4
 - 5
 - 6
 - 7
 - 8
 - 9
 - 10
 - 11
 - 12
 - 13
 - 14
 - 15
 - 16
 - 17
 - 18
 - 19
 - 20
 - 21
 - 22
 - 23
 - 24
 - 25
 - 26
 - 27
 - 28
 - 29
 - 30
 - 31
 - 32
 - 33
 - 34
 - 35
 - 36
 - 37
 - 38
 - 39
 - 40
 - 41
 - 42
 - 43
 - 44
 - 45
 - 46
 - 47
 - 48
 - 49
 - 50
 - 51
 - 52
 - 53
 - 54
 - 55
 - 56
 - 57
 - 58
 - 59
 - 60
 - 61
 - 62
 - 63
 - 64
 - 65
- 1 **Venus Looks Different at Different Wavelengths:**
- 2
- 3
- 4
- 5
- 6 **2 Morphology of the Global Day and Night Cloud Cover at Different Wavelengths**
- 7
- 8
- 9 **3 from Akatsuki Cameras**
- 10
- 11
- 12
- 13 4 Sanjay S. Limaye*, Space Science and Engineering Center, University of Wisconsin,
- 14
- 15
- 16 5 Madison, Wisconsin 53706, USA
- 17
- 18
- 19
- 20 6 Sanjay.Limaye@ssec.wisc.edu
- 21
- 22
- 23
- 24 7 Shigeto Watanabe, Space Information Center, Hokkaido Information University, Ebetsu,
- 25
- 26
- 27 8 Hokkaido 069-8585, Japan
- 28
- 29
- 30 9 shw@ep.sci.hokudai.ac.jp
- 31
- 32
- 33
- 34 10 Atsushi Yamazaki, Institute of Space and Astronautical Science, Japan Aerospace
- 35
- 36
- 37 11 Exploration Agency, 3-1-1, Yoshinodai, Chuo-ku, Sagamihara 252-5210, Japan,
- 38
- 39
- 40
- 41 12 yamazaki@stp.isas.jaxa.jp
- 42
- 43
- 44
- 45 13 Manabu Yamada, Planetary Exploration Research Center, Chiba Institute of Technology,
- 46
- 47
- 48 14 2-17-1, Tsudanuma, Narashino, Chiba, 275-0016, Japan
- 49
- 50
- 51 15 manabu@perc.it-chiba.ac.jp
- 52
- 53
- 54
- 55 16 Takehiko Satoh, Institute of Space and Astronautical Science, Japan Aerospace
- 56
- 57
- 58
- 59
- 60
- 61
- 62
- 63
- 64
- 65

- 1
2 17 Exploration Agency, 3-1-1, Yoshinodai, Chuo-ku, Sagamihara 252-5210, Japan
3
4
5 18 satoh@stp.isas.jaxa.jp
6
7
8
9 19 Takao M. Sato, Institute of Space and Astronautical Science, Japan Aerospace
10
11
12 20 Exploration Agency
13
14
15 21 takao@stp.isas.jaxa.jp
16
17
18
19 22 Masato Nakamura, Institute of Space and Astronautical Science, Japan Aerospace
20
21
22
23 23 Exploration Agency, 3-1-1, Yoshinodai, Chuo-ku, Sagamihara 252-5210, Japan
24
25
26 24 mnakamur@isas.jaxa.jp
27
28
29
30 25 Makoto Taguchi, College of Science, Rikkyo University, 3-34-1 Nishi-Ikebukuro,
31
32
33
34 26 Toshima-ku, Tokyo 171-8501, Japan
35
36
37 27 taguchi@rikkyo.ac.jp
38
39
40
41 28 Tetsuya Fukuhara, College of Science, Rikkyo University, 3-34-1 Nishi-Ikebukuro,
42
43
44 29 Toshima-ku, Tokyo 171-8501, Japan
45
46
47 30 tetsuyaf@rikkyo.ac.jp
48
49
50
51 31 Takeshi Imamura, Department of Complexity Science and Engineering, Graduate
52
53
54
55 32 School of Frontier Sciences, The University of Tokyo, Kiban-tou 4H7, 5-1-5
56
57
58
59
60
61
62
63
64
65

- 1
2 33 Kashiwanoha, Kashiwa, Chiba 277-8561,
3
4
5
6 34 t_imamura@edu.k.u-tokyo.ac.jp
7
8
9 35 Toru Kouyama, Artificial Intelligence Research Center, National Institute of Advanced
10
11
12 36 Industrial Science and Technology
13
14
15
16 37 t.kouyama@aist.go.jp
17
18
19 38 Yeon Joo Lee, Institute of Space and Astronautical Science, Japan Aerospace
20
21
22
23 39 Exploration Agency, 3-1-1, Yoshinodai, Chuo-ku, Sagamihara 252-5210, Japan
24
25
26
27 40 leeyj@ac.jaxa.jp
28
29
30 41 Takeshi Horinouchi, Faculty of Environmental Earth Science, Hokkaido University,
31
32
33
34 42 N10W5, Sapporo, Hokkaido 060-0810, Japan
35
36
37 43 horinout@ees.hokudai.ac.jp
38
39
40
41 44 Javier Peralta, Institute of Space and Astronautical Science, Japan Aerospace
42
43
44 45 Exploration Agency, 3-1-1, Yoshinodai, Chuo-ku, Sagamihara 252-5210, Japan,
45
46
47
48 46 javier.peralta@ac.jaxa.jp
49
50
51 47 Naomoto Iwagami, School of Commerce, Senshu University, 2-1-1 Higashimita, Tama-
52
53
54
55 48 ku, Kawasaki, Kanagawa 214-8580, Japan
56
57
58
59
60
61
62
63
64
65

1
2 49 iwagamina@hotmail.co.jp
3
4

5 50 George L. Hashimoto, Department of Earth Sciences, Okayama University, 3-1-1
6
7

8
9 51 Tsushimanaka, Kita-ku, Okayama 700-8530, Japan
10

11
12 52 george@gfd-dennou.org
13
14

15
16 53 Seiko Takagi, Tokai University, Research and Information Center, 4-1-1 Kitakaname,
17
18

19 54 Hiratsuka-shi, Kanagawa 259-1292, Japan
20
21

22
23 55 seiko@tokai-u.jp
24
25

26
27 56 Shoko Ohtsuki, School of Commerce, Senshu University, 2-1-1 Higashimita, Tama-ku,
28
29

30 57 Kawasaki, Kanagawa, 78 214-8580, Japan
31
32

33
34 58 oh@isc.senshu-u.ac.jp
35
36

37 59 Shin-ya Murakami, Institute of Space and Astronautical Science, Japan Aerospace
38
39

40
41 60 Exploration Agency, 3-1-1, Yoshinodai, Chuo-ku, Sagamihara 252-5210, Japan,
42
43

44 61 murashin@gfd-dennou.org
45
46

47
48 62 Yukio Yamamoto, Institute of Space and Astronautical Science, Japan Aerospace
49
50

51 63 Exploration Agency, 3-1-1 Yoshinodai, Chuo-ku, Sagamihara, Kanagawa 252-5210,
52
53

54
55 64 yamamoto.yukio@jaxa.jp
56
57
58
59
60
61
62
63
64
65

- 1
2 65 Kazunori Ogohara, School of Engineering, University of Shiga Prefecture
3
4
5
6 66 ogohara.k@e.usp.ac.jp
7
8
9 67 Hiroki Ando, Faculty of Science, Kyoto Sangyo University, Motoyama, Kamigamo,
10
11
12 68 Kita-ku, Kyoto-City 603-8555 Japan,
13
14
15
16 69 hando@cc.kyoto-su.ac.jp
17
18
19 70 Ko-ichiro Sugiyama, Department of Information Engineering, National Institute of
20
21
22
23 71 Technology, Matsue College, 14-4 Nishi-Ikuma, Matsue, Shimane 690-8518 Japan,
24
25
26
27 72 sugiyama@matsue-ct.jp
28
29
30 73 Nobuaki Ishii, Institute of Space and Astronautical Science, Japan Aerospace
31
32
33
34 74 Exploration Agency, 3-1-1 Yoshinodai, Chuo-ku, 49 Sagamihara, Kanagawa 252-5210,
35
36
37 75 ishii@isas.jaxa.jp
38
39
40
41 76 Takumi Abe, Institute of Space and Astronautical Science, Japan Aerospace
42
43
44 77 Exploration Agency, 3-1-1 Yoshinodai, Chuo-ku, Sagamihara, Kanagawa 252-5210,
45
46
47
48 78 abe.takumi@jaxa.jp
49
50
51 79 Chikako Hirose, Institute of Space and Astronautical Science, Japan Aerospace
52
53
54
55 80 Exploration Agency, 3-1-1, Yoshinodai, Chuo-ku, Sagamihara 252-5210, Japan,
56
57
58
59
60
61
62
63
64
65

- 1
2 81 hirose.chikako@jaxa.jp
3
4
5
6 82 Makoto Suzuki, Institute of Space and Astronautical Science, Japan Aerospace
7
8
9 83 Exploration Agency, 3-1-1 Yoshinodai, Chuo-ku, Sagamihara, Kanagawa 252-5210,
10
11
12
13 84 suzuki.makoto@jaxa.jp
14
15
16 85 Naru Hirata, ARC-Space, CAIST, The University of Aizu, 90 Kami-Iawase,
17
18
19 86 Tsuruga, Ikki-machi, Aizu-Wakamatsu, Fukushima 965-8580, Japan
20
21
22
23 87 naru@u-aizu.ac.jp
24
25
26
27 88 Eliot F. Young
28
29
30 89 Southwest Research Institute, 1050 Walnut St., Suite 300, Boulder, CO 80302, USA
31
32
33
34 90 efy@boulder.swri.edu
35
36
37 91 Adriana C. Ocampo
38
39
40
41 92 NASA Headquarters, 300 E Street SW, Washington, DC 20546, USA
42
43
44 93 adriana.c.ocampo@nasa.gov
45
46
47
48 94
49
50
51 95
52
53
54
55 96 *Corresponding author
56
57
58
59
60
61
62
63
64
65

1 97 **Abstract**
2
3

4 98 Since insertion into orbit around Venus on December 7, 2015, Akatsuki orbiter has
5
6 99 returned unprecedented global images of Venus from its four imaging cameras at
7
8 100 ultraviolet (283 and 365 nm), near infrared (0.9 to 2.3 μm) and at thermal infrared (8-12
9
10 101 μm) showing the dynamic morphology of its day and night time cloud cover nearly
11
12 102 continuously. Past orbiting or fly-by missions to Venus did not provide such long-term
13
14 103 global, wide spectral range or frequency of observations. The day side cloud cover
15
16 104 imaged at the ultraviolet wavelengths shows morphologies similar to what was observed
17
18 105 from Mariner 10, Pioneer Venus, Galileo, Venus Express and MESSENGER, but the day
19
20 106 time images at 0.9 and 2.02 μm also reveal some interesting features which bear similarity
21
22 107 to the ultraviolet images. The night time images at 1.74, 2.26 and 2.32 μm and at 8-
23
24 108 12 μm reveal features not seen before and show new details on the night side structure and
25
26 109 ribbon like narrow width, long scale waves, frontal boundaries and even small vortices.
27
28 110 Some features seen previously, such as Circum-Equatorial Belts (CEBs) and occasional
29
30 111 brightenings at ultraviolet (seen in Venus Express observations) of the cloud cover at
31
32 112 ultraviolet have not been seen so far. Evidence for the hemispheric vortex organization of
33
34 113 the global circulation can be seen at all wavelengths on day and night side.

35
36
37
38
39
40
41
42
43
44
45
46
47
48
49
50
51
52
53
54
55
56
57
58
59
60
61
62
63
64
65

114
115 The cloud morphologies provide some clues to the processes occurring in the atmosphere
116 and are thus a key diagnostic tool when quantitative dynamical analysis is not feasible
117 due to lack of sufficient information.

118

119 **Keywords**

120 Venus Clouds, Morphology, Day-side, Night-side, Ultraviolet, Near Infrared

121

122 **Akatsuki Observations**

123 Akatsuki orbiter was originally planned to be inserted into orbit around Venus on 7
124 December 2010 after a successful launch on 21 May 2010. However, a malfunction
125 during the procedure led to the spacecraft miss the orbit insertion and ended up in a ~ 205
126 day orbit around the Sun (Nakamura et al., 2016), changing to 199 day period by
127 November 2011. Heroic rescue efforts by the Akatsuki team orbit insertion was finally
128 achieved on 7 December 2015, a rare reprieve for a planetary mission. Akatsuki orbiter
129 is providing images of Venus comparable to or better than those obtained from the Venus
130 Express VMC instrument. Only the LIR camera images are much smaller (~ 18 pixel
131 diameter) at apoapsis. Imaging in reflected light is performed in portions of the orbit
132 when the phase angle is appropriate with imaging at roughly two hour intervals.
133 Imaging of the night side of Venus is limited to portions of the orbit when the angular
134 separation between the Sun and Venus is larger than 26.5° to avoid stray light. Also,
135 pointing is adjusted to keep as much of the saturated day-side portion of the planet out of
136 the field of view of IR2 and IR1 cameras as possible to minimize contamination of the
137 data by the bright dayside portion of the planet. Additionally, data communication to
138 the 64 m Usuda Deep Space Station near Nagano, Japan occurs daily for about eight hours
139 when observations are not possible. The three filters with band pass centered at 0.9,
140 0.97 and $1.07 \mu\text{m}$ are used for imaging the surface in the CO_2 windows where the
141 atmosphere and the clouds are largely transparent and hence do not reveal any cloud
142 morphology, but can be useful perhaps to retrieve some of the properties.

144 **Introduction**

145 The cloud cover on Venus is ubiquitous, unlike on Earth and Mars. That it shows no
146 contrast at most reflected wavelengths except ultraviolet has been known for a long
147 time. The ultraviolet contrasts were first discovered by Quénisset in 1911 visually and
148 recorded as drawings (Dollfus, 1975; Ross, 1927) and photographed by several
149 observers in blue-violet in 1920s (Ross, 1927), and it was subsequently when more
150 frequent ultraviolet images were obtained and showed variability that the images
151 revealed clouds and not features on the surface. First spacecraft images were obtained

1 152 over an eight day period during the Mariner 10 fly-by of Venus in February 1974
2
3 153 (Murray et al., 1974). The morphology of the cloud cover from these images and their
4
5 154 relationship to the Y-features seen prominently in earth based images has been presented
6
7 155 by Dollfus (1975). Pioneer Venus orbiter imaged Venus at spatial resolution of ~ 25-
8
9 156 40 km at 370 nm using a spin scan technique but it took between 2 and 5 hours to
10
11 157 complete one image in the eccentric orbit (Travis et al., 1979a; Travis et al., 1979b).
12
13 158 Most of the features identified in Mariner 10 images during its short coverage were also
14
15 159 seen in the longer duration of Pioneer Venus orbiter and the morphology was presented
16
17 160 by Rossow et al. (Rossow et al., 1980). Venera 9 and 10 orbiters also obtained 17
18
19 161 images covering a limited portion of the sun-lit planet during 26 October – 25
20
21 162 December 1975 using the motion of the orbiters with a 512 element linear photometer
22
23 163 array with 30° wide field of view at violet and ultraviolet wavelengths (Keldysh, 1977).
24
25 164 Pioneer Venus orbiter (PVO) also obtained lower resolution images (365 nm global
26
27 165 images with a few limb images at 365 and 690 nm) and polarization data (~ 100 km per
28
29 166 pixel) in reflected sunlight at four wavelengths (270, 365, 550 and 935 nm) which
30
31 167 showed morphology to be similar at 270 and 365 nm in unpolarized light, but also
32
33 168 showed similar features in polarization data at the two longer wavelengths (Limaye,
34
35 169 1984). The Orbiter Infrared Radiometer (OIR), a 6 filter instrument on PVO also
36
37 170 yielded thermal infrared views of the northern hemisphere cloud tops at 10.6 -12.6 μm
38
39 171 for about two months (Apt et al., 1980; Taylor, 1980). Galileo orbiter took images of
40
41 172 Venus (Belton et al., 1991) over a very short period (2.5 days) in February 1990 at two
42
43 173 different wavelengths in reflected light (420 and 990 nm effective wavelengths) which
44
45 174 showed morphologies to be similar to the Mariner 10 and Pioneer Venus observations
46
47 175 (Belton et al., 1992), but at near infrared wavelengths (1-3 μm) showed surprising detail
48
49 176 on the night side (Carlson et al., 1991). The Venus Monitoring Camera (VMC)
50
51 177 (Markiewicz et al., 2007) on Venus Express orbiter (Svedhem et al., 2007) imaged
52
53 178 Venus at 365, 513, 950 and 1010 nm and the mapping channel of the Visible Infrared
54
55 179 Thermal Imaging Spectrometer (VIRTIS) imaged Venus between 0.28 – 5.1 μm during
56
57 180 15 April 2006 – 27 November 2014 and predominantly provided a polar view of the
58
59 181 Venus cloud cover at ~ 25-45 km per pixel size and detailed views of the equatorial and
60
61 182 northern latitudes at a spatial scale of as high as 1-2 km per pixel. The VIRTIS-M used
62
63 183 separate detectors of the short wave and infrared regions. The shortwave data are still
64
65 184 being fully calibrated to remove instrumental effects. The near infrared data showed

1 185 new details of the polar regions of Venus not readily accessible to Akatsuki and imaged
2 186 primarily the southern hemisphere between 200 nm – 5 μ m wavelngths at moderate
3 187 spectral resolution. At tne near infrared (NIR) wavelengths these data showed the
4 188 morphologies of features formed by CO₂ non-LTE emmissions (Garcia et al., 2009) in
5 189 the upper atmosphere, details of the nightside upper oxygen airglow (Soret et al., 2014).
6 190 The NIR data also showed nightside upper clouds (Peralta et al., 2017) and lower clouds
7 191 (Hueso et al., 2012). VIRTIS also revealed the intricacies of the inner region of the
8 192 (southern) hemispheric vortex circulation (Garate-Lopez et al., 2015; Luz et al., 2011)
9 193 which were not seen in the ultraviolet views that revealed the vortex from space-time
10 194 composites of Mariner 10 day-side images (Suomi & Limaye, 1978).

11 195
12 196 In Venus Express observations the 365 nm morphologies seen showed the same basic
13 197 features detected from previous missions, but showed some new aspects of the cloud
14 198 cover, particularly because of its polar vantage point ((Markiewicz et al., 2014; Titov et
15 199 al., 2012). The VIRTIS experiment (Piccioni et al., 2007a) of Venus Express imaged
16 200 Venus from 0.3 to 4.3 μ m and showed the intricacies of the inner region of the
17 201 (southern) hemispheric vortex circulation (Limaye et al., 2009; Suomi & Limaye, 1978)
18 202 about the poles of Venus in each hemisphere. MESSENGER spacecraft imaged Venus
19 203 from its wide and narrow angle cameras in June 2007 and provided more than two
20 204 hundred images of Venus in 10 nm spectral bands (wide angle only) at a twelve
21 205 wavelengths over about two days.

22 206
23 207 It is useful to note that on Earth cloud morphologies look very similar from blue to
24 208 thermal infrared wavelengths (Figure 1), unlike on Venus (Figure 2). Images taken from
25 209 Himawari satellite at sixteen different wavelengths between 410 nm and 15 μ m are
26 210 shown in Figure 1 while similar wavelength coverage for Venus is shown in Figure 2
27 211 from recent missions. Unlike the Earth images which are concurrent, we have only
28 212 limited concurrent coverage over the same spectral range from MESSENGER fly-by
29 213 data and is supplemented by Galileo and Akatsuki for illustrative purpose. The
30 214 MESSENGER images are taken from the MDIS Wide Angle camera (Hawkins et al.,
31 215 2009; Robinson et al., 2007) with narrow band filters (10 nm) comparable to the band
32 216 pass of the Akatsuki images at 283and 365 nm (Table 1).

33 217
34
35
36
37
38
39
40
41
42
43
44
45
46
47
48
49
50
51
52
53
54
55
56
57
58
59
60
61
62
63
64
65

1 218 The difference between the wavelength similarity for Earth and for Venus is striking and
2
3 219 suggestive of the compositional differences between Earth and Venus clouds. Venus
4
5 220 clouds are complex as we have discovered. Although the ultraviolet contrasts were
6
7 221 first discovered more than a century ago (Dollfus, 1975), and that the clouds are
8
9 222 composed of sulfuric acid for nearly five decades (Hansen & Hovenier, 1974) we still
10
11 223 do not know what substance(s) are responsible for them except that sulfur dioxide gas is
12
13 224 one of them and there is at least another absorber which is as yet unknown (Travis,
14
15 225 1975). Morphologies provide a good diagnostic tool for relating the atmospheric
16
17 226 processes involved with the sources and sinks of the aerosols, condensates and trace
18
19 227 gases that are involved. There are more than one hundred and forty chemical reactions
20
21 228 involving sulfur in the atmosphere of Venus and may more involving other elements.
22
23 229 Venera and VeGa landers, four Pioneer Venus probes and two VeGa balloons have
24
25 230 sampled the clouds below 62 km and obtained useful measurements, but these are
26
27 231 proving to be insufficient in understanding the clouds of Venus.

28 232
29 233 Against this background, the observations from Akatsuki cameras are providing high
30
31 234 quality global images at wavelengths where Venus over an extended period enabling a
32
33 235 study of the global morphologies and shedding new light on the clouds of Venus.
34
35 236 Akatsuki orbiter's cameras are now imaging Venus at thirteen wavelengths from 283 nm
36
37 237 to 10 μ m. These images provide global views of the day and night side of Venus at
38
39 238 spatial scales from \sim 70 km to as high as 0.2 km per pixel. Concerning cloud
40
41 239 morphology, Akatsuki provides the best global views of Venus at several wavelengths
42
43 240 for the first time – 283, 900, 2020 nm on the day side and at 0.97, 1.01, 1.74, 2.26 and
44
45 241 2.32 μ m on the night side while the LIR camera provides day and night side views of
46
47 242 Venus at the thermal wavelengths.

48 243
49 244 The morphological investigation at the multiple wavelengths enabled by Akatsuki
50
51 245 cameras presented here provides new constraints on the clouds – both ultraviolet
52
53 246 absorbers responsible for day side patterns and local variations in cloud opacity for the
54
55 247 night side patterns. We describe here the morphology of the day side cloud cover (283,
56
57 248 365, 900 and 2020 nm) for the first time and also the night time morphology from 1.74,
58
59 249 2.26 and 2.32 μ m images that shows amazing detail not previously seen in either the
60
61 250 ground based observations or from the VIRTIS/Venus Express coverage.
62
63
64
65

251 Akatsuki Multispectral Images of Venus: Cameras on board

252 There are five cameras on Akatsuki to image Venus at UV to thermal infrared – UVI
 253 [Yamazaki et al. submitted to EPS, same issue], IR1 (Iwagami, 2011), IR2 (Satoh et al.,
 254 2016), and LIR (Fukuhara et al., 2011) wavelengths and Lightning and Airglow Camera
 255 (LAC) which does not produce an image (Takahashi et al., 2008) which is operated
 256 when the night side of Venus is visible to Akatsuki to detect lightening and airglow.
 257 Table 1 provides the characteristics of the four imaging cameras. The 1.65 μm filter in
 258 the IR2 camera was used for zodiacal imaging during cruise and is not used to image
 259 Venus and hence is not listed in this table. The focal lengths are nominal values and
 260 have been updated from star fields during the mission for IR2 camera, and updates are
 261 expected for the other cameras. During the long interval between the first attempt in
 262 December 2010 and the successful one in December 2015, Akatsuki came much closer
 263 to the Sun than anticipated with 11 perihelion passages. Thus the camera performance
 264 was affected somewhat, particularly for the IR1 camera, requiring new procedures for
 265 calibration of the data.

266
 267 Table 1. Characteristics of cameras on Akatsuki Orbiter

Camera	Channel Name	Band Center (μm)	Bandwidth (micron)	Transmittance	Pixel Size (mm)	# Lines	# Samples	Focal Length (mm)	Day/Night
IR1	090d	0.900	0.00910	0.0027	0.017	1024	1024	84.2	Day
	090n	0.898	0.02890	0.74	0.017	1024	1024	84.2	Night
	097	0.969	0.03860	0.78	0.017	1024	1024	84.2	Night
	101	1.009	0.03910	0.75	0.017	1024	1024	84.2	Night
IR2	174	1.735	0.041	0.85	0.017	1024	1024	85.41	Night
	226	2.26	0.052	0.67	0.017	1024	1024	85.44	Night
	232	2.32	0.036	0.67	0.017	1024	1024	85.41	Night
	202	2.02	0.039	0.06	0.017	1024	1024	85.50	Day
	165	1.65	0.283	0.93	0.034	520	520	85.35	-
UVI	283	0.283	0.014	0.280	0.013	1024	1024	63.3	Day
	365	0.365	0.014	0.509	0.013	1024	1024	63.3	Day
LIR		10.00	4.00	-	0.037	328	248	42.2	Day and Night

268
 269
 270 Generally, when Akatsuki orbiter predominantly views the night hemisphere of Venus
 271 from its position in its ~ 11-day orbit around Venus, the UVI camera is not used, and

1 272 only IR1 (IR1_9N and IR1_101 filters) and IR2 (IR2_174, IR2_226 and IR2_232
2 filters) cameras image the night side of Venus in selected filters. The 1.65 μm filter of
3 273 IR2 is for zodiacal light studies and was used only during cruise. The LIR camera
4 274 images Venus throughout the orbit – day and night as it senses radiation emitted to space
5 275 by the planet from the cloud tops. Dayside images are taken from the UVI camera at
6 276 283 and 365 nm wavelengths as well as at 0.9, 1.01 (IR1) and 2.02 μm (IR2)
7 277 wavelengths. Instrumental constraints prevent concurrent images from different filters
8 278 from the same camera but the time interval is relatively short (about 214 seconds for
9 279 UVI) which provides near simultaneous imaging at different wavelengths except at
10 280 close approach to Venus.
11 281
12 282

283 **Temporal Coverage**

284 Only four hours after Venus Orbit Insertion (VOI), the IR1, UVI and LIR
285 cameras took Venus images. Only IR2 waited to be cooled down for 10 days
286 and took “first light” images after a long hibernation period also in
287 December 2015, but the first Venus images from IR2 were obtained in
288 January 2016. Akatsuki began its systematic data collection in April 2016 from its
289 near equatorial orbit with periapsis altitude of ~ 1000 km and a 10.5-day period and an
290 eccentricity of about 0.92 (Figure 3). Routine imaging from all four cameras began on
291 1 April 2016 and has continued on every orbit. In November 2016 a technical problem
292 prevented imaging from IR1 and IR2 cameras which share some electronics, and
293 currently those two cameras are not returning any data. The cadence of most of the
294 images from UVI, IR1 and IR2 cameras is two hours, but some have been acquired one
295 hour apart for better temporal sampling. Generally, UVI camera makes three
296 exposures for one “image” and a median filter is applied to reduce the dark noise and
297 this procedure takes 210 seconds. But at close approach to Venus the median filter is not
298 applied and images can be acquired quicker (150 seconds apart). The LIR camera can
299 image Venus every four seconds. The total number of images returned from Akatsuki
300 is thus somewhat less than the number of images returned from VMC, but the overall
301 quality and image resolution are better, and provide global views of the planet than only
302 a south polar view from the majority of the images.

303 **Day Side Morphology**

304 *283 nm, 365 nm (UVI) Images*

305 A representative sampling of images taken through the 283 and 365 nm filters are
306 shown in Figure 4. At first impression the cloud forms seen at these two wavelengths
307 are very similar as the clouds absorb some of the incident ultraviolet radiation, however
308 some differences in the relative brightness and contrasts are seen. In general, the
309 contrast of the images is somewhat lower at 283 nm than at 365 nm. This is somewhat
310 unexpected as SO₂ is expected to absorb some of the radiation at this wavelength, along
311 with another absorber (Esposito, 1980; Esposito et al., 1983). The intensity data
312 acquired from Pioneer Venus Orbiter Cloud Photopolarimeter showed somewhat larger
313 contrasts at 270 nm compared to 365 nm at 0 - 90° phase angle, at least when contrast
314 was defined in terms of absolute deviation from the intensity expected from a Minnaert
315 law behavior. Despite the somewhat lower contrast, 283 nm images show generally
316 the same morphology as 365 nm images, but the smaller scale details are muted or
317 absent.

318
319 The Akatsuki images show features seen before – discrete smaller scale features at low
320 latitudes, bright spiraling streaks and bands at mid-latitude, bow like features near the
321 sub-solar point and the Y-like feature in different shapes. As before, the contrasts are
322 lower near terminators. A more detailed study of the Y-feature and a study of the
323 evolution of morphology and contrasts at 283 and 365 nm data are underway and will be
324 reported by others in the near future. Scattering properties of the clouds at 283 and 365
325 nm as deduced from Akatsuki data have been reported recently (Lee et al., 2017) which
326 confirm that SO₂ and the unknown UV absorber are necessary factors to explain the
327 decreasing trend of the observed relative albedo at phase angles larger than 10°.

328 *Day side Images at 900 nm (IR1)*

329 Images taken through the 0.9d filter on the day side of Venus are shown in Figure 5.
330 As expected from previous observations (Coffeen et al., 1971), the full disk image of
331 Venus shows little detail as the contrast is very low. Low to medium spatial resolution
332 full disk images show somewhat less bright polar regions compared to the ultraviolet,

1 333 showing similar darkening as seen at 2.02 μm . Digital filtering brings out subtle
2 334 contrasts on very small scales ($\sim 10\text{-}20$ km) at 0.9 and 2.02 μm . Some examples are
3 335 shown in Figure 5 – images B,D, and F are high pass filtered images. Images C and D
4 336 are mapped at 0.025° per pixel in latitude and longitude to present the same scale since
5 337 Image E was obtained at a range of 16,467 km and “F” at 17,458 km (3.38 and 3.52
6 338 km/pixel respectively) and the two images are only about 12 minutes apart, showing
7 339 rapid changes in the small scale contrasts. Both E and F images show the equatorial
8 340 region and span an area approximately 400 x 400 km. On this small scale the
9 341 origination of the bright streaks at 365 nm is almost orthogonal to the latitude circles,
10 342 unlike the general pattern of streaks seen over larger scales which are inclined at a
11 343 smaller angle, giving the impression that they are streak lines (Smith & Gierasch, 1996).
12 344
13 345 Similar to the variable correlation between the 283 and 365 nm brightness distribution
14 346 over concurrent images from Akatsuki UVI camera, the correlation between the
15 347 wavelengths covered by Galileo and MESSENGER images was also found to vary.
16 348 During the Galileo flyby there seemed to be an "anticorrelation" in brightness between
17 349 the violet and near-infrared images (Belton et al., 1991), but this anticorrelation was not
18 350 apparent during the MESSENGER fly-by (Peralta et al. 2017a). Analysis of the
19 351 Akatsuki data correlation between short and long wavelengths is underway and will be
20 352 reported later.

353 *Day side Images at 2.02 μm*

354 Full disk day side 2.02 μm images from the IR2 camera are shown in Figure 6. The
355 polar regions ($> 60^\circ$ latitude), appear noticeably darker at this wavelength close to the
356 equatorial boundary of the “cold collar” seen in the thermal data. At this wavelength
357 some of the radiation reflected from the clouds is absorbed by CO₂, the dominant
358 constituent of the Venus atmosphere. The darker regions thus suggest lower cloud tops,
359 which would be consistent with the lower cloud tops inferred from VIRTIS data at 1.74
360 μm using the same approach by Ignatiev et al. (2009). The equatorial and mid-latitude
361 regions show faint details somewhat similar to those seen at ultraviolet wavelengths.
362 The classic Y-shaped feature can be discerned often. There also appears to be some
363 phase angle dependence as very few details are visible at phase angles $> 120^\circ$.

1 364 *Morphology at Smaller scales (~2 to ~5 km/pixel)*
2
3

4 365 The structures on smaller scale are somewhat different from the patterns seen on a
5
6 366 global scale. VMC images showed fine scale gravity waves in northern latitudes
7
8 367 (Piccialli et al., 2014) which were not seen previously and have not yet been seen in
9
10 368 Akatsuki images at any wavelength. Images at ~2 to ~5 km/pixel scale are generally
11
12 369 acquired by Akatsuki cameras at low latitudes and show somewhat surprising structures.
13
14 370 Figures 7a shows a selection of views from UVI and IR1 cameras. Only contrast
15
16 371 filtered versions are shown as the calibrated images do not show any discernable details.
17
18 372 Figure 7b shows 2.02 images in both calibrated and contrast filtered versions. In
19
20 373 general the contrasts are even lower on such small spatial scales and are brought out
21
22 374 only after some filtering. The contrast filtered versions were created by dividing the root
23
24 375 mean square deviation over a box (9x9 or 11x11) centered over a pixel by the average of
25
26 376 the pixels within the box. Images A and B show thin, string like features of variable
27
28 377 lengths, curvature and inclinations to latitude circles. Image C however is surprisingly
29
30 378 devoid of such features but shows a bright region core surrounded by a dark ring like
31
32 379 the classic signature of the glory feature which has been seen in the Venus Monitoring
33
34 380 Camera at 365, 550, 950 and 1050 nm (Markiewicz et al., 2014), but the geometry is not
35
36 381 consistent with the backscatter angle and the feature is believed to be due to low
37
38 382 frequency bias and cross-talk between the four quadrants of the IR2 readout electronics
39
40 383 (Sato et al, this issue).
41
42 384

43 385 Near simultaneous global images of Venus at 283, 365, 900 and 2020 nm on three
44
45 386 separate days (almost one orbit apart) are shown in Figure 8. The near infrared images
46
47 387 are shown in filtered versions to bring out the contrasts. The transition between lower
48
49 388 and higher brightness matches well at 283 and 2.02 μ m while the transition occurs at a
50
51 389 slightly lower latitude at 365 nm. Poleward of this quasi linear streaks can be seen at all
52
53 390 four wavelengths which are equivalent to the spiral arms of the vortex over the pole.
54
55 391 The two longer wavelengths should probe the deeper levels of the clouds compared to
56
57 392 the UV wavelengths, but at 2.02 μ m CO₂ absorption also plays a role. Thus when
58
59 393 similar features or structures are seen at all four wavelengths, the features extend from
60
61 394 near the top to at least a scale height deeper. When the features are not similar, the
62
63 395 cloud cover is likely layered.
64
65

1 396 *Variations in Cloud Properties: Contemporaneous views at 283, 365 nm,*
2
3 397 *1.02 μm and 2.02 μm*
4
5

6 398 Figure 9 shows images obtained close together in time and at spatial scale of about 6 km
7
8 399 per pixel at 283, 365nm and 2.02 μm in the top row mapped in latitude and longitude.
9
10 400 The lower column shows a color composite with 283 nm shown in blue, 2.02 μm in red
11 401 and 365 nm image in green. Subtle color variations over the overlapping area from
12 402 yellow to purple or brown are suggestive of differences in the distribution of sub-micron
13 403 haze ($\sim 0.2 \mu\text{m}$ radius), the cloud particles ($\sim 1.2 \mu\text{m}$ radius), larger particles and
14 404 possible differential CO₂ amounts over the “cloud-tops”. More bluish and/or greenish
15 405 indicate less abundances of UV absorbers, while reddish indicates higher cloud top level
16 406 than that over rest area owing to less CO₂ absorption above the cloud top altitude at the
17 407 CO₂ band (2.02 μm). Figure 9 shows yellowish in the 10° S -10° N latitude, implying
18 408 the area has less unknown UV absorber and the cloud top level is higher than
19 409 surrounding region.
20
21
22
23
24
25
26
27

28 410 **Night Side Morphology**
29
30

31 411 *1.74, 2.26 and 2.32 μm Images from IR2 Camera*
32
33

34 412 Figure 10 shows a selection of night time images taken from the IR2 camera at 1.74,
35 413 2.26 and 2.32 μm which reveal a very different morphology than that seen on the day
36 414 side. Also included are two sample images (U and X) from the NASA Infrared
37 415 Telescope Facility (IRTF) located at Mauna Kea, Hawaii. These two images are part of a
38 416 ground based campaign to collect supplemental images in support of Akatsuki mission.
39 417 Although the NIMS (Galileo) and VIRTIS (Venus Express) instruments also provided
40 418 images at these wavelengths, the temporal coverage was too short due to the fly-by
41 419 nature of Galileo observations and VIRTIS was not able to image the low latitudes or
42 420 provide global views of the planet from an equatorial perspective due to the elongated,
43 421 polar orbit of Venus Express.
44
45
46
47
48
49
50

51 422
52

53 423 Thus Akatsuki images reveal for the first time the complex and puzzling morphology of
54 424 the cloud cover on the night side. At the wavelengths near 2 μm , the features seen in
55 425 the images have been interpreted as being seen as back-lit silhouettes illuminated by the
56
57
58
59
60
61
62
63
64
65

1 426 radiation emitted by the increasingly warming atmosphere below the clouds towards the
2
3 427 surface and the surface itself. While differences in either the amount of UV absorbers
4
5 428 or cloud altitudes as on the dayside lead to changes in the day side appearance of Venus,
6
7 429 the varying near infrared opacity of the clouds is responsible for the features seen at
8
9 430 near infrared wavelengths seen in previous ground based, Galileo/NIMS and
10
11 431 VEX/VIRTIS images. However, the features seen in the Akatsuki IR2 images suggest
12
13 432 that dynamics may play a significant role in the night side morphology. For example,
14
15 433 images G, H and I of Figure 10 at 1.74, 2.26 and 2.32 μm show a long linear dark streak
16
17 434 (low intensity) at some angle to the latitude circles as well as a very bright (high
18
19 435 intensity). Different processes may be producing a very high linear opacity feature in
20
21 436 the case of the dark streak and a very localized “hole” in the overlying cloud to let the
22
23 437 near infrared radiation leak through from the lower atmosphere to space.

24 438 *Sharp Boundaries or Frontal Zones?*

25
26
27 439 Some night side IR2 images show a sharp linear boundary running north-south across
28
29 440 which the intensity varies noticeably. What is remarkable is the sharpness of the
30
31 441 boundary with changing orientation. Origins of such sharp opacity regions are not
32
33 442 easy to explain dynamically without invoking “different air masses” as was suggested to
34
35 443 explain the VeGa balloon dynamical results (Blamont et al., 1986), but then the
36
37 444 challenge is explaining the origins of different air masses.

38
39 445
40
41 446 Another example is illustrated by images J, K L as well as M, N and O of Figure 10 in
42
43 447 which a very sharp, irregular boundary with a very sharp right angle boundary is seen at
44
45 448 all three wavelengths between high and low intensity. Figure 11a shows another
46
47 449 example with very striking intensity boundary in a 2.26 μm image, reminiscent of a
48
49 450 front. This boundary remains more or less intact for some time before dissipating,
50
51 451 much as the expanding plume from a volcanic eruption or a dust storm front. On Earth
52
53 452 sharp boundaries are also seen in water vapor channel images are seen often (Figure
54
55 453 11b) revealing different mid-low tropospheric water vapor abundances. The right
56
57 454 angled between dry (dark) and moist (gray) seen in Figure 11b southeast of Japan is
58
59 455 similar to the feature in images M, N and O in Figure 10. Trace gases such as water
60
61 456 vapor, HF, CO and COS are optically active in the 2.3 μm region and can be responsible
62
63
64
65

1 457 for such discontinuities but the cause for such demarkation in the species abundances
2
3 458 are unclear, but volcanic eruptions can be one. Since such boundaries are not apparent
4
5 459 in the UVI images, the differences in the abundances are restricted to middle and lower
6
7 460 part of the cloud, perhaps due to the increasing stability of the atmosphere. Magurno et
8
9 461 al. (2017) have examined VIRTIS data between 25-55° latitude to explore cloud particle
10
11 462 properties and trace species and find that sulfuric acid concentrating making up the
12
13 463 cloud particles may be varying vertically and that near 2.3 μm , water vapor, CO and
14
15 464 COS affect the observed intensities (they did not include CS₂). Regional dynamics
16
17 465 must therefore be responsible to create the observed sharp boundaries which leads to the
18
19 466 question of the sources and sinks of the trace species.

20
21 467
22 468 Images S and T of Figure 10 also show a similarly sharp boundary, but in this case the
23
24 469 low intensity region is shaped like a dark streak. Ground based IRTF images (U and
25
26 470 X) also show large contrasts in the intensities in the K-continuum filter. Once again, it
27
28 471 is not easy to explain the causes of such features, except to say that somehow the local
29
30 472 dynamics must play a role in affecting the distribution of aerosols at the levels involved.
31
32 473 These features serve as a caution against basing interpretations of the observations on
33
34 474 the VIRA model globally as the local deviations are clearly significant. At this point it
35
36 475 is premature to assess the impact of these opacity variations on the heat deposition in
37
38 476 the atmosphere which is believed to be driving the superrotation of the deep atmosphere
39
40 477 of Venus.

41
42 478
43 479 At high spatial resolution all three wavelengths show bright, thin, sinuous wispy streaks
44
45 480 like features against a darker (lower intensity) background (Images P, Q and R).
46
47 481 Such features have not been detected on the day side at any wavelength in the images
48
49 482 obtained so far. Often these features are seen to criss-cross, suggesting perhaps some
50
51 483 altitude difference analogous to terrestrial cirrus, but we have little additional data or
52
53 484 information at this time. Regardless, their presence is undoubtedly due to some cloud
54
55 485 particle formation process in the middle of the cloud layer which is affected by trace
56
57 486 species, condensation nuclei and temperature and cloud forming substances such as
58
59 487 sulfuric acid which is believed to form in the upper portion of the cloud layer, but not
60
61 488 photochemistry.

62
63
64
65
66 489

1 490 *The Y-Feature absent on night side?*

2
3 491 The Y-feature and its numerous shape varieties seen in the ultraviolet images of Venus is
4
5 492 conspicuously missing in the night time images taken at 1.74, 2.26 and 2.32 μm . This
6
7 493 suggests some vertical limits on the dynamical processes that produce this recurring
8
9 494 feature, e.g. that it is the result of the distortion of an equatorial wave as it propagates
10
11 495 within a latitudinal varying zonal wind differing from solid body rotation (Peralta et al.,
12
13 496 2015). To some extent, the appearance or the perception of the Y-shaped features
14
15 497 appears to be related to the relative spatial resolution of the images. It is far easier to
16
17 498 this feature in lower spatial resolution images than in high resolution images. This is
18
19 499 probably due to the scale dependence of the contrasts seen in the cloud cover of Venus.
20
21 500 The contrasts on small spatial scales ($\ll 100$ km) is very low compared to the contrasts
22
23 501 seen at large scales ($\gg 100$ km), as can be seen from images shown in Figures 4 and 5.

24

25 502
26 503 *Small scale vortices*

27 504 Small scale, local circulations, including vortices are also seen in a few of the images
28
29 505 for the first time on Venus (D,E,F in Figure 10) which resemble “mushroom” like
30
31 506 features seen in water vapor images of Earth from synchronous weather satellites
32
33 507 (Houghton & Suomi, 1978). These features are being presented by Limaye et al.
34
35 508 (2017). Origin of such small scale circulations was not expected due to the low
36
37 509 rotation rate which places Venus in a “symmetric” circulation regime rather than a
38
39 510 planetary wave regime as was discovered by R. Hide (Hide, 1953) and D. Fultz from
40
41 511 dish pan or rotating annulus experiments to simulate atmospheric circulations many
42
43 512 decades ago and analyzed extensively since then (Read, 2011; Sugata & Yoden, 1993).

44

45 513
46 514 *Ribbons or narrow width waves*

47 515 Small scale waves along a sharp boundary parallel to latitude circles have been seen in
48
49 516 2.32 μm images at low latitudes ($\sim 15^\circ$ S latitude) from Akatsuki’s IR2 camera, that
50
51 517 resembles sharp boundary between the low to mid latitude clouds and the bright band
52
53 518 seen at 365 nm in most Venus images situated typically between 45-50 $^\circ$ latitudes in both
54
55 519 hemispheres (Rossow et al., 1980; Suomi & Limaye, 1978; Titov et al., 2012). Figure
56
57 520 12 shows an example of an 2.26 μm image in perspective view from IR2 camera (left)
58
59 521 and in a latitude-longitude view (right). The wavelike boundary is at about -17.3°
60
61 522 latitude. The larger intensities at higher latitudes suggest thinner (lower opacity)

62
63
64
65

1 523 overlying clouds. VIRTIS observations indicated only lower cloud tops in polar regions
2
3 524 (Ignatiev et al., 2009).

4
5 525

6
7 526 *High Resolution Detail on the Nightside*

8 527 Figure 13 shows a color composite of co-located 1.74 μm (red), 2.26 μm (green) and
9
10 528 2.32 μm (blue) images obtained from the IR2 camera at a spatial scale of ~ 11 km/pixel.
11
12 529 All three images are shown as latitude –longitude maps with 0.1° / pixel scale. Color
13
14 530 differences reveal subtle differences in opacity of the Venus clouds at the three
15
16 531 wavelengths in this color composite. Thus white features have similar opacity values
17
18 532 and different colors indicate higher or lower values of opacity. Thus areas that appear
19
20 533 yellowish in the overlap region should indicate somewhat higher opacity at 2.32 μm
21
22 534 compared to the other two wavelengths, and the reverse in areas where the features
23
24 535 appear somewhat bluish. These differences appear consistent with influences of CO
25
26 536 contribution (2.32 μm , (Tsang et al., 2009), H_2SO_4 absorption (1.74 vs. 2.2 μm (Barstow
27
28 537 et al., 2012)), and cloud particle size (1.74 vs 2.3 μm (Wilson et al., 2008)) have been
29
30 538 identified from Venus Express data. It seems that the compositional differences do not
31
32 539 appear to be due to local time differences.

31
32 540

33 541 *Thermal Infrared: Cloud Top Brightness Temperature Morphology from*
34
35 542 *LIR*

36 543 Pioneer Venus OIR experiment provided the first spacecraft observations of Venus at the
37
38 544 thermal wavelengths where the emission from its cloud tops can be sensed (Taylor et al.,
39
40 545 1980) but these were limited to northern polar regions. Akatsuki LIR camera provides
41
42 546 the first global views of the brightness temperature distribution over the cloud cover
43
44 547 continuously. Figure 14 shows two sample images. One of the first major
45
46 548 discoveries was a bright band (Image A in Figure 14) aligned almost north-south with a
47
48 549 slight curvature which has been interpreted as a standing gravity wave triggered by
49
50 550 surface topography (Fukuhara et al., 2017). Such waves have been seen often in
51
52 551 Akatsuki data and it has been observed that they last for a few days before dissipating.
53
54 552 Further, these waves occur only near the evening temperature with temperature contrast
55
56 553 of about 5-6 K with the bright and dark portions corresponding to about 230 and 225 K
57
58 554 respectively. Surprisingly, the signature of these standing waves can also be detected
59
60 555 at 283 nm (Fukuhara et al., 2017), and have been detected at 365 nm also.

1 556 These waves were also seen in the 986 nm images of Venus from the Galileo Solid State
2
3 557 Imager (SSI), but were not identified as such and was described as a north south
4
5 558 brightness discontinuity but moving with the ambient wind by Belton et al. (1991).
6

7 559

8 560 Except for the presence of such standing waves, the cloud cover shows very small
9
10 561 brightness temperatures over most of the planet (Image B in Figure 14), less than 2K.
11
12 562 Only at polar latitudes is any brightness temperature variation seen. The “cold collar”
13
14 563 can be often identified as a darker ring surrounding the warm core region of the vortex
15
16 564 over the pole which appears bright due to emissions from the deeper atmosphere.
17

17 565

18
19 566 What remains a mystery is that the brightness temperature contrasts related to the
20
21 567 standing wave are much larger than any temperature contrasts between bright and dark
22
23 568 ultraviolet features, even though a very large fraction of the absorbed solar energy is
24
25 569 taking place at ultraviolet wavelengths. Thus the question that arises is whether the
26
27 570 standing wave brightness temperature contrast is due to vertical altitude differences
28
29 571 since the ambient temperature decreases with altitudes near 65 km altitude at about
30
31 572 6K.km^{-1} or more rapidly.
32

31 573

33 574 *Global Organization of the Cloud Cover - Vortex situated over the poles*

34 575 One morphological feature that spans both day and night cloud cover of Venus is the
35
36 576 hemispheric global vortices in each hemisphere rotating asymmetrically about each
37
38 577 pole. First discovered from Mariner 10 images taken in February 1974 (Suomi &
39
40 578 Limaye, 1978), the vortex organization of the cloud level circulation has been seen in
41
42 579 Pioneer Venus (Limaye, 1985), Galileo (Peralta et al., 2007), and Venus Express
43
44 580 (Limaye et al., 2009) data and hence now can be assumed to be a quasi-permanent state
45
46 581 of the global circulation. The VIRTIS experiment (Piccioni et al., 2007b) with its wide
47
48 582 spectral coverage from UV to NIR was able to capture the complete day and night
49
50 583 portions of the southern vortex. Akatsuki’s near equatorial orbit does not provide an
51
52 584 over the pole view of Venus, and thus the complete vortex in any day or night side filter
53
54 585 cannot be seen and can be seen only as a space-time composite. Figure 15 presents a
55
56 586 view of the vortex organization as obtained from Akatsuki observations at three
57
58 587 wavelengths. An example is shown in Figure 14a by using only two 365 nm images
59
60 588 separated by two days with one image rotated by 180 degrees to show the
61
62
63
64
65

1 589 correspondence of the spiral features. The central oval shaped core region which is
2
3 590 somewhat depressed in altitude can be seen. Figure 15b shows the finer structure in
4
5 591 the north and south hemisphere vortices from 2.02 μm observations. The fine scale
6
7 592 structure could be due to variations in cloud altitudes if the absorption from CO_2 is
8
9 593 considered. This is consistent with the warmer brightness temperatures from the LIR
10
11 594 data shown in Figure 15c.

12 595

13 596 Muto and Imamura (2017); (Piccioni et al., 2007b) discuss the structure of the oval
14
15 597 shaped core region of this vortex as observed from Venus Express VMC ultraviolet
16
17 598 images. The thermal infrared also shows the core region is warmer and also exhibits
18
19 599 the vortex morphology (Figure 15 b). Images taken through 2 μm filters from IR2
20
21 600 suggest that the vortex structure persists in the middle cloud layer seen on the night side,
22
23 601 consistent with the VIRTIS observations,

24 602

27 603 **Summary**

30 604 Akatsuki data at near infrared wavelengths provide new information about the global
31
32 605 cloud morphology on the day and night side in reflected and transmitted radiation. At
33
34 606 ultraviolet wavelengths the new observations reveal same morphology as seen from
35
36 607 previous missions. The day side longer wavelength images show morphologies
37
38 608 somewhat resembling what is observed at shorter wavelengths but the details are
39
40 609 different at the longer wavelengths, confirming the impression from the very limited
41
42 610 images obtained during the second fly-by past Venus by the MESSENGER spacecraft
43
44 611 on its way to Mercury. On the night side Akatsuki observations from the IR2 camera
45
46 612 reveal new aspects of the cloud structure not seen in VIRTIS images – small scale
47
48 613 vortices, waves. Surprisingly many wispy or string like features like cirrus clouds on
49
50 614 Earth are also seen on the night side at low and mid latitudes which correspond to low
51
52 615 opacity regions indicating higher radiances from the atmosphere due to warmer
53
54 616 temperatures. How such features develop is a mystery.

53 617

55 618 What is puzzling is the impression from the motions of the VeGa balloons (Sagdeev et
56
57 619 al., 1990) with the morphologies seen in the 2 μm band images – the VeGa balloons

1 620 moved fairly smoothly horizontally about 6.5° away from the equator in the north and
2
3 621 south hemispheres over most of their 48 hour trajectory, yet the images show a rather
4
5 622 chaotic, dynamical situation. VeGa balloons, floating near 54 km altitude did
6
7 623 experience some large vertical accelerations at times, some were correlated with
8
9 624 topography. The standing gravity waves seen in LIR and UVI (283 nm) images are
10
11 625 absent in the IR2 day side images ($2.02 \mu\text{m}$) or on the night side. At the thermal
12
13 626 wavelengths standing waves and core region of the vortices situated over the Northern
14
15 627 and Southern poles are the prominent features seen. Global brightness temperature
16
17 628 contrasts are low ($< \sim 5\text{K}$). Analysis of the Akatsuki data from all cameras is
18
19 629 continuing and these and future investigations should give us a better idea of the variety
20
21 630 of different processes occurring in the atmosphere of Venus on both the day and night
22
23 631 sides.

- 24 632 • Venus cloud cover appears different at different wavelengths on day side and
25 633 night side compared to global cloud cover on Earth.
- 26 634 • Differences due to different cloud forming processes appear to be active on
27 635 Venus resulting in different cloud particle constituents and responding to the
28 636 temperature and pressure conditions and trace gases.
- 29 637 • It is not well understood why the contrasts peak at 365 nm on the day side and
30 638 near $2.3 \mu\text{m}$ on the night side. Photochemistry, ambient temperatures,
31 639 dynamics may all be responsible in the appearance of Venus at these
32 640 wavelengths in particular.
- 33 641 • Absorbers of incident sunlight at $\lambda < 600 \text{ nm}$ include SO_2 , CS_2 , COS which
34 642 have been detected in the atmosphere of Venus and some others whose nature
35 643 could be organic (Limaye et al., 2017) cannot be ruled out
- 36 644 • There is a clear boundary in the morphology patterns at mid latitudes at all
37 645 wavelengths except at thermal infrared ($8\text{-}12 \mu\text{m}$) where the boundary is
38 646 between $60\text{-}70^\circ$ latitude.
- 39 647 • Regional dynamics must be involved in creating variations in trace gas
40 648 abundances which must control the cloud opacity and reflectivity variations.
41 649 But how these variations come about cannot be determined due to any
42 650 information about their sources as most trace species are affected by
43 651 photochemistry. The differences in the day and night and the reaction rates of
44 652 the numerous chemical reactions possible in the cloud layer are somehow

1 653 responsible, but the spatial variations remain a puzzle.

2 654

3 655

4 656

5 657 **Availability of data and materials**

6 658 Akatsuki data will be available from the Akatsuki Project as well as NASA's Planetary

7 659 Data System in summer 2017.

8 660

9 661 **Competing interests**

10 662 There are no financial and non-financial competing interests.

11 663

12 664 **Funding**

13 665 S.S. Limaye is funded by NASA Grant NNX16AC79G (Participating Scientist in

14 666 Residence) for Akatsuki mission. Drs. Nakamura, Imamura, and Horinouchi are funded

15 667 by JSPS KAKENHI Grant Number JP16H02231. T. Satoh was supported by JSPS

16 668 KAKENHI Grant Number 16H05738.

17 669 **Authors' contributions**

18 670 Drs. Watanabe, Yamazaki, Satoh, Iwagami, Taguchi and Fukuhara have been

1
2 671 responsible for camera development, calibration and observations while Prof. Nakamura
3
4
5
6 672 has been shepherding the Akatsuki mission and operations. Dr. Sato, Yamada, Suzuki,
7
8
9 673 Hirata, Sugiyama and Ando have been involved in instrument calibration, spacecraft
10
11
12 674 operations. Dr. Abe has guided the technical aspects of Akatsuki Project. Prof.
13
14
15
16 675 Yamada contributed to Venus atmospheric dynamics. Dr. Yamamoto, Ohtsuki,
17
18
19 676 Sugiyama, Suzuki, Naru and Takagi have been involved in instrument calibration and
20
21
22
23 677 operations. Drs. Lee and Peralta contributed to the interpretation of the data. Dr.
24
25
26
27 678 Murakami has been responsible for pipe-line data processing operations. Dr. Nishii
28
29
30 679 and Hirose have been leading spacecraft operations and trajectory. Dr. Hashimoto and
31
32
33
34 680 Murakami are overseeing systematic data processing. Dr. Young has been collecting
35
36
37 681 Venus night side imaging data from IRTF in support of Akatsuki mission. Dr. Ocampo
38
39
40
41 682 has played a key role in the NASA-ISAS/JAXA collaboration for Akatsuki mission and
42
43
44 683 overseeing the Participating Scientist Program.

45
46
47
48 684 **Declarations**

49
50
51 685 **Ethics approval and consent to participate**

52
53
54 686 Not applicable.
55
56
57
58
59
60
61
62
63
64
65

1
2 **687 Acknowledgements**
3

4
5
6 **688** We thank Mr. Patrick Fry (SSEC) for processing the MESSENGER images.
7

8
9 **689 Authors' information**
10

11
12 **690** SSL has been studying Venus with data from Mariner 10, Pioneer Venus and Venus
13
14

15
16 **691** Express missions prior to Akatsuki. Drs. Satoh, Iwagami have been studying Venus
17
18

19
20 **692** with ground based observations as well as spacecraft for a long time. Drs. Lee and
21
22

23 **693** Peralta have experience with Venus Express and ground based observations of Venus.
24
25

26
27 **694** Other co-authors have been responsible for instrument calibration, observation
28
29

30 **695** planning, ground processing and spacecraft operations.
31
32

33
34 **696**
35
36

37
38 **697 References**
39

40
41 **698** Coffeen, D. L., Owen, T. C., & Smith, H. J. (1971). *Venus Cloud Contrasts*.
42

43 **699** Paper presented at the Planetary Atmospheres.
44

45 **700** <http://adsabs.harvard.edu/abs/1971IAUS...40...84C>
46

47 **701** Hawkins, S. E., III, Murchie, S. L., Becker, K. J., Selby, C. M., Turner, F. S.,
48

49 **702** Noble, M. W., Chabot, N. L., Choo, T. H., Darlington, E. H., Denevi, B.
50

51 **703** W., Domingue, D. L., Ernst, C. M., Holsclaw, G. M., Laslo, N. R.,
52

53 **704** McClintock, W. E., Prockter, L. M., Robinson, M. S., Solomon, S. C., &
54

55 **705** Sterner, R. E., II. (2009). *In-flight performance of MESSENGER's*
56

57 **706** *Mercury Dual Imaging System*. Paper presented at the Instruments
58

59 **707** and Methods for Astrobiology and Planetary Missions XII.
60
61
62
63
64
65

- 1 708 <http://adsabs.harvard.edu/abs/2009SPIE.7441E..0ZH>
2
3 709 Limaye, S., Slowik, G., Ansari, A., Smith, D., Mogul, R., & Vaishampayan, P.
4
5 710 (2017). *Short wavelength abedo, contrasts and micro-organisms on*
6
7 711 *Venus*. Paper presented at the EGU General Assembly Conference
8
9 712 Abstracts. <http://adsabs.harvard.edu/abs/2017EGUGA..19.5913L>

10
11 713 **Uncategorized References**

- 12
13 714 Apt, J., Brown, R. A., & Goody, R. M. (1980). The character of the thermal
14
15 715 emission from Venus. *Journal of Geophysical Research*, *85*, 7934-
16
17 716 7940.
- 18 717 Barstow, J. K., Tsang, C. C. C., Wilson, C. F., Irwin, P. G. J., Taylor, F. W.,
19
20 718 McGouldrick, K., Drossart, P., Piccioni, G., & Tellmann, S. (2012).
21
22 719 Models of the global cloud structure on Venus derived from Venus
23
24 720 Express observations. *Icarus*, *217*, 542-560.
- 25 721 Belton, M. J. S., Gierasch, P., Klaasen, K. P., Anger, C. D., Carr, M. H.,
26
27 722 Chapman, C. R., Davies, M. E., Greeley, R., Greenberg, R., & Head, J.
28
29 723 W. (1992). Imaging of Venus from Galileo - Early results and camera
30
31 724 performance. *Advances in Space Research*, *12*, 91-103.
- 32 725 Belton, M. J. S., Gierasch, P. J., Smith, M. D., Helfenstein, P., Schinder, P. J.,
33
34 726 Pollack, J. B., Rages, K. A., Morrison, D., Klaasen, K. P., & Pilcher, C.
35
36 727 B. (1991). Images from Galileo of the Venus cloud deck. *Science*, *253*,
37
38 728 1531-1536.
- 39 729 Blamont, J. E., Young, R. E., Seiff, A., Ragent, B., Sagdeev, R., Linkin, V. M.,
40
41 730 Kerzhanovich, V. V., Ingersoll, A. P., Crisp, D., Elson, L. S., Preston, R.
42
43 731 A., Golitsyn, G. S., & Ivanov, V. N. (1986). Implications of the VEGA
44
45 732 balloon results for Venus atmospheric dynamics. *Science*, *231*, 1422-
46
47 733 1425.
- 48 734 Carlson, R. W., Baines, K. H., Kamp, L. W., Weissman, P. R., Smythe, W. D.,
49
50 735 Ocampo, A. C., Johnson, T. V., Matson, D. L., Pollack, J. B., &
51
52 736 Grinspoon, D. (1991). Galileo infrared imaging spectroscopy
53
54 737 measurements at Venus. *Science*, *253*, 1541-1548.
- 55 738 Dollfus, A. (1975). Venus - Evolution of the upper atmospheric clouds.
56
57 739 *Journal of Atmospheric Sciences*, *32*, 1060-1070.
58
59
60
61
62
63
64
65

- 1 740 Esposito, L. W. (1980). Ultraviolet contrasts and the absorbers near the
2
3 741 Venus cloud tops. *Journal of Geophysical Research*, *85*, 8151-8157.
4
5 742 Esposito, L. W., Knollenberg, R. G., Marov, M. I., Toon, O. B., Turco, R. P.,
6
7 743 Colin, L., Donahue, T. M., & Moroz, V. I. (1983). The clouds are hazes
8
9 744 of Venus. In D. M. Hunten (Ed.), *Venus* (pp. 484-564).
- 10 745 Fukuhara, T., Futaguchi, M., Hashimoto, G. L., Horinouchi, T., Imamura, T.,
11
12 746 Iwagami, N., Kouyama, T., Murakami, S. Y., Nakamura, M.,
13
14 747 Ogohara, K., Sato, M., Sato, T. M., Suzuki, M., Taguchi, M., Takagi,
15
16 748 S., Ueno, M., Watanabe, S., Yamada, M., & Yamazaki, A. (2017). Large
17
18 749 stationary gravity wave in the atmosphere of Venus. *Nature*
19
20 750 *Geoscience*, *10*(2), 85-+. doi:10.1038/Ngeo2873
- 21 751 Fukuhara, T., Taguchi, M., Imamura, T., Nakamura, M., Ueno, M., Suzuki,
22
23 752 M., Iwagami, N., Sato, M., Mitsuyama, K., Hashimoto, G. L.,
24
25 753 Ohshima, R., Kouyama, T., Ando, H., & Futaguchi, M. (2011). LIR:
26
27 754 Longwave Infrared Camera onboard the Venus orbiter Akatsuki.
28
29 755 *Earth, Planets and Space*, *63*(9), 1009-1018.
30
31 756 doi:10.5047/eps.2011.06.019
- 32 757 Garate-Lopez, I., García Muñoz, A., Hueso, R., & Sánchez-Lavega, A. (2015).
33
34 758 Instantaneous three-dimensional thermal structure of the South
35
36 759 Polar Vortex of Venus. *Icarus*, *245*, 16-31.
- 37 760 Garcia, R. F., Drossart, P., Piccioni, G., López-Valverde, M., & Occhipinti, G.
38
39 761 (2009). Gravity waves in the upper atmosphere of Venus revealed by
40
41 762 CO₂ nonlocal thermodynamic equilibrium emissions. *Journal of*
42
43 763 *Geophysical Research (Planets)*, *114*.
- 44 764 Hansen, J. E., & Hovenier, J. W. (1974). Interpretation of the polarization of
45
46 765 Venus. *Journal of Atmospheric Sciences*, *31*, 1137-1160.
- 47 766 Hide, R. (1953). Some experiments on thermal convection in a rotating
48
49 767 liquid. *Quarterly Journal of the Royal Meteorological Society*, *79*(339),
50
51 768 161-161. doi:10.1002/qj.49707933916
- 52 769 Houghton, D. D., & Suomi, V. E. (1978). Information content of satellite
53
54 770 images. *Bulletin of the American Meteorological Society*, *59*(12), 1614-
55
56 771 1617.
- 57
58 772 Hueso, R., Peralta, J., & Sánchez-Lavega, A. (2012). Assessing the long-term
59
60
61
62
63
64
65

- 1 773 variability of Venus winds at cloud level from VIRTIS-Venus Express.
2
3 774 *Icarus*, 217, 585-598.
4
5 775 Ignatiev, N. I., Titov, D. V., Piccioni, G., Drossart, P., Markiewicz, W. J.,
6 776 Cottini, V., Roatsch, T., Almeida, M., & Manoel, N. (2009). Altimetry
7 777 of the Venus cloud tops from the Venus Express observations. *Journal*
8 778 *of Geophysical Research (Planets)*, 114.
9
10 779 Iwagami, N. (2011). Science requirements and description of the 1 μm
11 780 camera onboard the Akatsuki Venus Orbiter. *Earth Planets Space*, 63.
12 781 doi:10.5047/eps.2011.03.007
13
14 782 Keldysh, M. V. (1977). Venus exploration with the Venera 9 and Venera 10
15 783 spacecraft. *Icarus*, 30(4), 605-625. doi:[http://dx.doi.org/10.1016/0019-](http://dx.doi.org/10.1016/0019-1035(77)90085-9)
16 784 [1035\(77\)90085-9](http://dx.doi.org/10.1016/0019-1035(77)90085-9)
17
18 785 Lee, Y. J., Yamazaki, A., Imamura, T., Yamada, M., Watanabe, S., Sato, T.
19 786 M., Ogohara, K., Hashimoto, G. L., & Murakami, S. (2017). Scattering
20 787 Properties of the Venusian Clouds Observed by the UV Imager on
21 788 board Akatsuki. *The Astronomical Journal*, 154.
22
23 789 Limaye, S. S. (1984). Morphology and movements of polarization features on
24 790 Venus as seen in the Pioneer Orbiter Cloud Photopolarimeter data.
25 791 *Icarus*, 57, 362-385.
26
27 792 Limaye, S. S. (1985). Venus atmospheric circulation - Observations and
28 793 implications of the thermal structure. *Advances in Space Research*, 5,
29 794 51-62.
30
31 795 Limaye, S. S., Kossin, J. P., Rozoff, C., Piccioni, G., Titov, D. V., &
32 796 Markiewicz, W. J. (2009). Vortex circulation on Venus: Dynamical
33 797 similarities with terrestrial hurricanes. *Geophysical Research*
34 798 *Letters*, 36.
35
36 799 Luz, D., Berry, D. L., Piccioni, G., Drossart, P., Politi, R., Wilson, C. F.,
37 800 Erard, S., & Nuccilli, F. (2011). Venus's Southern Polar Vortex Reveals
38 801 Precessing Circulation. *Science*, 332(6029), 577-580.
39 802 doi:10.1126/science.1201629
40
41 803 Magurno, D., Maestri, T., Grassi, D., Piccioni, G., & Sindoni, G. (2017).
42 804 Retrieval of Venus' cloud parameters from VIRTIS nightside spectra
43 805 in the latitude band 25°-55°N. *Planetary and Space Science*, 144, 16-

- 1 806 31. doi:<http://dx.doi.org/10.1016/j.pss.2017.06.004>
2
3 807 Markiewicz, W. J., Petrova, E., Shalygina, O., Almeida, M., Titov, D. V.,
4
5 808 Limaye, S. S., Ignatiev, N., Roatsch, T., & Matz, K. D. (2014). Glory on
6
7 809 Venus cloud tops and the unknown UV absorber. *Icarus*, *234*, 200-203.
8
9 810 Markiewicz, W. J., Titov, D. V., Ignatiev, N., Keller, H. U., Crisp, D., Limaye,
10 811 S. S., Jaumann, R., Moissl, R., Thomas, N., Esposito, L., Watanabe,
11 812 S., Fiethe, B., Behnke, T., Szemerey, I., Michalik, H., Perplies, H.,
12 813 Wedemeier, M., Sebastian, I., Boogaerts, W., Hviid, S. F., Dierker, C.,
13 814 Osterloh, B., Böker, W., Koch, M., Michaelis, H., Belyaev, D.,
14 815 Dannenberg, A., Tschimmel, M., Russo, P., Roatsch, T., & Matz, K. D.
15 816 (2007). Venus Monitoring Camera for Venus Express. *Planetary and*
16 817 *Space Science*, *55*, 1701-1711.
17
18 818 Murray, B. C., Belton, M. J. S., Danielson, G. E., Davies, M. E., Gault, D.,
19 819 Hapke, B., O'Leary, B., Strom, R. G., Suomi, V., & Trask, N. (1974).
20 820 Venus: Atmospheric Motion and Structure from Mariner 10 Pictures.
21 821 *Science*, *183*, 1307-1315.
22
23 822 Muto, K., & Imamura, T. (2017). Morphology and temporal variation of the
24 823 polar oval of Venus revealed by VMC/Venus express visible and UV
25 824 images. *Icarus*, *295*, 110-118.
26
27 825 Nakamura, M., Imamura, T., Ishii, N., Abe, T., Kawakatsu, Y., Hirose, C.,
28 826 Satoh, T., Suzuki, M., Ueno, M., Yamazaki, A., Iwagami, N.,
29 827 Watanabe, S., Taguchi, M., Fukuhara, T., Takahashi, Y., Yamada, M.,
30 828 Imai, M., Ohtsuki, S., Uemizu, K., Hashimoto, G. L., Takagi, M.,
31 829 Matsuda, Y., Ogohara, K., Sato, N., Kasaba, Y., Kouyama, T., Hirata,
32 830 N., Nakamura, R., Yamamoto, Y., Horinouchi, T., Yamamoto, M.,
33 831 Hayashi, Y.-Y., Kashimura, H., Sugiyama, K.-i., Sakanoi, T., Ando, H.,
34 832 Murakami, S.-y., Sato, T. M., Takagi, S., Nakajima, K., Peralta, J.,
35 833 Lee, Y. J., Nakatsuka, J., Ichikawa, T., Inoue, K., Toda, T., Toyota, H.,
36 834 Tachikawa, S., Narita, S., Hayashiyama, T., Hasegawa, A., & Kamata,
37 835 Y. (2016). AKATSUKI returns to Venus. *Earth, Planets, and Space*,
38 836 *68*.
39
40 837 Peralta, J., Hueso, R., & Sánchez-Lavega, A. (2007). A reanalysis of Venus
41 838 winds at two cloud levels from Galileo SSI images. *Icarus*, *190*(2),
42
43
44
45
46
47
48
49
50
51
52
53
54
55
56
57
58
59
60
61
62
63
64
65

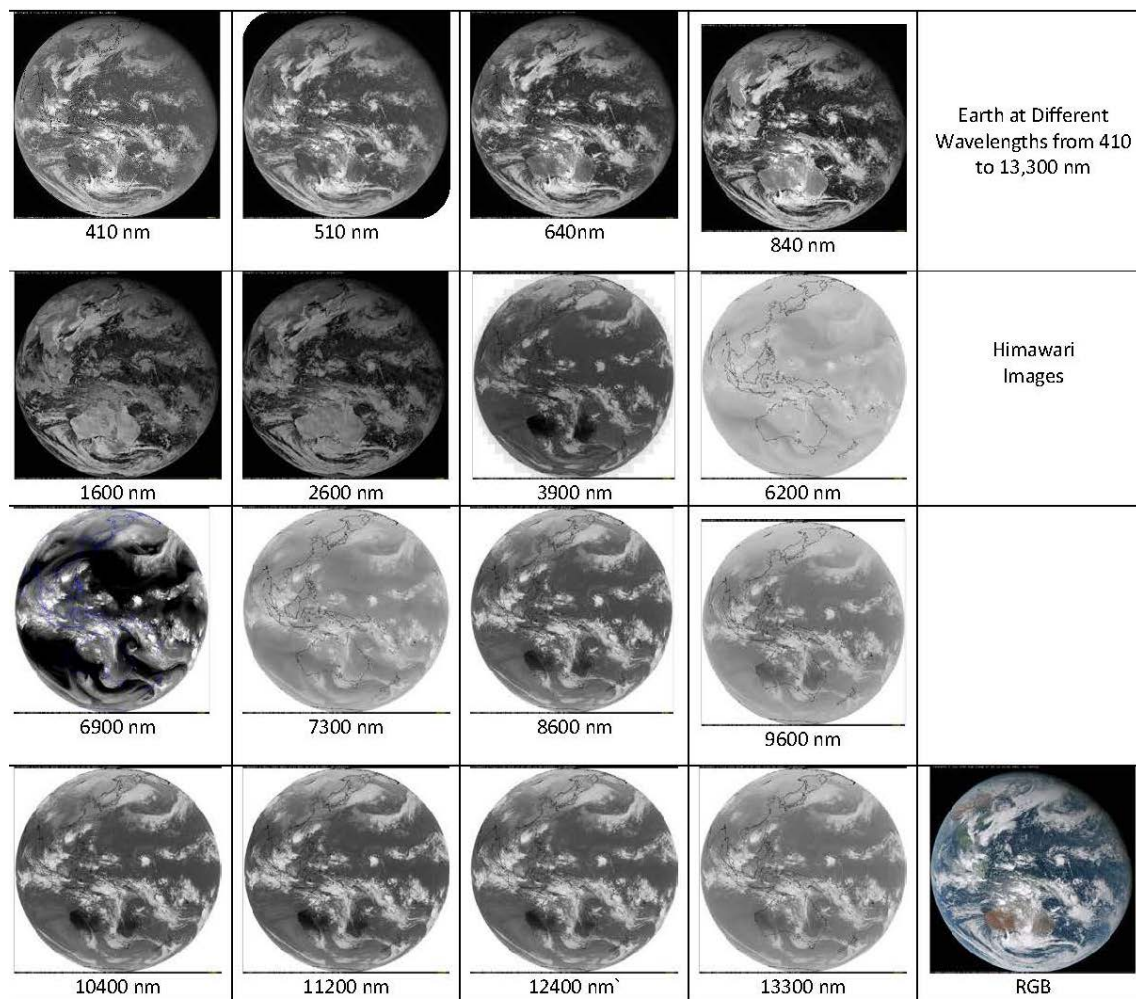
- 1 839 469-477. doi:<http://dx.doi.org/10.1016/j.icarus.2007.03.028>
2
3 840 Peralta, J., Lee, Y. J., McGouldrick, K., Sagawa, H., Sánchez-Lavega, A.,
4
5 841 Imamura, T., Widemann, T., & Nakamura, M. (2017). Overview of
6
7 842 useful spectral regions for Venus: An update to encourage
8
9 843 observations complementary to the Akatsuki mission. *Icarus*, *288*,
10 844 235-239.
- 11 845 Peralta, J., Sánchez-Lavega, A., López-Valverde, M. A., Luz, D., & Machado,
12 846 P. (2015). Venus's major cloud feature as an equatorially trapped
13 847 wave distorted by the wind. *Geophysical Research Letters*, *42*(3), 705-
14 848 711. doi:10.1002/2014GL062280
- 15 849 Piccioni, G., Drossart, P., Sanchez-Lavega, A., Hueso, R., Taylor, F. W.,
16 850 Wilson, C. F., Grassi, D., Zasova, L., Moriconi, M., Adriani, A.,
17 851 Lebonnois, S., Coradini, A., Bezard, B., Angrilli, F., Arnold, G., Baines,
18 852 K. H., Bellucci, G., Benkhoff, J., Bibring, J. P., Blanco, A., Blecka, M.
19 853 I., Carlson, R. W., Di Lellis, A., Encrenaz, T., Erard, S., Fonti, S.,
20 854 Formisano, V., Fouchet, T., Garcia, R., Haus, R., Helbert, J., Ignatiev,
21 855 N. I., Irwin, P. G., Langevin, Y., Lopez-Valverde, M. A., Luz, D.,
22 856 Marinangeli, L., Orofino, V., Rodin, A. V., Roos-Serote, M. C., Saggin,
23 857 B., Stam, D. M., Titov, D., Visconti, G., Zambelli, M., Team, V. I.-V. E.
24 858 T., Ammannito, E., Barbis, A., Berlin, R., Bettanini, C., Boccaccini, A.,
25 859 Bonnelo, G., Bouye, M., Capaccioni, F., Moinelo, A. C., Carraro, F.,
26 860 Cherubini, G., Cosi, M., Dami, M., De Nino, M., Del Vento, D., Di
27 861 Giampietro, M., Donati, A., Dupuis, O., Espinasse, S., Fabbri, A.,
28 862 Fave, A., Veltroni, I. F., Filacchione, G., Garceran, K., Ghomchi, Y.,
29 863 Giustini, M., Gondet, B., Hello, Y., Henry, F., Hofer, S., Huntzinger,
30 864 G., Kachlicki, J., Knoll, R., Driss, K., Mazzoni, A., Melchiorri, R.,
31 865 Mondello, G., Monti, F., Neumann, C., Nuccilli, F., Parisot, J., Pasqui,
32 866 C., Perferi, S., Peter, G., Piacentino, A., Pompei, C., Reess, J. M.,
33 867 Rivet, J. P., Romano, A., Russ, N., Santoni, M., Scarpelli, A., Semery,
34 868 A., Soufflot, A., Stefanovitch, D., Suetta, E., Tarchi, F., Tonetti, N.,
35 869 Tosi, F., & Ulmer, B. (2007a). South-polar features on Venus similar to
36 870 those near the north pole. *Nature*, *450*(7170), 637-640.
37 871 doi:10.1038/nature06209
38
39
40
41
42
43
44
45
46
47
48
49
50
51
52
53
54
55
56
57
58
59
60
61
62
63
64
65

- 1 872 Piccioni, G., Drossart, P., Suetta, E., Cosi, M., Amannito, E., Barbis, A.,
2
3 873 Berlin, R., Bocaccini, A., Bonello, G., Bouyé, M., Capaccioni, F.,
4
5 874 Cherubini, G., Dami, M., Dupuis, O., Fave, A., Filacchione, G., Hello,
6
7 875 Y., Henry, F., Hofer, S., Huntzinger, G., Melchiorri, R., Parisot, J.,
8
9 876 Pasqui, C., Peter, G., Pompei, C., Rèess, J. M., Semery, A., Soufflot, A.,
10
11 877 Adriani, A., Angrilli, F., Arnold, G., Baines, K., Bellucci, G., Benkhoff,
12
13 878 J., Bezdard, B., Bibring, J.-P., Blanco, A., Blecka, M. I., Carlson, R.,
14
15 879 Coradini, A., Di Lellis, A., Encrenaz, T., Erard, S., Fonti, S.,
16
17 880 Formisano, V., Fouchet, T., Garcia, R., Haus, R., Helbert, J., Ignatiev,
18
19 881 N. I., Irwin, P., Langevin, Y., Lebonnois, S., Lopez Valverde, M. A.,
20
21 882 Luz, D., Marinangeli, M., Orofino, V., Rodin, A. V., Roos-Serote, M. C.,
22
23 883 Saggin, B., Sanchez-Lavega, A., Stam, B. M., Taylor, F., Titov, D.,
24
25 884 Visconti, G., Zambelli, M., Drossart, P., Suetta, E., Cosi, M.,
26
27 885 Amannito, E., Barbis, A., Berlin, R., Bocaccini, A., Bonello, G., Bouyé,
28
29 886 M., Capaccioni, F., Cherubini, G., Dami, M., Dupuis, O., Fave, A.,
30
31 887 Filacchione, G., Hello, Y., Henry, F., Hofer, S., Huntzinger, G.,
32
33 888 Melchiorri, R., Parisot, J., Pasqui, C., Peter, G., Pompei, C., Rèess, J.
34
35 889 M., Semery, A., Soufflot, A., Adriani, A., Angrilli, F., Arnold, G.,
36
37 890 Baines, K., Bellucci, G., Benkhoff, J., Bezdard, B., Bibring, J.-P.,
38
39 891 Blanco, A., Blecka, M. I., Carlson, R., Coradini, A., Di Lellis, A.,
40
41 892 Encrenaz, T., Erard, S., Fonti, S., Formisano, V., Fouchet, T., Garcia,
42
43 893 R., Haus, R., Helbert, J., Ignatiev, N. I., Irwin, P., Langevin, Y.,
44
45 894 Lebonnois, S., Lopez Valverde, M. A., Luz, D., Marinangeli, M.,
46
47 895 Orofino, V., Rodin, A. V., Roos-Serote, M. C., Saggin, B., Sanchez-
48
49 896 Lavega, A., Stam, B. M., Taylor, F., Titov, D., Visconti, G., & Zambelli,
50
51 897 M. (2007b, December 1, 2007). *VIRTIS: The Visible and Infrared*
52
53 898 *Thermal Imaging Spectrometer*. Paper presented at the ESA Special
54
55 899 Publication.
56
57 900 Read, P. L. (2011). Dynamics and circulation regimes of terrestrial planets.
58
59 901 *Planetary and Space Science*, 59(10), 900-914.
60
61 902 doi:<http://dx.doi.org/10.1016/j.pss.2010.04.024>
62
63 903 Robinson, M. S., Harch, A. P., Hawkins, S. E., Head, J. W., Kang, H., Laslo,
64
65 904 N. R., Murchie, S. L., Prockter, L. M., Solomon, S. C., Vaughan, R. M.,

- 1 905 & Watters, T. R. (2007). MDIS Observations from the Second
2
3 906 MESSENGER Venus Flyby. *AGU Fall Meeting Abstracts*, 33.
4
5 907 Ross, F. E. (1927). Photographs of Venus. *Popular Astronomy*, 35, 492.
6
7 908 Rossow, W. B., del Genio, A. D., Limaye, S. S., & Travis, L. D. (1980). Cloud
8
9 909 morphology and motions from Pioneer Venus images. *Journal of*
10
11 910 *Geophysical Research*, 85, 8107-8128.
12
13 911 Sagdeev, R. Z., Kerzhanovich, V. V., Kogan, L. R., Kostenko, V. I., Linkin, V.
14
15 912 M., Matveenko, L. I., Nazirov, R. R., Pogrebenko, S. V., Strukov, I. A.,
16
17 913 Preston, R., Purcell, G. H., Jr., Hildebrand, C., Blamont, J., Boloh, L.,
18
19 914 Laurans, G., Spencer, R. E., Golt, J., Grishmanovskii, V. A., Kozlov, A.
20
21 915 N., Molotov, E. P., Yatskiv, Y. S., Martirosyan, R. M., Moiseev, I. G.,
22
23 916 Rogers, A. E. E., Biraud, F., Boichaut, A., Kaufmann, P., Mezger, P.,
24
25 917 Schwarz, R., Ronang, B. O., & Nicolson, G. (1990). Measurements of
26
27 918 the Dynamics of Air Mass Motion in the Venus Atmosphere with
28
29 919 Balloon Probes - VEGA Project. *Soviet Astronomy Letters*, 16, 357.
30
31 920 Satoh, T., Nakamura, M., Ueno, M., Uemizu, K., Suzuki, M., Imamura, T.,
32
33 921 Kasaba, Y., Yoshida, S., & Kimata, M. (2016). Development and in-
34
35 922 flight calibration of IR2: 2- μ m camera onboard Japan's Venus orbiter,
36
37 923 Akatsuki. *Earth, Planets and Space*, 68(1), 74. doi:10.1186/s40623-
38
39 924 016-0451-z
40
41 925 Smith, M. D., & Gierasch, P. J. (1996). Global-Scale Winds at the Venus
42
43 926 Cloud-Top Inferred from Cloud Streak Orientations. *Icarus*, 123, 313-
44
45 927 323.
46
47 928 Soret, L., Gérard, J.-C., Piccioni, G., & Drossart, P. (2014). Time variations
48
49 929 of O₂(a¹ Δ) nightglow spots on the Venus nightside and dynamics of
50
51 930 the upper mesosphere. *Icarus*, 237, 306-314.
52
53 931 Sugata, S., & Yoden, S. (1993). A Numerical Study on Regime Transitions of
54
55 932 the Rotating Annulus Flow with a Semi-Spectral Model. *Journal of*
56
57 933 *the Meteorological Society of Japan. Ser. II*, 71(4), 491-501.
58
59 934 doi:10.2151/jmsj1965.71.4_491
60
61 935 Suomi, V. E., & Limaye, S. S. (1978). Venus - Further evidence of vortex
62
63 936 circulation. *Science*, 201, 1009-1011.
64
65 937 Svedhem, H., Titov, D. V., McCoy, D., Lebreton, J.-P., Barabash, S., Bertaux,

- 1 938 J.-L., Drossart, P., Formisano, V., Häusler, B., Korablev, O.,
2
3 939 Markiewicz, W. J., Nevejans, D., Pätzold, M., Piccioni, G., Zhang, T.
4
5 940 L., Taylor, F. W., Lellouch, E., Koschny, D., Witasse, O., Eggel, H.,
6
7 941 Warhaut, M., Accomazzo, A., Rodriguez-Canabal, J., Fabrega, J.,
8
9 942 Schirmann, T., Clochet, A., & Coradini, M. (2007). Venus Express—
10 943 The first European mission to Venus. *Planetary and Space Science*,
11 944 *55*, 1636-1652.
- 13 945 Takahashi, Y., Yoshida, J., Yair, Y., Imamura, T., & Nakamura, M. (2008).
14 946 Lightning Detection by LAC Onboard the Japanese Venus Climate
15 947 Orbiter, Planet-C. *Space Science Reviews*, *137*(1), 317-334.
16
17 948 doi:10.1007/s11214-008-9400-x
18
19 949 Taylor, F. W. (1980). Structure and meteorology of the middle atmosphere of
20 950 Venus: infrared remote sensing from the Pioneer orbiter. *J. Geophys.*
21 951 *Res.*, *85*, 7963-8006.
- 23 952 Taylor, F. W., Beer, R., Chahine, M. T., Diner, D. J., Elson, L. S., Haskins, R.
24 953 D., McCleese, D. J., Martonchik, J. V., Reichley, P. E., Bradley, S. P.,
25 954 Delderfield, J., Schofield, J. T., Farmer, C. B., Froidevaux, L., Leung,
26 955 J., Coffey, M. T., & Gille, J. C. (1980). Structure and meteorology of
27 956 the middle atmosphere of Venus Infrared remote sensing from the
28 957 Pioneer orbiter. *Journal of Geophysical Research*, *85*, 7963-8006.
- 30 958 Titov, D. V., Markiewicz, W. J., Ignatiev, N. I., Song, L., Limaye, S. S.,
31 959 Sanchez-Lavega, A., Hesemann, J., Almeida, M., Roatsch, T., Matz,
32 960 K.-D., Scholten, F., Crisp, D., Esposito, L. W., Hviid, S. F., Jaumann,
33 961 R., Keller, H. U., & Moissl, R. (2012). Morphology of the cloud tops as
34 962 observed by the Venus Express Monitoring Camera. *Icarus*, *217*, 682-
35 963 701.
- 37 964 Travis, L. D. (1975). On the origin of ultraviolet contrasts on Venus.
38 965 *Journal of Atmospheric Sciences*, *32*, 1190-1200.
- 40 966 Travis, L. D., Coffeen, D. L., Hansen, J. E., Kawabata, K., Lacis, A. A., Lane,
41 967 W. A., Limaye, S. S., & Stone, P. H. (1979a). Orbiter cloud
42 968 photopolarimeter investigation. *Science*, *203*, 781-785.
- 44 969 Travis, L. D., Coffeen, D. L., Hansen, J. E., Kawabata, K., Lacis, A. A., Lane,
45 970 W. A., Rossow, W. B., del Genio, A. D., Limaye, S. S., & Stone, P. H.

- 1 971 (1979b). Images of the Venus Clouds from the Pioneer Orbiter
2
3 972 Photopolarimeter. *EOS Transactions*, 60.
4
5 973 Tsang, C. C. C., Taylor, F. W., Wilson, C. F., Liddell, S. J., Irwin, P. G. J.,
6
7 974 Piccioni, G., Drossart, P., & Calcutt, S. B. (2009). Variability of CO
8
9 975 concentrations in the Venus troposphere from Venus Express/VIRTIS
10
11 976 using a Band Ratio Technique. *Icarus*, 201, 432-443.
12
13 977 Wilson, C. F., Guerlet, S., Irwin, P. G. J., Tsang, C. C. C., Taylor, F. W.,
14
15 978 Carlson, R. W., Drossart, P., & Piccioni, G. (2008). Evidence for
16
17 979 anomalous cloud particles at the poles of Venus. *Journal of*
18
19 980 *Geophysical Research: Planets*, 113(E9), n/a-n/a.
20
21 981 doi:10.1029/2008JE003108
22
23
24
25
26
27
28
29
30
31
32
33
34
35
36
37
38
39
40
41
42
43
44
45
46
47
48
49
50
51
52
53
54
55
56
57
58
59
60
61
62
63
64
65



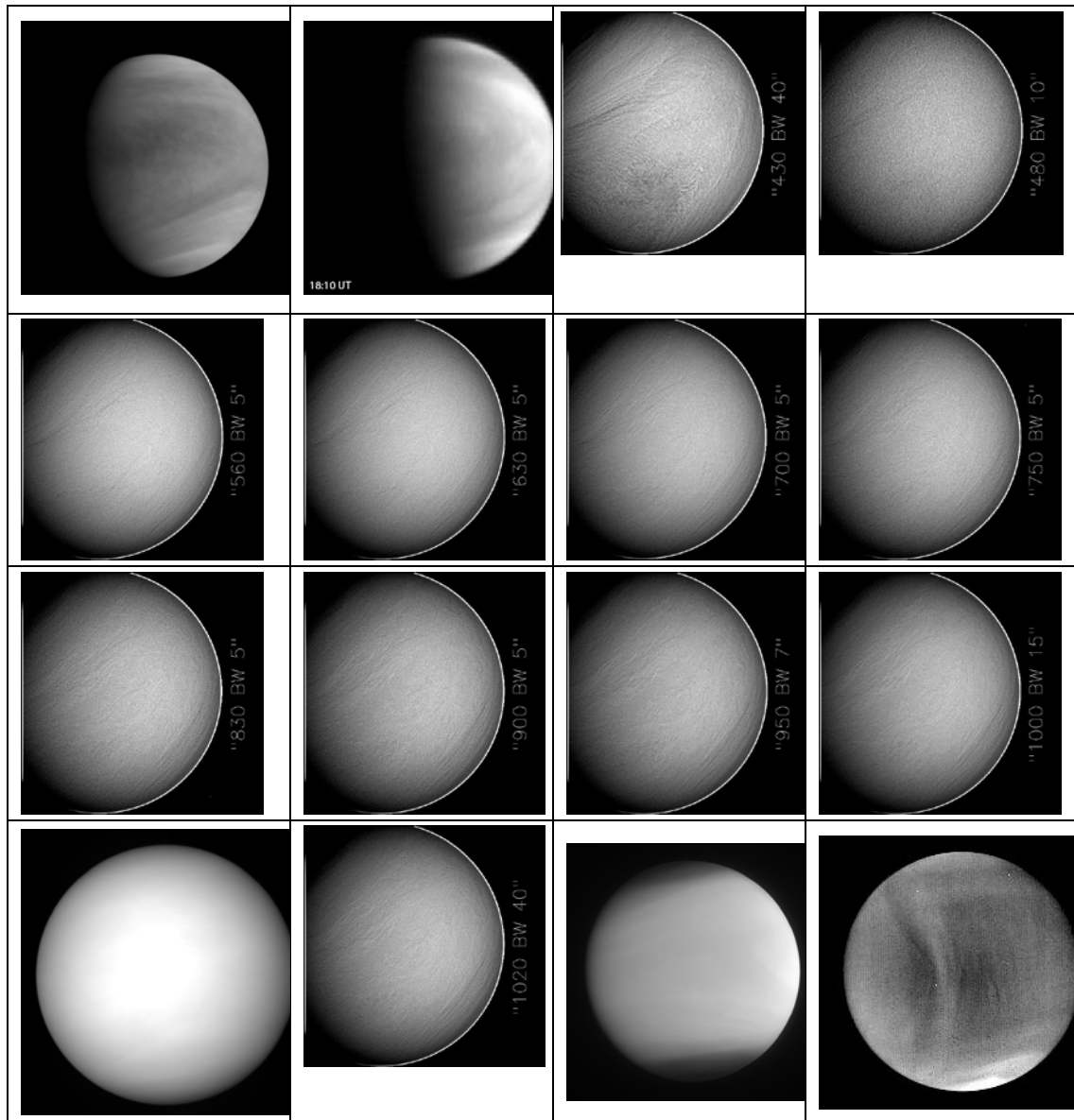
1

2 Figure 1. An example of Earth clouds imaged by Himawari weather satellite (27

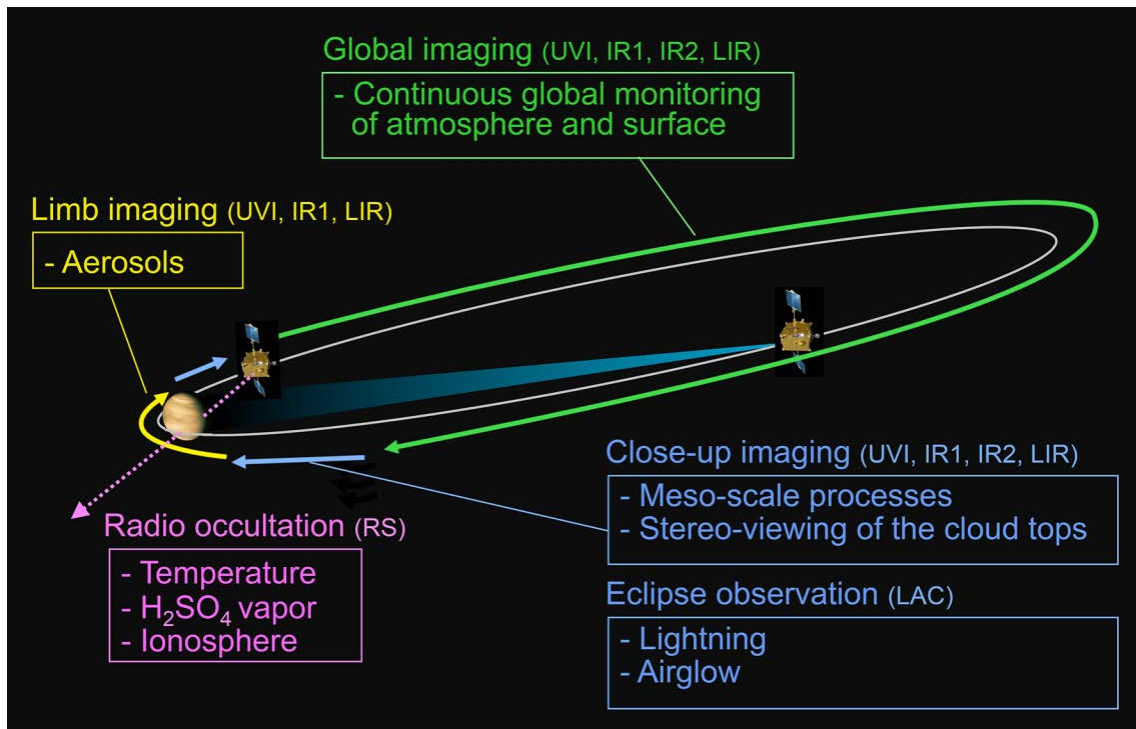
3 December 2016, 04:00 UT) in geosynchronous orbit at sixteen different wavelengths.

4 The cloud features show a great deal of similarity from 410 nm to 13.3 μm .

5



6 Figure 2. Venus at different wavelengths imaged by Akatsuki and MESSENGER
 7 cameras. Top row – (left to right) 283 nm, 365 nm (UVI Akatsuki), 430 nm, and 480 nm
 8 (MESSENGER –MDIS/WA). Second row – 560, 630, 700 and 750 nm (MDIS-WA).
 9 Third row- 830, 900, 950 and 1000 nm (MDIS-WA). Bottom row – 900 nm (IR1) 1020
 10 nm (MDIS-WA), 2020 nm (IR2) and 10-14 μm (LIR). All MESSENGER images have
 11 been high pass filtered to bring out the very low contrast features.



12

13 Figure 3. Schematic view of orbit of Akatsuki orbiter around Venus and general

14 observing plan during the ~ 10.5-day orbit.

15

16

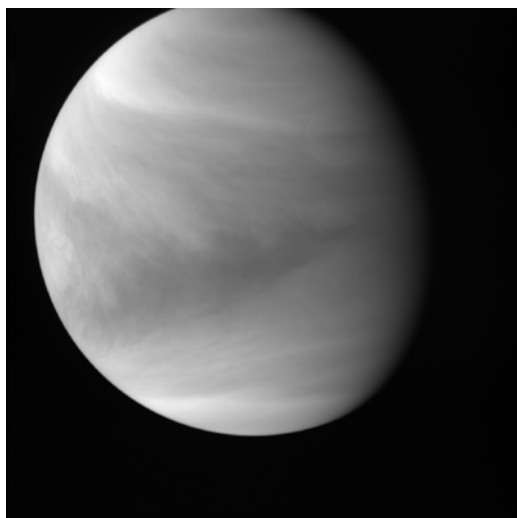
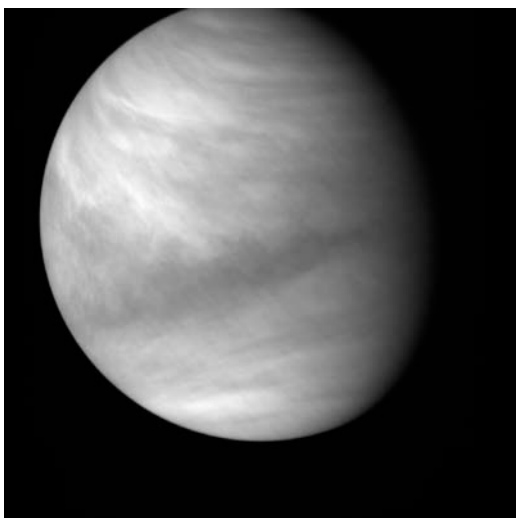
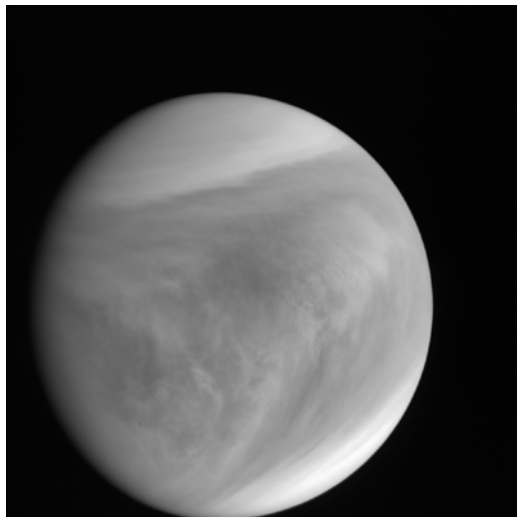
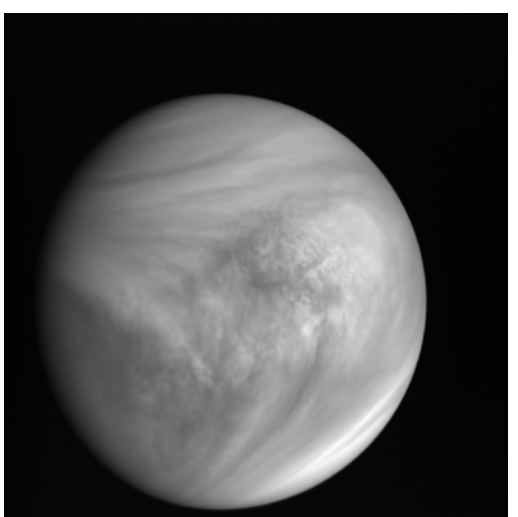
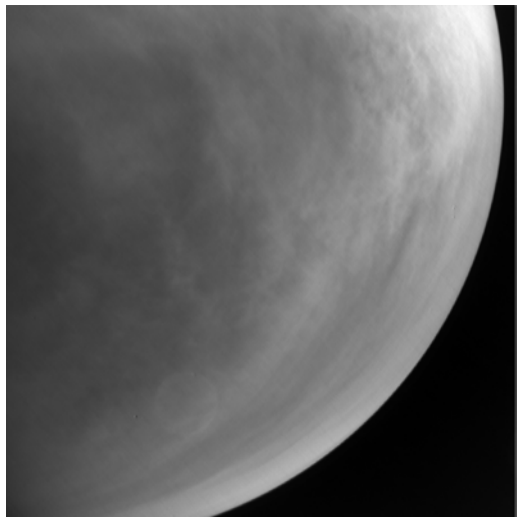
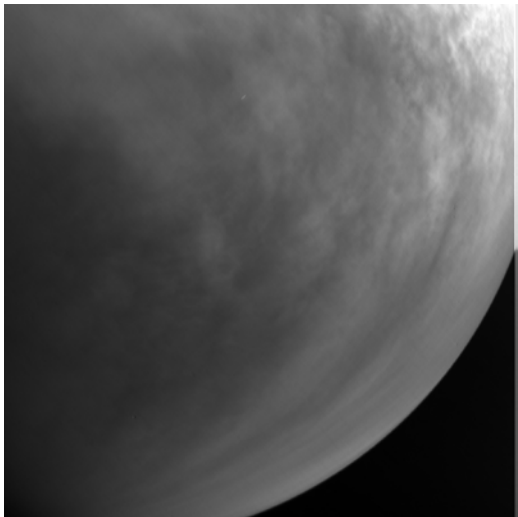
17

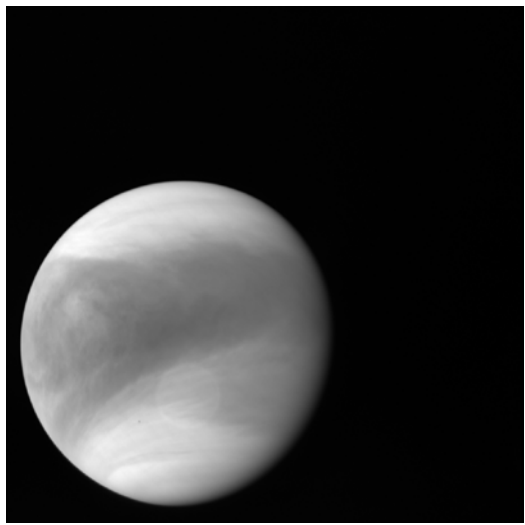
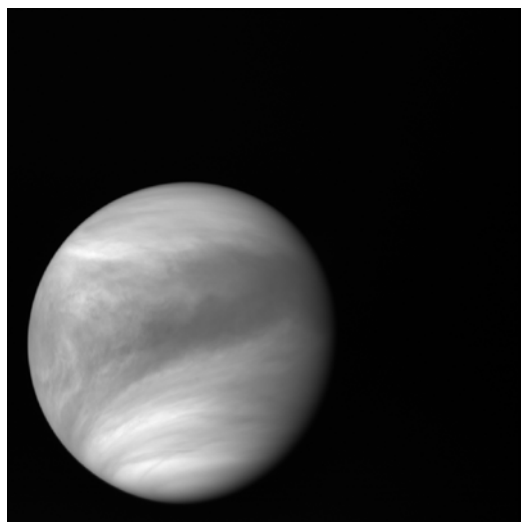
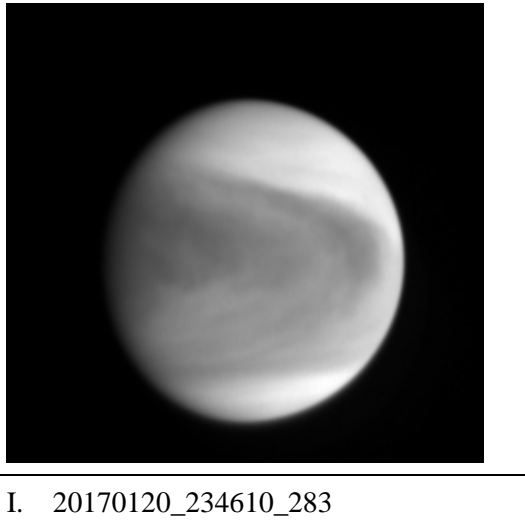
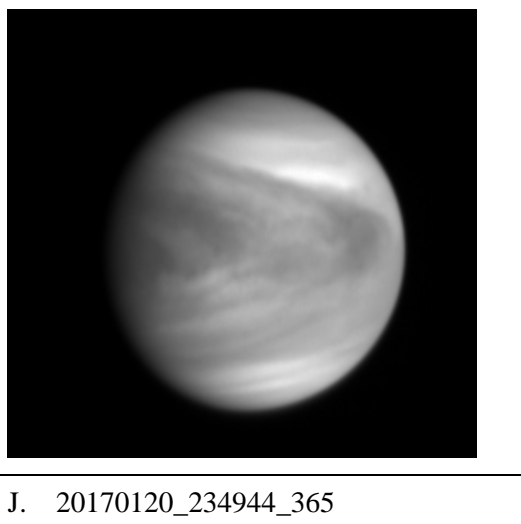
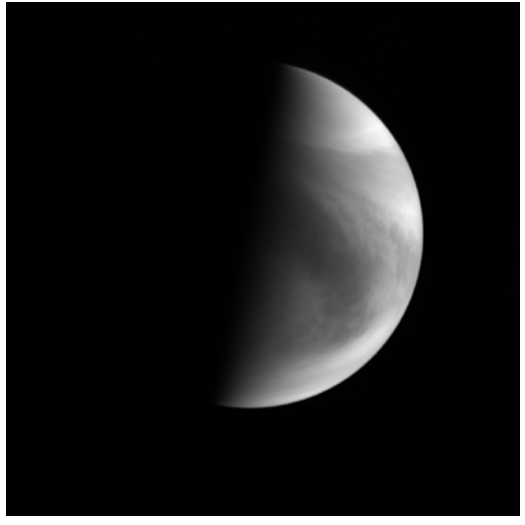
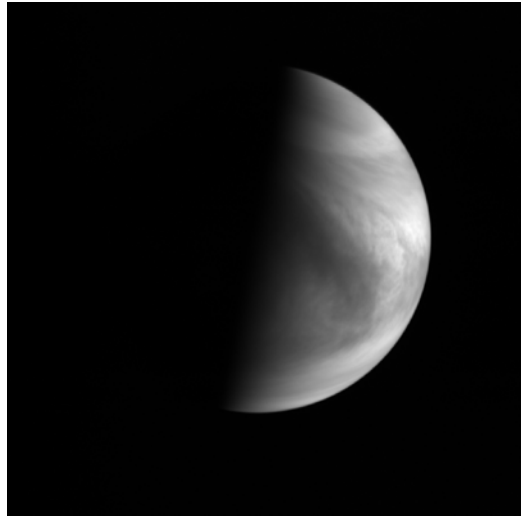
18

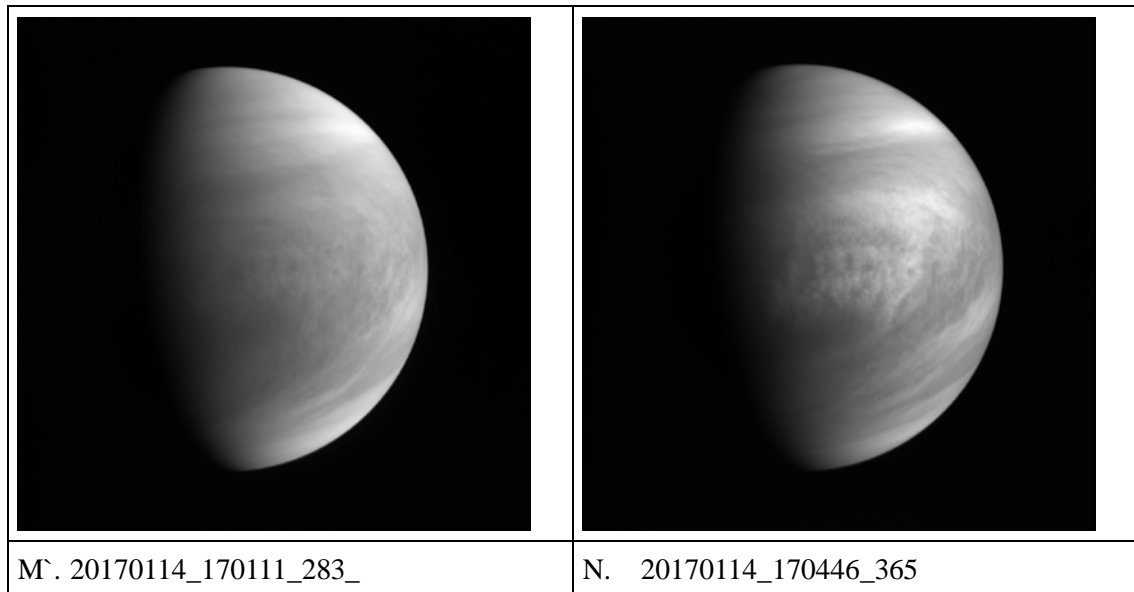
19

20

21

	
A. 20161120_132347_283	B. 20161120_132721_365
	
C. uvi_20161223_101110_283	D. uvi_20161223_101445_365
	
E. uvi_20161223_141058_283	F. uvi_20161223_141334_365

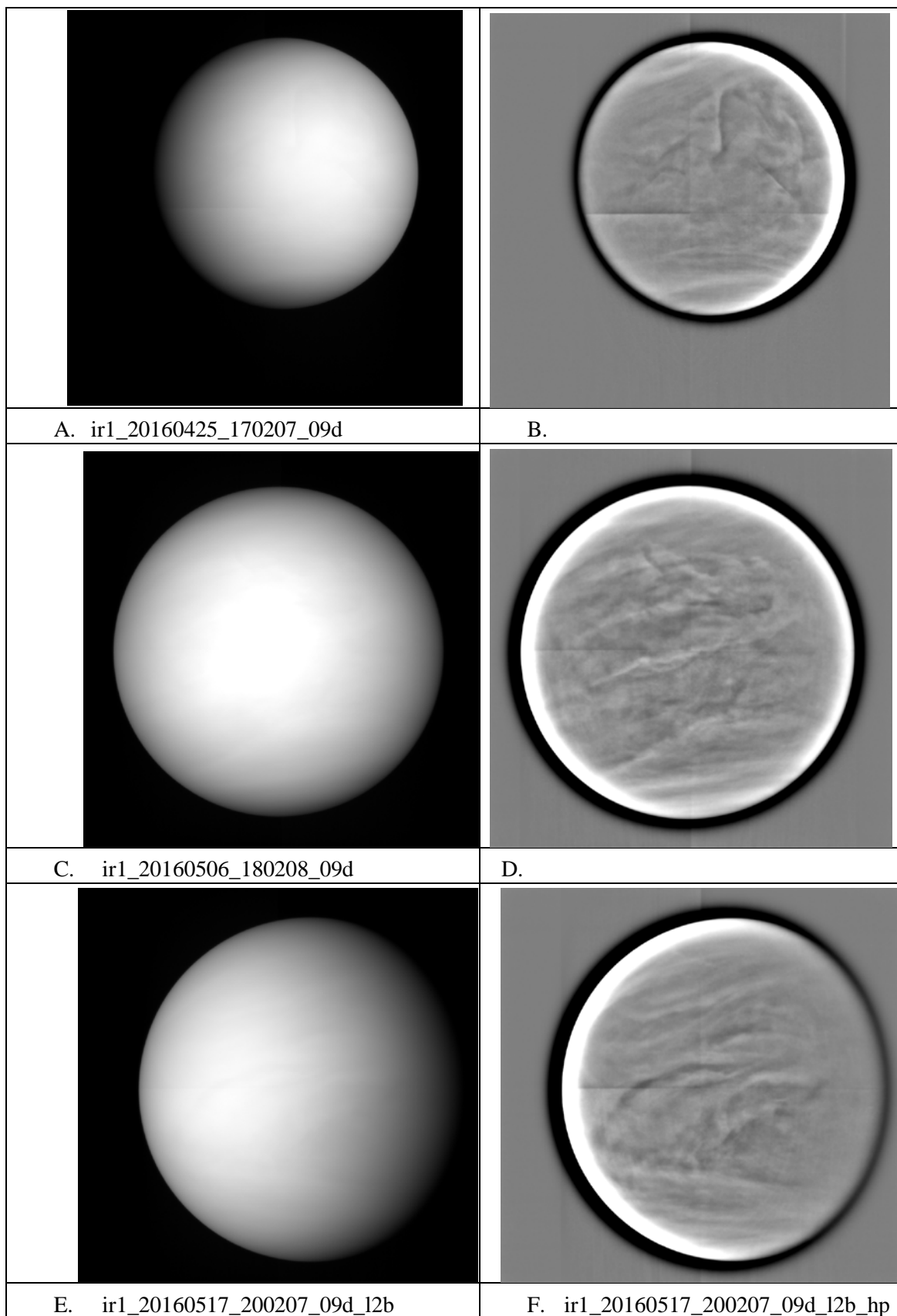
	
G. uvi_20170115_083111_283	H. uvi_20170115_083445_365
	
I. 20170120_234610_283	J. 20170120_234944_365
	
K. 20170205_180111_283	L. 20170205_180445_365



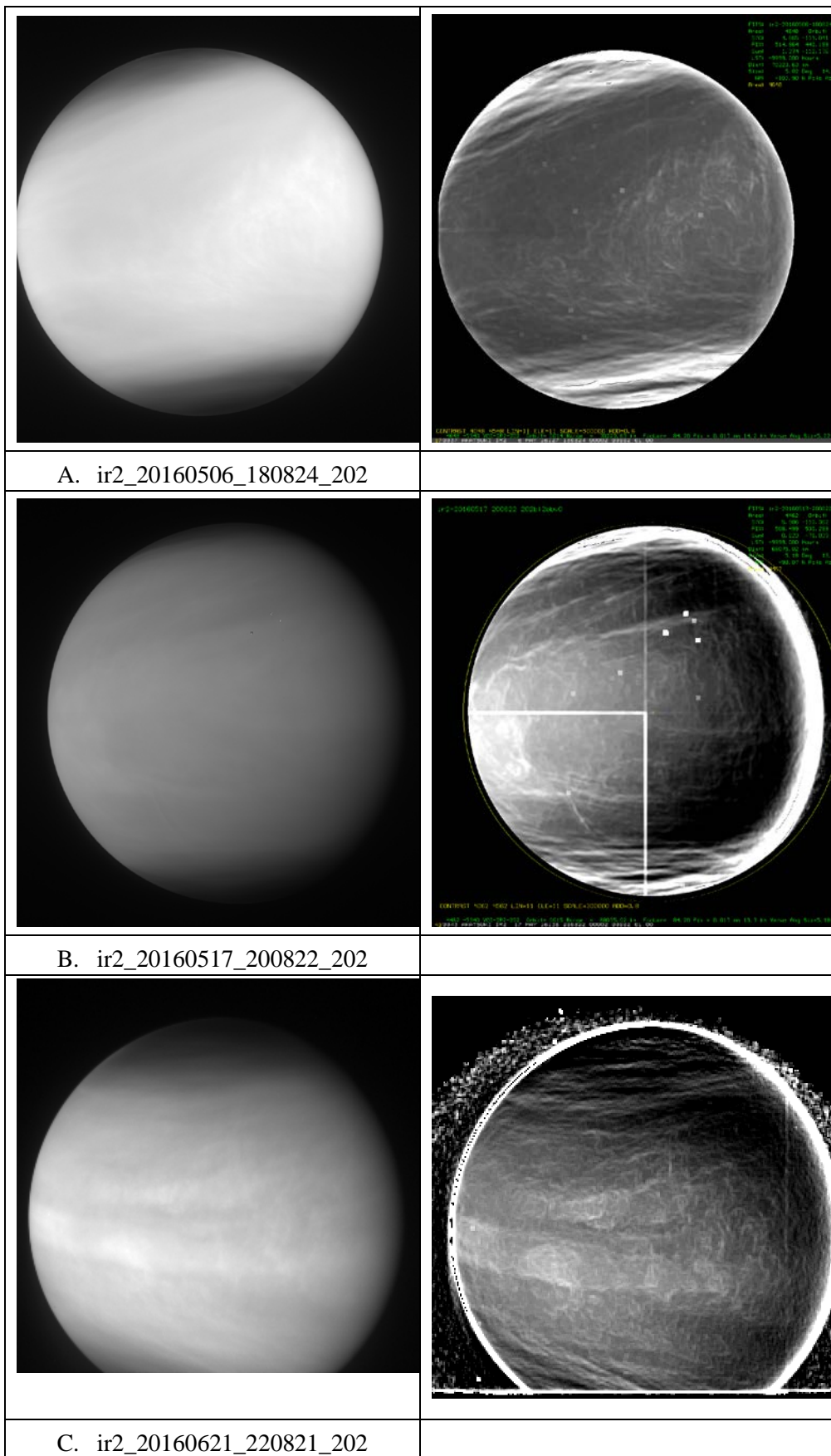
22

23 Figure 4. Selected images from UVI camera taken from the 283 nm (left column) and
24 365 nm (right column) showing representative features seen in the collection of images
25 taken from Akatsuki. Generally images taken through the 283 nm and 365 nm filters
26 are very close together in time. Simultaneous imaging is not possible from the camera
27 in the two filters, the time difference between them is about 150 seconds, so only at very
28 close approach to Venus is overlap between 283 and 365 nm images is not possible due
29 to the fast movement of Akatsuki in its orbit .

30

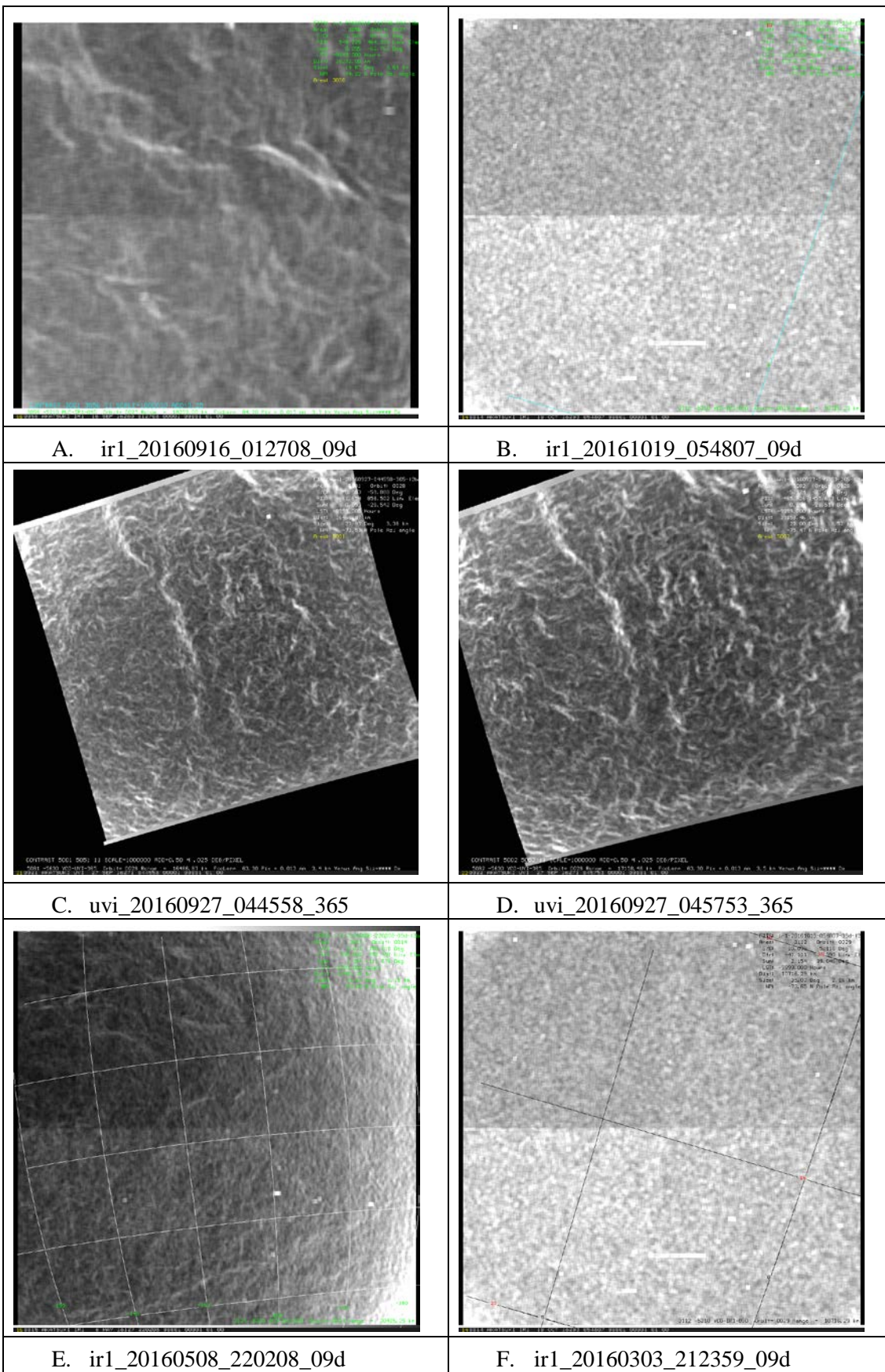


32 Figure 5. Selected global images taken at $0.97\ \mu\text{m}$ on the day side from the IR1 camera.
33 Calibrated images are shown in the left column and high pass filtered versions are shown in the
34 column on the right. Contrasts are much lower at $900\ \text{nm}$ than at $365\ \text{nm}$ as expected and the
35 spatial scales and morphology are similar, but the global organization is not as apparent as at
36 $365\ \text{nm}$. In images taken closer to the planet which show the planet at $\sim 2\text{-}6\ \text{km/pixel}$ scale,
37 muted contrasts are seen. This is opposite to what is observed at the ultraviolet wavelengths
38 where the contrasts are much weaker on the very small spatial scales of $\sim 5\text{-}10\ \text{km}$ and are seen
39 only over scales about 10 times larger. Because Akatsuki spends only a short time at close
40 proximity to Venus in its highly elliptic orbit, global coverage at high spatial resolution is not
41 feasible as the field of view of the camera is too small compared to the angular size of the planet
42 and Akatsuki moves relative to the planet very quickly.
43

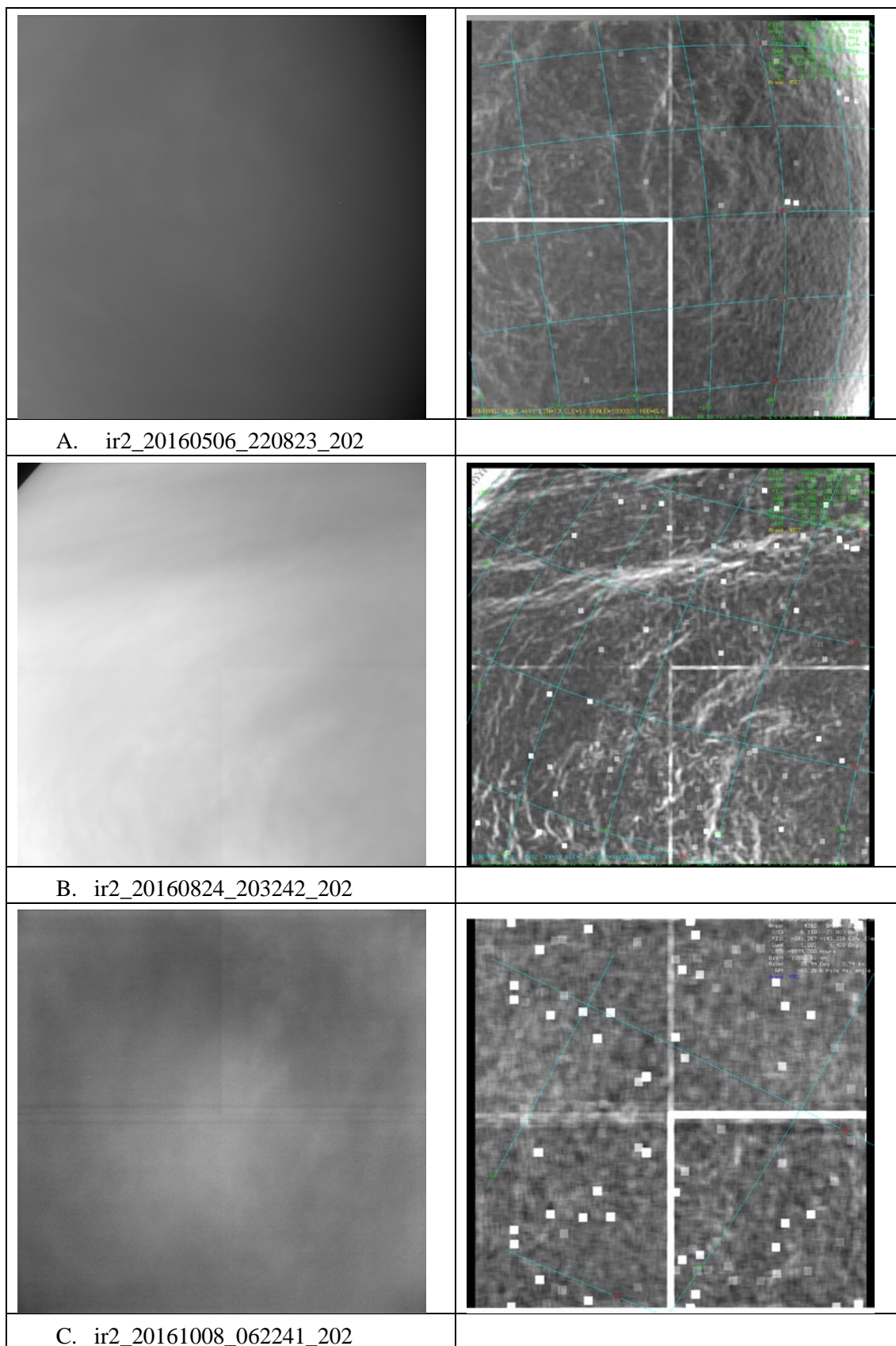


44 Figure 6. A sample of full disk day side 2.02 μm images from the IR2 camera. The
45 calibrated versions are shown in the left column and contrast filtered versions are shown
46 in the right column to bring out the very low contrast details present in the data.

47 A close up view of Venus, one the highest resolution ones from Akatsuki orbiter on the
48 day side at ultraviolet and 2.02 μm is shown in Figure 9. The scale is almost 6 km per
49 pixel. Contrasts are seen on scales of about 100 km at 283 and 365 nm, and perhaps on a
50 little larger scale at 2.02 μm , but it may be due to the lower level of contrasts and the
51 dynamic range of the data.

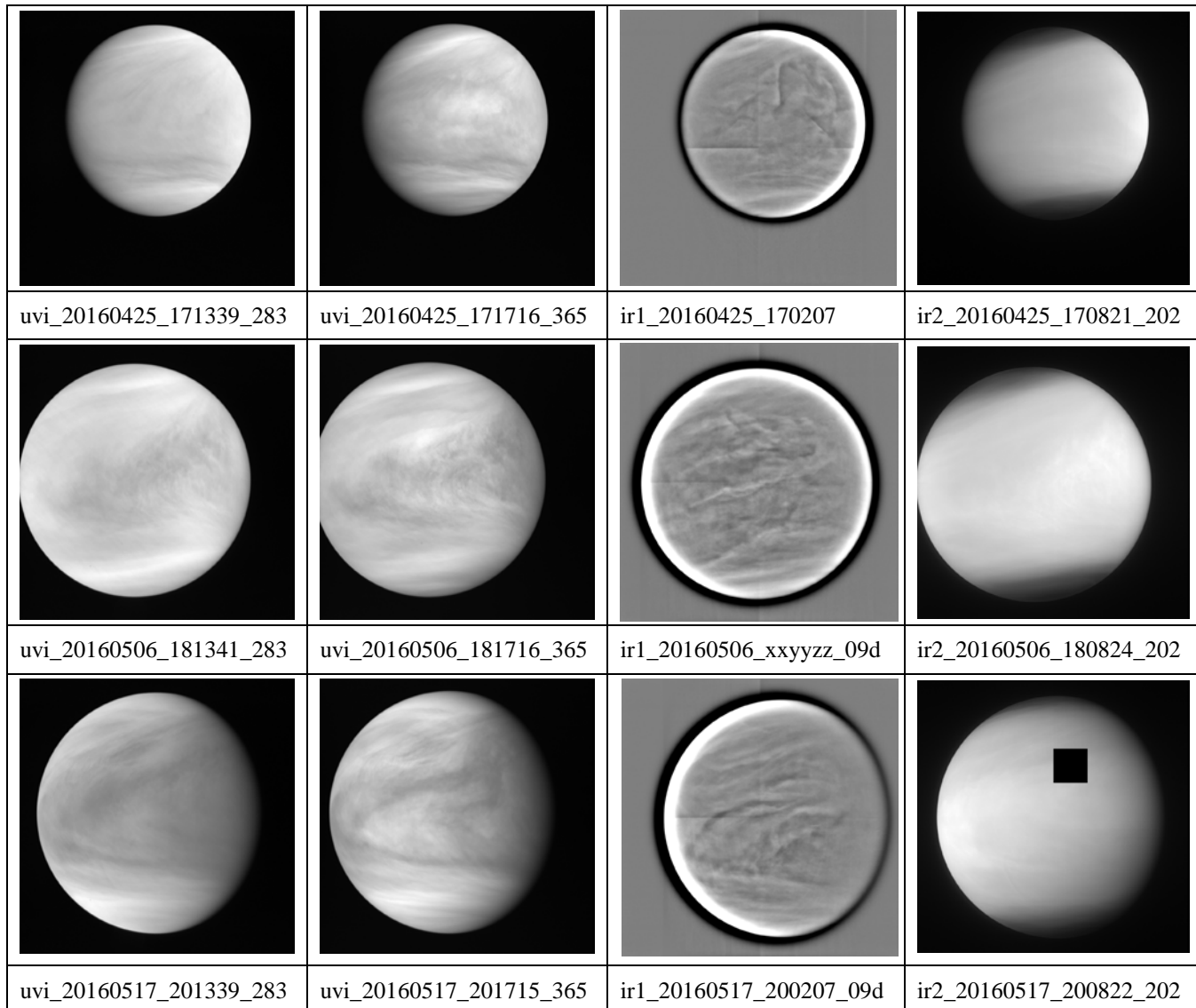


52 Figure 7a. High resolution images from IR1 camera (top and bottom rows) in the 09d
53 filter and two UVI images taken through the 365 nm filter (middle row). Only contrast
54 filtered images are shown to emphasize the details.

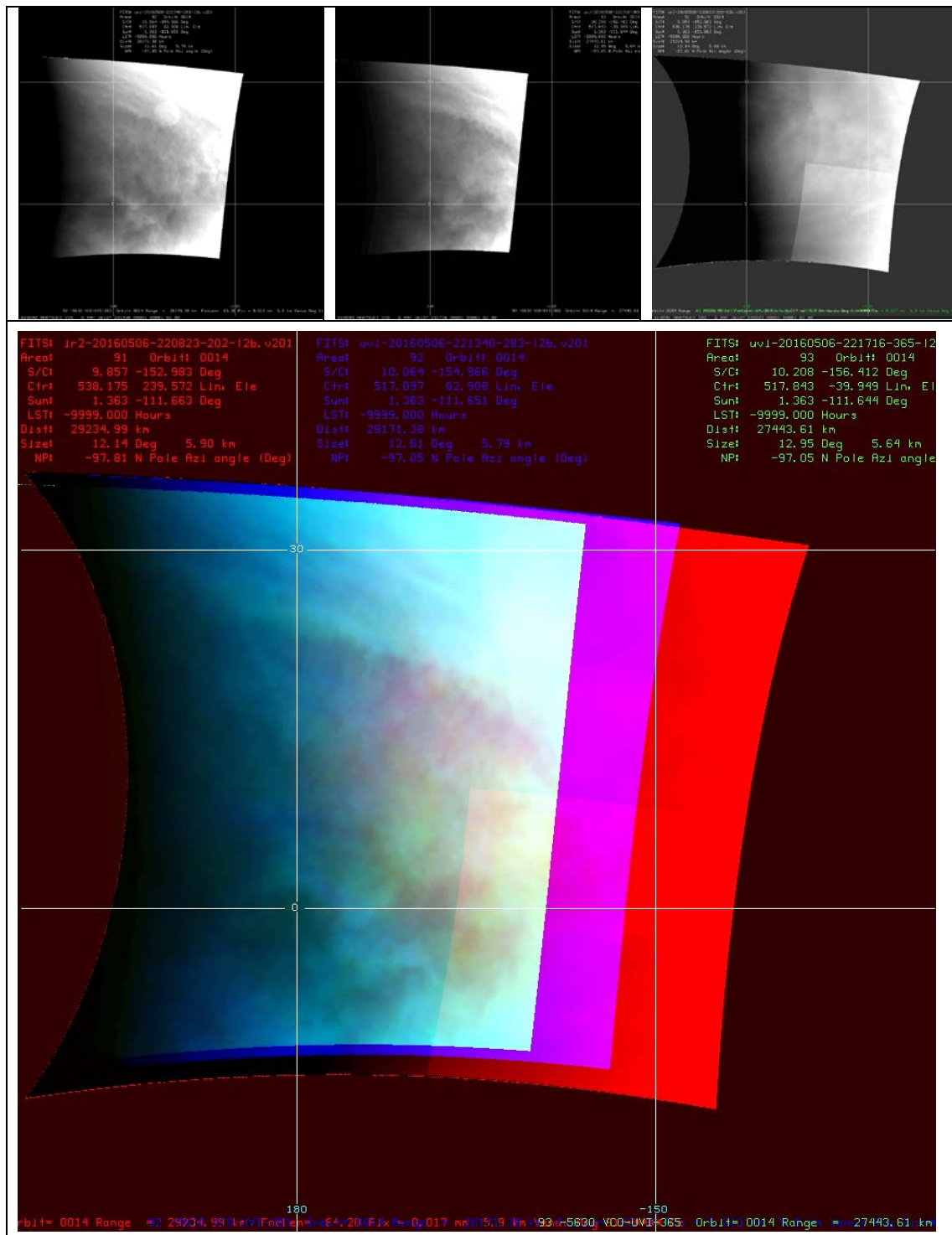


55 Figure 7b. A sample of high spatial resolution images of the day side 2.02 μm images

56 from the IR2 camera, each at a pixel scale of approximately 5 km. Very subtle sinuous
57 or string like structures are seen with widths of about 20-40 km and with variable
58 lengths and inclinations to latitude circles are seen in A and B. Image B shows bow like
59 waves seen at ultraviolet wavelengths, often seen with the Y-feature. Image C is
60 devoid of such patterns, but instead shows a bright area surrounded by a poorly defined
61 dark ring which is suggestive of the glory feature seen on Venus at other wavelengths
62 but the phase angle is far from 0° and is believed to be due to the electronic noise due to
63 the cross-talk between the readout of the four quadrants of the image (Satoh et al., this
64 issue).

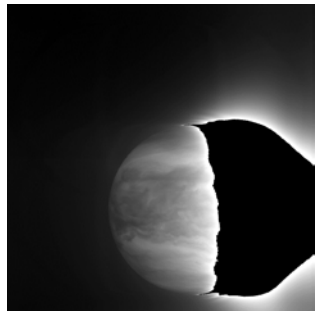
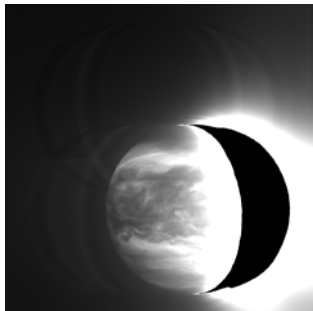
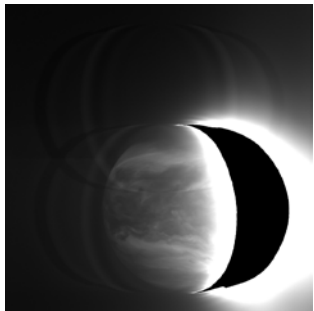
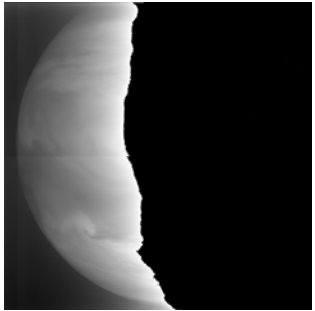
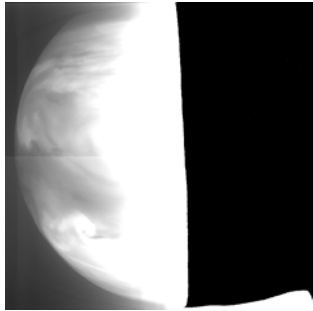
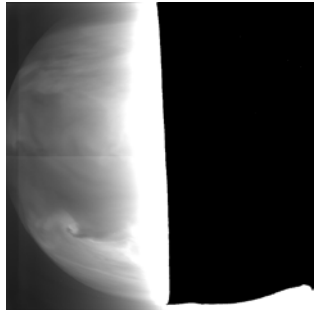
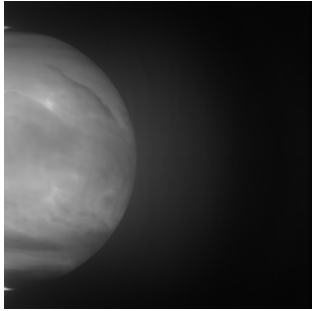
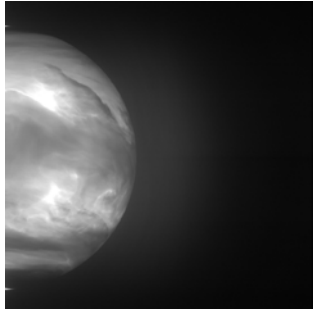
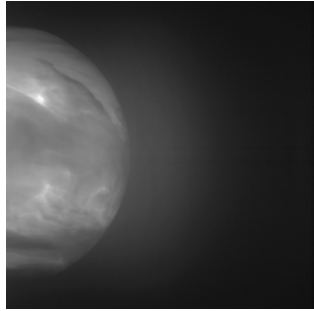
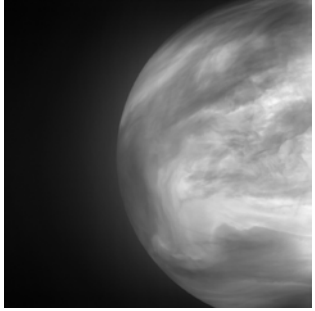
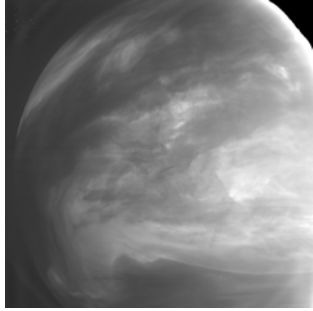
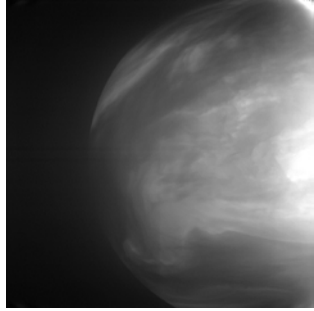


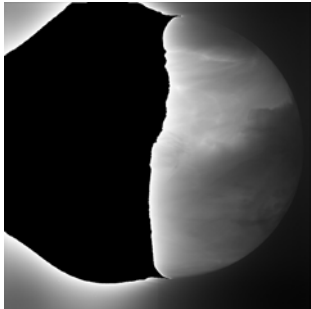

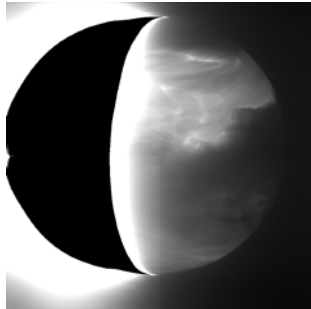
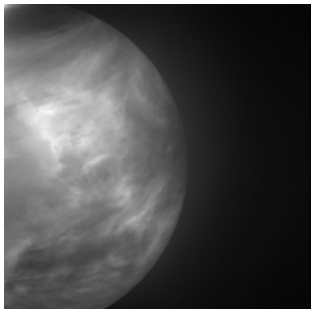
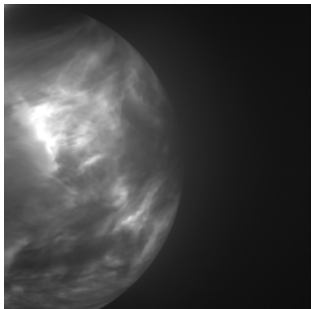
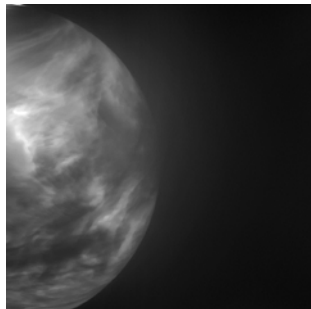
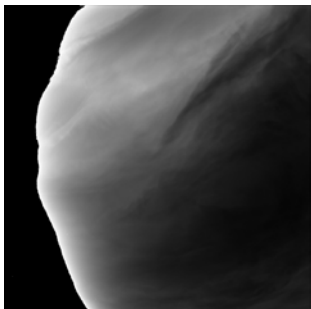
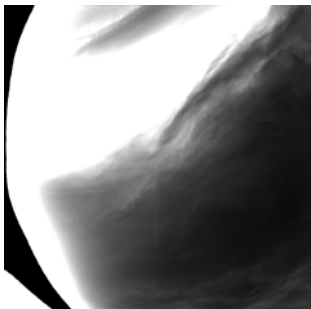
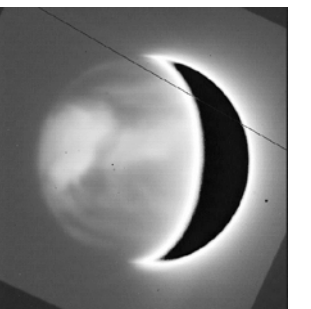
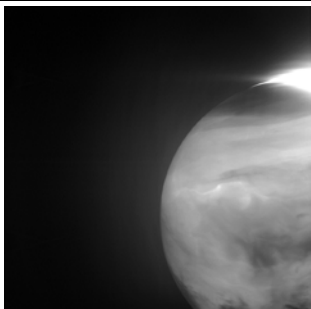
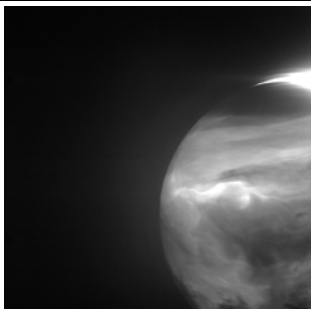
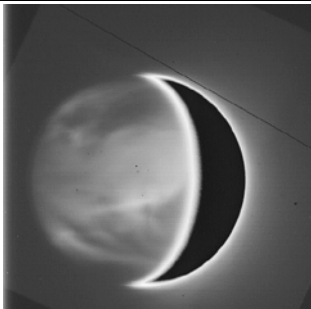
65 Figure 8. Concurrent views of the dayside hemisphere of Venus at 283, 365, 900 and
 66 2020 nm. The 900 nm images are shown after applying a high pass filter to bring out
 67 subtle detail. The high latitude regions appear darker at 2020 nm due to the increased
 68 absorption by CO₂ indicating somewhat lower cloud tops. The black square in the
 69 May 17 IR2 image is an artifact of the processing.



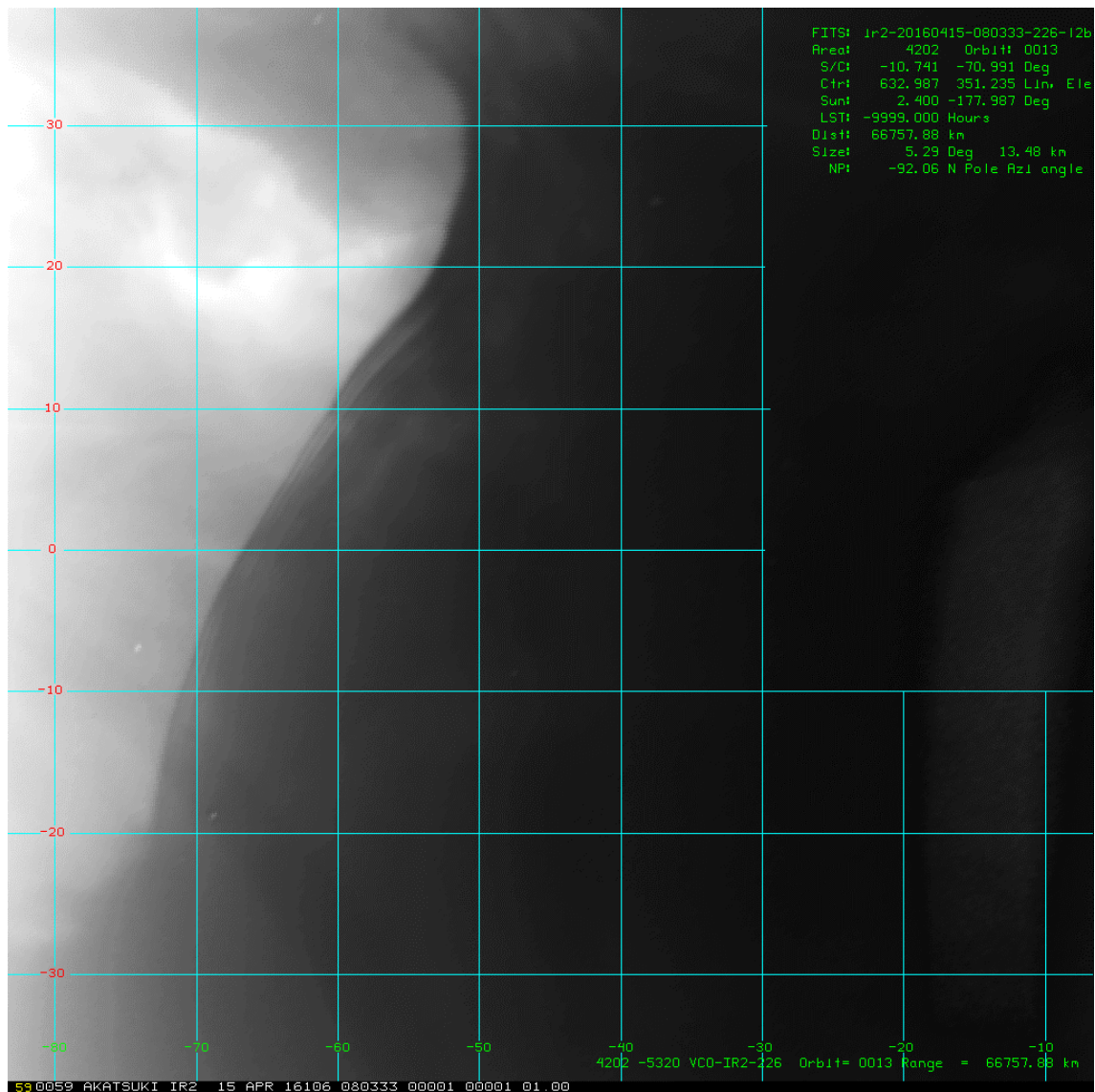
70 Figure 9. A high resolution view of Venus at 283 nm, 365 nm and 2.02 μ m (~ 6 km per
 71 pixel) from Akatsuki UVI and IR2 cameras on 6 May 2016. The lower right quadrant
 72 boundary of the 2.02 μ m image is an artifact. The lower right image is a color

73 composite of these images in a latitude-longitude view (Red- 2.02 μm , Green- 365 nm
74 and Blue – 283 nm). The oval shaped bright spot seen in the 283 image is an artifact.
75

		
A 20160325_073211_174	B 20160325_073333_226	C 20160325_074039_232
		
D 20160507_040211_174	E 20160507_040333_226	F 20160507_041037_232
		
G 20160712_020212_174	H 20160712_020333_226	I 20160712_021127_232
		
J 20160904_170212_174	K 20160904_180128_226	L 20160904_171123_232

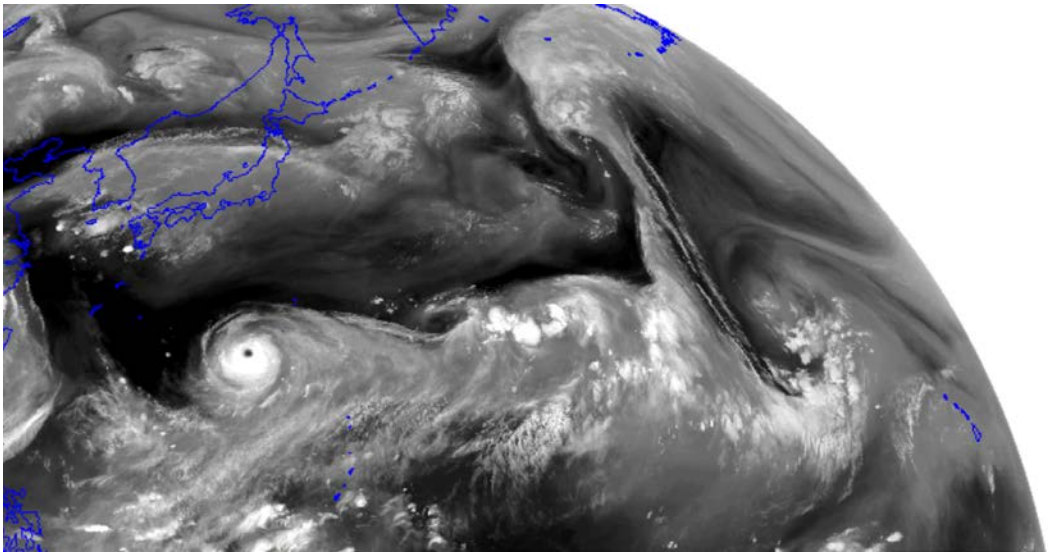
		
M ir2_20160905_033211_174	N 20160905_033333_226	O ir2_20160905_034120_232
		
P ir2_20160927_090209_174	Q 20160927_090331_226	R ir2_20160927_091120_232
		
S ir2_20161008_090056_174	T 20161008_090127_226	U IRTF Cont_K April 27
		
V ir2_20161030_080211_174	W 20161030_080333_226	X IRTF Cont_K April 28

76 Figure 10. Selected images at 1.74, 2.26 and 2.32 μm taken from the IR2 camera on the
 77 night side of Venus. Images U and X are part of supplemental IRTF images for IR2.

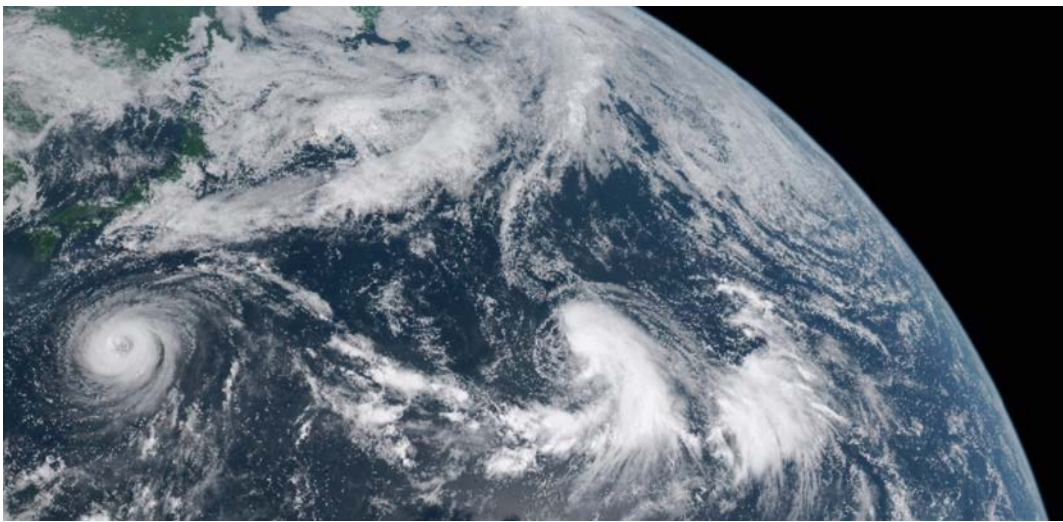


78

79 Figure 11a. A latitude-longitude map of 2.26 μm nightside image obtained from the
80 IR2 camera on April 25 showing an unusual sharp boundary in the intensity. Such
81 sharp boundaries are seen on Earth only in water vapor channels, thereby showing the
82 dry and moist airmasses (Figure 11b).



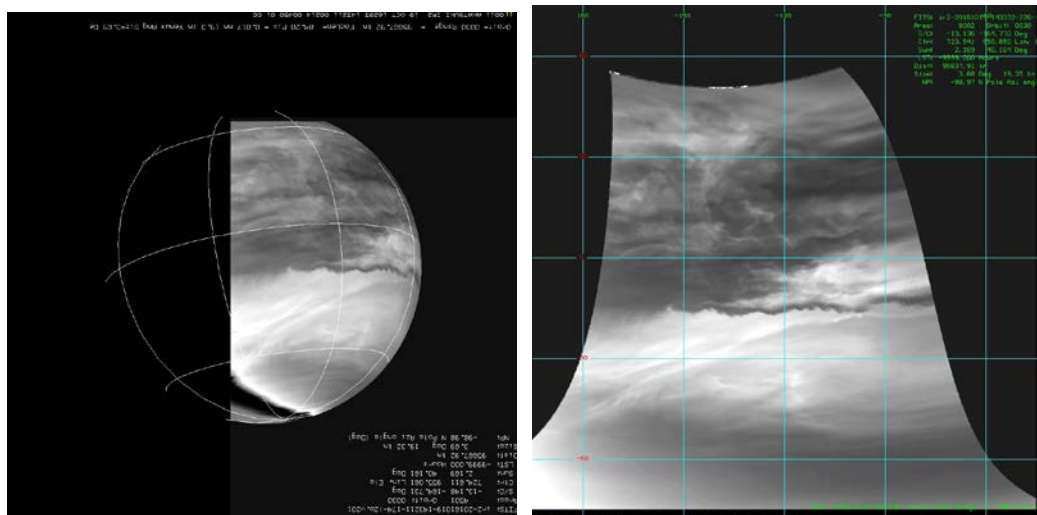
83



84

85 Figure 11b. Sharp boundaries are also seen in images of Earth taken from weather
86 satellites in the water vapor channel (top). This image taken from Himari on 1 August
87 2017 at 23:50 UT in the $6.9 \mu\text{m}$ channel shows several sharp boundaries depicting
88 different air masses with different lower tropospheric water vapor amounts. The
89 bottom image is a RGB composite view taken at the same time where the boundary is
90 not so easily discerned but can be inferred from the destruction of the clouds due to
91 entrainment of the the dry air in the western half of the cyclonic region (central part of
92 the color image). By analogy, the sharp boundaries seen on Venus in the IR2 night time

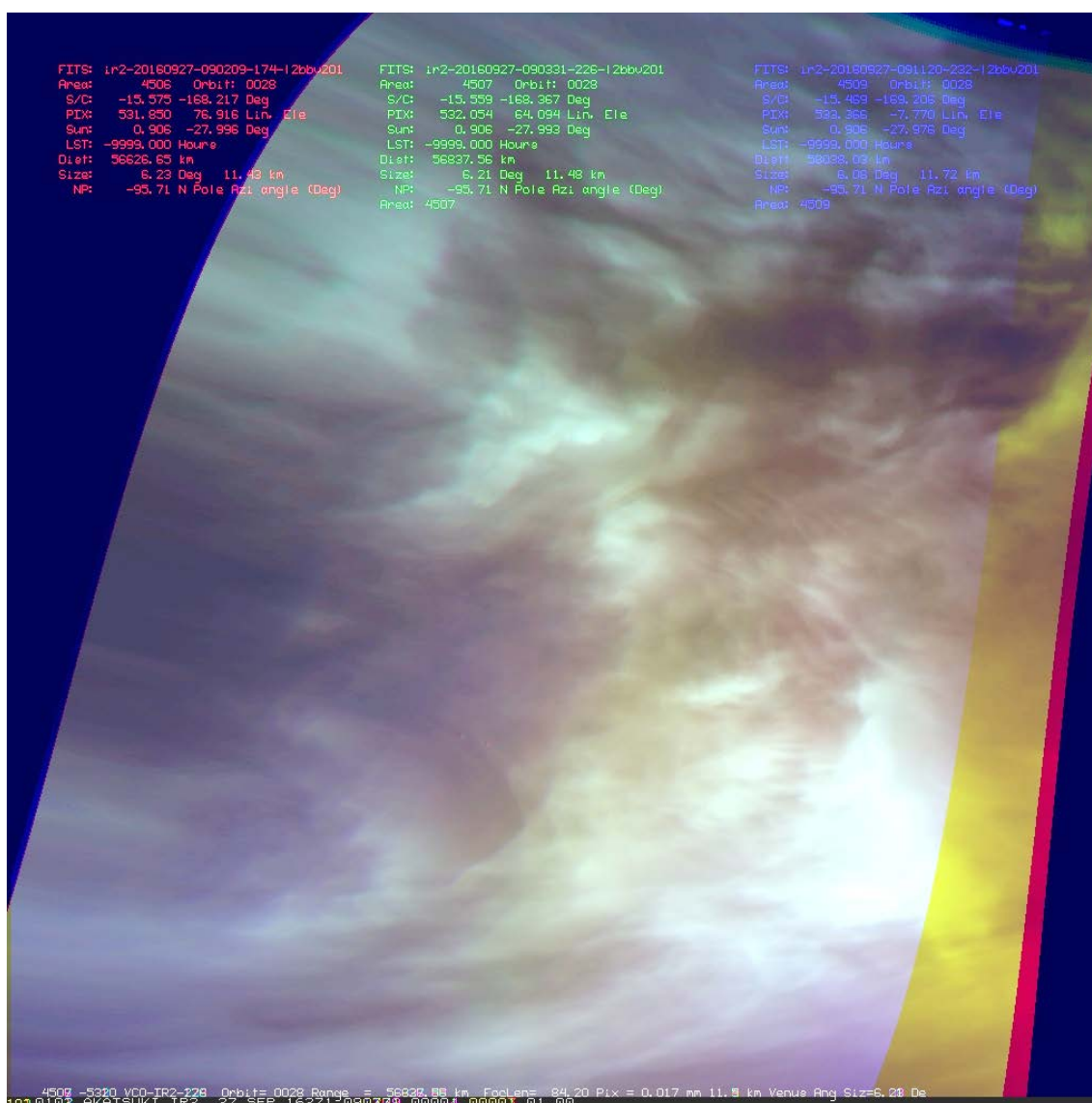
- 93 images may suggest different “air masses” due to differing trace gas abundance(s) on
- 94 Venus in the Venus cloud layer.



95

96 Figure 12. This 2.32 μm image (ir2_20161019_143211_226) suggests a wave like

97 boundary between cloud masses at some unknown altitude.



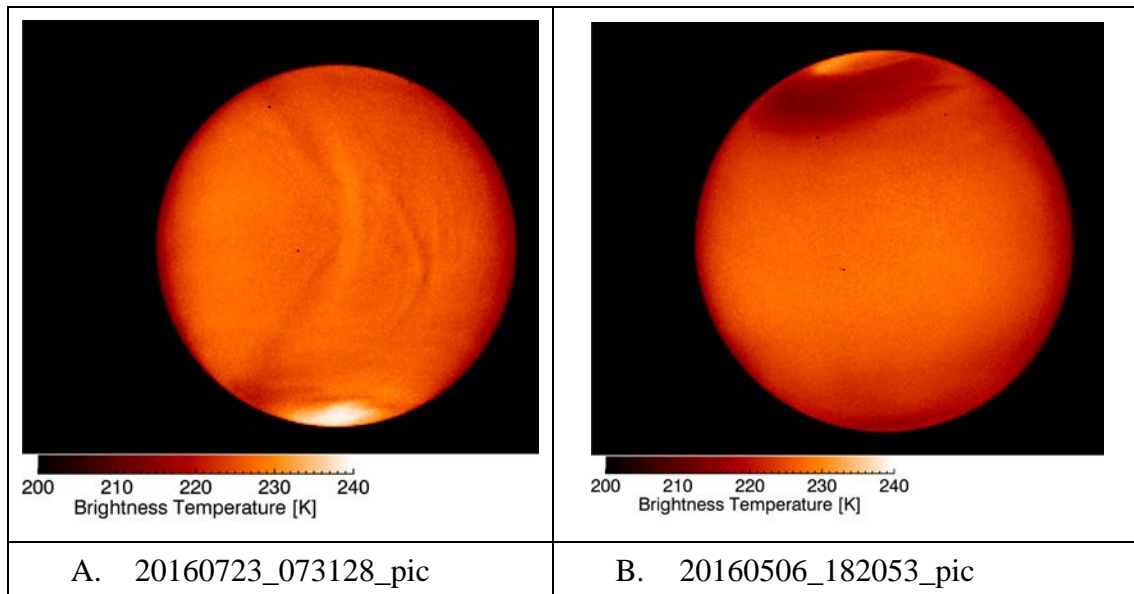
98

99 Figure 13. Subtle variations in the opacities are revealed in this color composite

100 generated from mapped 1.74 μm (red), 2.26 μm and 2.32 μm images. The image scale

101 is 0.1°/pixel in latitude and longitude.

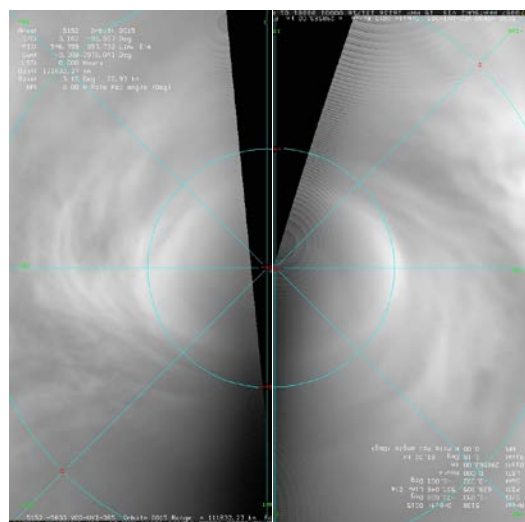
102



103 Figure 14. Representative images of Venus taken by the LIR camera at 8-12 μm .

104 Panel A shows the standing gravity waves discovered by Akatsuki from such
 105 observations (Fukuhara et al., 2017), while B shows Venus when the standing wave is
 106 not present. Generally the equator ward edge of the vortex over the poles is seen in all
 107 the LIR images depicting its temporal evolution due to the vortex dynamics (Garate-
 108 Lopez et al., 2015; Garate-Lopez et al., 2013; Limaye et al., 2009; Piccioni et al., 2007).

109

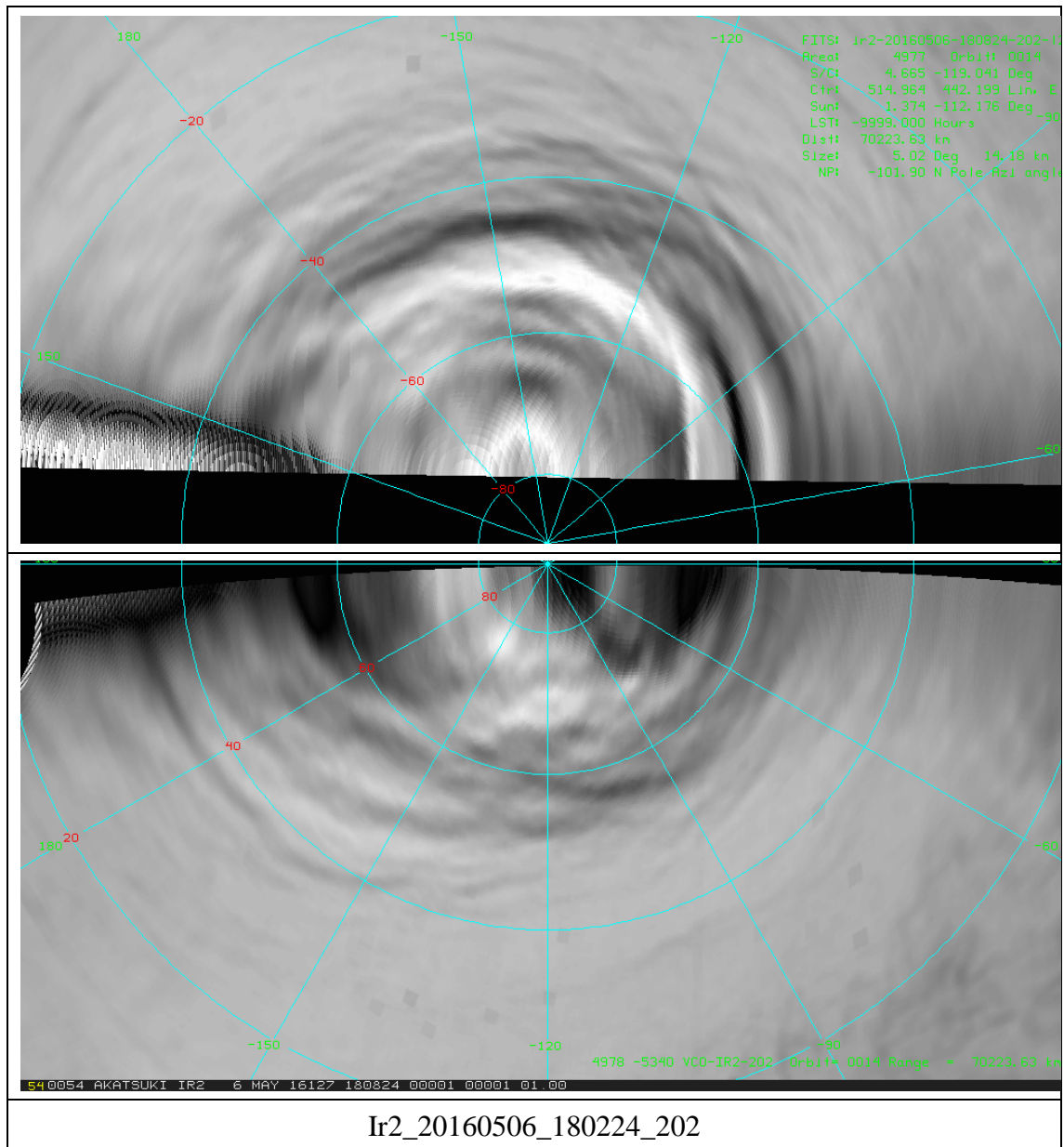


110 Figure 15a. The cloud cover at the ultraviolet shows the same vortex morphology over

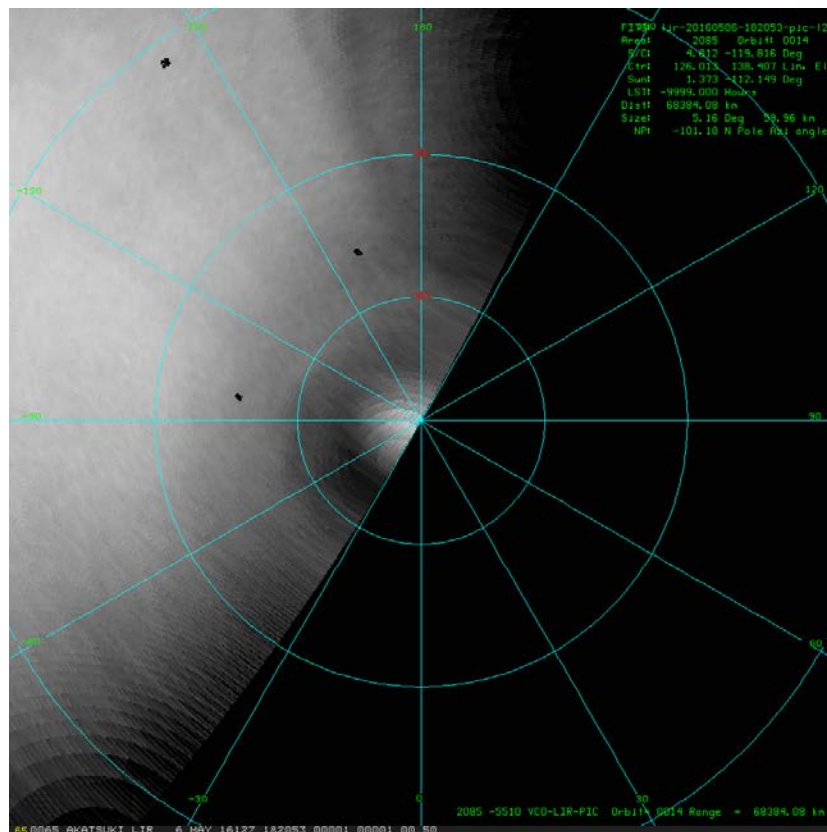
111 both hemispheres. This composite view is from two 365 nm images taken on 15 May
112 (right) and 17 May (left) on orbit 15 of Akatsuki and show the southern hemisphere
113 vortex. The 15 May image is rotated by 180°. A similar vortex is seen over the
114 northern pole.
115

116

117



118 Figure 15b. North (bototn) and south (top) hemispheres in polar stereographic
 119 projection of a 2.02 μm contrast filtered image with overlaid latitude and longitude
 120 grid.. The calibrated image was first subjected to a contrast filter to bring out the local
 121 structures and then projected. Although the pattern at higher latitudes show patterns
 122 similar to the spiral arms of the vortex seen at ultraviolet, there is considerable amount
 123 detail in the core region visible.
 124



125

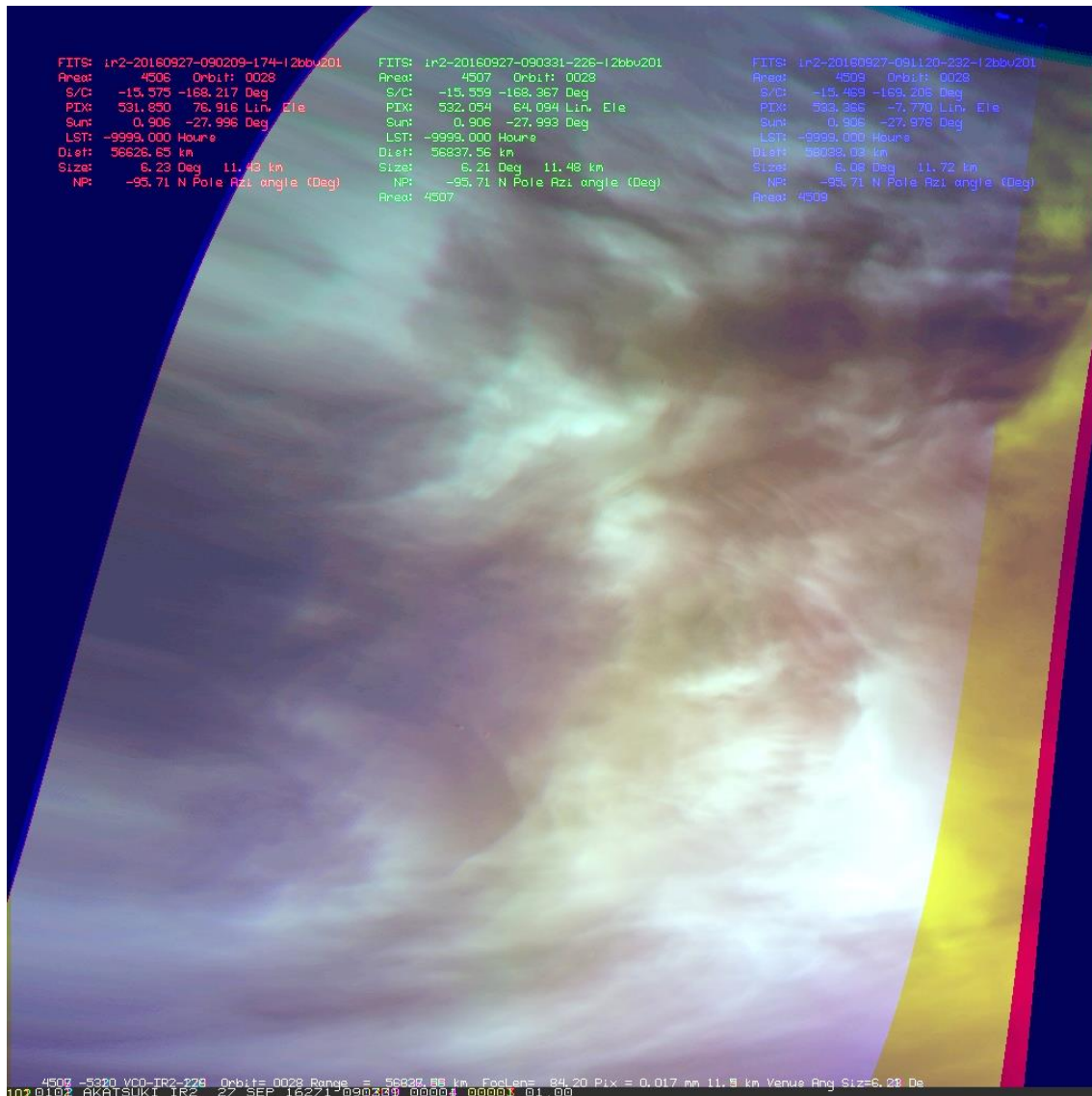
126 Figure 15c. Polar stereographic view of the northern hemisphere of the image B of
 127 Figure 14, also showing the warmer (deeper) core region of the vortex. This is
 128 consistent with the 2.02 μm image.

129

130 Uncategorized References

- 131 Fukuhara, T., Futaguchi, M., Hashimoto, G. L., Horinouchi, T., Imamura, T.,
 132 Iwagaimi, N., Kouyama, T., Murakami, S. Y., Nakamura, M.,
 133 Ogohara, K., Sato, M., Sato, T. M., Suzuki, M., Taguchi, M., Takagi,
 134 S., Ueno, M., Watanabe, S., Yamada, M., & Yamazaki, A. (2017). Large
 135 stationary gravity wave in the atmosphere of Venus. *Nature*
 136 *Geoscience*, *10*(2), 85-+. doi:10.1038/Ngeo2873
- 137 Garate-Lopez, I., García Muñoz, A., Hueso, R., & Sánchez-Lavega, A. (2015).
 138 Instantaneous three-dimensional thermal structure of the South
 139 Polar Vortex of Venus. *Icarus*, *245*, 16-31.
- 140 Garate-Lopez, I., Hueso, R., Sánchez-Lavega, A., Peralta, J., Piccioni, G., &
 141 Drossart, P. (2013). A chaotic long-lived vortex at the southern pole of

- 142 Venus. *Nature Geoscience*, 6, 254-257.
- 143 Limaye, S. S., Kossin, J. P., Rozoff, C., Piccioni, G., Titov, D. V., &
144 Markiewicz, W. J. (2009). Vortex circulation on Venus: Dynamical
145 similarities with terrestrial hurricanes. *Geophysical Research*
146 *Letters*, 36.
- 147 Piccioni, G., Drossart, P., Sanchez-Lavega, A., Hueso, R., Taylor, F. W.,
148 Wilson, C. F., Grassi, D., Zasova, L., Moriconi, M., Adriani, A.,
149 Lebonnois, S., Coradini, A., Bezaud, B., Angrilli, F., Arnold, G., Baines,
150 K. H., Bellucci, G., Benkhoff, J., Bibring, J. P., Blanco, A., Blecka, M.
151 I., Carlson, R. W., Di Lellis, A., Encrenaz, T., Erard, S., Fonti, S.,
152 Formisano, V., Fouchet, T., Garcia, R., Haus, R., Helbert, J., Ignatiev,
153 N. I., Irwin, P. G., Langevin, Y., Lopez-Valverde, M. A., Luz, D.,
154 Marinangeli, L., Orofino, V., Rodin, A. V., Roos-Serote, M. C., Saggin,
155 B., Stam, D. M., Titov, D., Visconti, G., Zambelli, M., Team, V. I.-V. E.
156 T., Ammannito, E., Barbis, A., Berlin, R., Bettanini, C., Boccaccini, A.,
157 Bonnelo, G., Bouye, M., Capaccioni, F., Moinelo, A. C., Carraro, F.,
158 Cherubini, G., Cosi, M., Dami, M., De Nino, M., Del Vento, D., Di
159 Giampietro, M., Donati, A., Dupuis, O., Espinasse, S., Fabbri, A.,
160 Fave, A., Veltroni, I. F., Filacchione, G., Garceran, K., Ghomchi, Y.,
161 Giustini, M., Gondet, B., Hello, Y., Henry, F., Hofer, S., Huntzinger,
162 G., Kachlicki, J., Knoll, R., Driss, K., Mazzoni, A., Melchiorri, R.,
163 Mondello, G., Monti, F., Neumann, C., Nuccilli, F., Parisot, J., Pasqui,
164 C., Perferi, S., Peter, G., Piacentino, A., Pompei, C., Reess, J. M.,
165 Rivet, J. P., Romano, A., Russ, N., Santoni, M., Scarpelli, A., Semery,
166 A., Soufflot, A., Stefanovitch, D., Suetta, E., Tarchi, F., Tonetti, N.,
167 Tosi, F., & Ulmer, B. (2007). South-polar features on Venus similar to
168 those near the north pole. *Nature*, 450(7170), 637-640.
169 doi:10.1038/nature06209
170



- 1
- 2 Akatsuki global images of Venus on the day and night side are providing new insights
- 3 into the behavior and properties of clouds on Venus and informing us about its dynamic
- 4 atmosphere.

1 **Venus' Spectral Signatures and the Potential for Life in the Clouds**

2
3
4 Sanjay S. Limaye (Sanjay.Limaye@ssec.wisc.edu)
5 University of Wisconsin,
6 Space Science and Engineering Center, 1225 West Dayton Street
7 Madison, Wisconsin 53706, USA

8
9 Rakesh Mogul (rmogul@cpp.edu)
10 California State Polytechnic University, Pomona
11 3801 W. Temple Ave., Pomona, CA 91768, USA

12
13 Arif H. Ansari (a.h.ansari@bsip.res.in)
14 Birbal Sahni Institute of Palaeosciences
15 53 University Road, Lucknow – 226007, India

16
17 Grzegorz P. Słowik (grzegslowik@o2.pl)
18 University of Zielona Góra
19 69 Wojska Polskiego Str., 65-762 Zielona Góra, Poland

20
21 David J. Smith (david.j.smith-3@nasa.gov)
22 NASA Ames Research Center, Moffett Field, CA 94035, USA
23 Space Biosciences Research Branch

24
25 Parag Vaishampayan (vaishamp@jpl.nasa.gov)
26 *Jet Propulsion Laboratory, California Institute of Technology, Pasadena, CA*
27 *4800 Oak Grove Dr., M/S 89-108, Pasadena, CA 91109, USA*

28
29
30 **Corresponding Author**

31 Sanjay S. Limaye, (Sanjay.Limaye@ssec.wisc.edu)
32 Space Science and Engineering Center,
33 1225 West Dayton Street, Madison, Wisconsin 53706, USA

34
35
36 Keywords: Venus, Clouds, Microorganisms, Albedo, Spectral bio-signatures

37
38 Submitted to Astrobiology
39 16 January 2017
40 Revised 16 October 2017
41

42 Abstract

43 The lower cloud layer of Venus (47.5-50.5 km) is an exceptional target for
44 exploration due to the favorable conditions for microbial life including moderate
45 temperatures and pressures (~60 °C and 1 atm), and the presence of micron-sized
46 sulfuric acid aerosols. Nearly a century after the ultraviolet contrasts of Venus'
47 cloud layer were discovered using Earth-based photographs, the substances and
48 mechanisms responsible for the changes in Venus' contrasts and albedo are still
49 unknown. While current models include sulfur dioxide and iron chloride as the
50 ultraviolet absorbers, the temporal and spatial changes in contrasts, and albedo
51 between 330-500 nm, remain to be fully explained. Within this context, we
52 present a discussion regarding the potential for microorganisms to survive in
53 Venus' lower clouds and contribute to the observed bulk spectra. In this
54 hypothesis paper, we provide an overview of Venus spectroscopy, characterize
55 the spectral and physical properties of terrestrial biological materials compared to
56 Venus' clouds, review the potential for an iron and sulfur-centered metabolism in
57 the clouds, and discuss conceivable mechanisms of transport from the surface
58 towards a more habitable zone present in the lower clouds. Together, our
59 hypothetical lines of reasoning suggest that particles in Venus' lower clouds
60 contain sufficient mass balance to harbor microorganisms, water, and solutes, and
61 potentially sufficient biomass to be detected by optical methods. As such, the
62 spectral overlaps between Venus and terrestrial biomolecules potentially warrant
63 further investigations into the prospect of biosignatures in Venus' clouds.

64 **Introduction**

65 The habitability of Venus' clouds has been a subject of discussion for
66 several decades, but has gained limited traction as a popular target in astrobiology
67 research. Initially stirring excitement, Cockell (1999) concluded that the
68 conditions between the lower and middle Venus atmosphere were conducive to
69 (terrestrial) biology, and that conditions in the higher Venus altitudes would
70 freeze but not necessarily kill microorganisms. Since then, subsequent studies
71 have highlighted the potential for life in Venus' cloud layers due to favorable
72 chemical and physical conditions, including the presence of sulfur compounds,
73 CO₂, and water, and moderate temperatures (0-60 °C) and pressures (~0.4-2 atm)
74 (Schulze-Makuch et al., 2004; Schulze-Makuch & Irwin, 2002). In this hypothesis
75 paper, we further consider these conditions and examine the potential for
76 microorganisms to survive in the clouds and contribute to the bulk spectral
77 properties of Venus.

78

79 **Overview of Venus Spectroscopy**

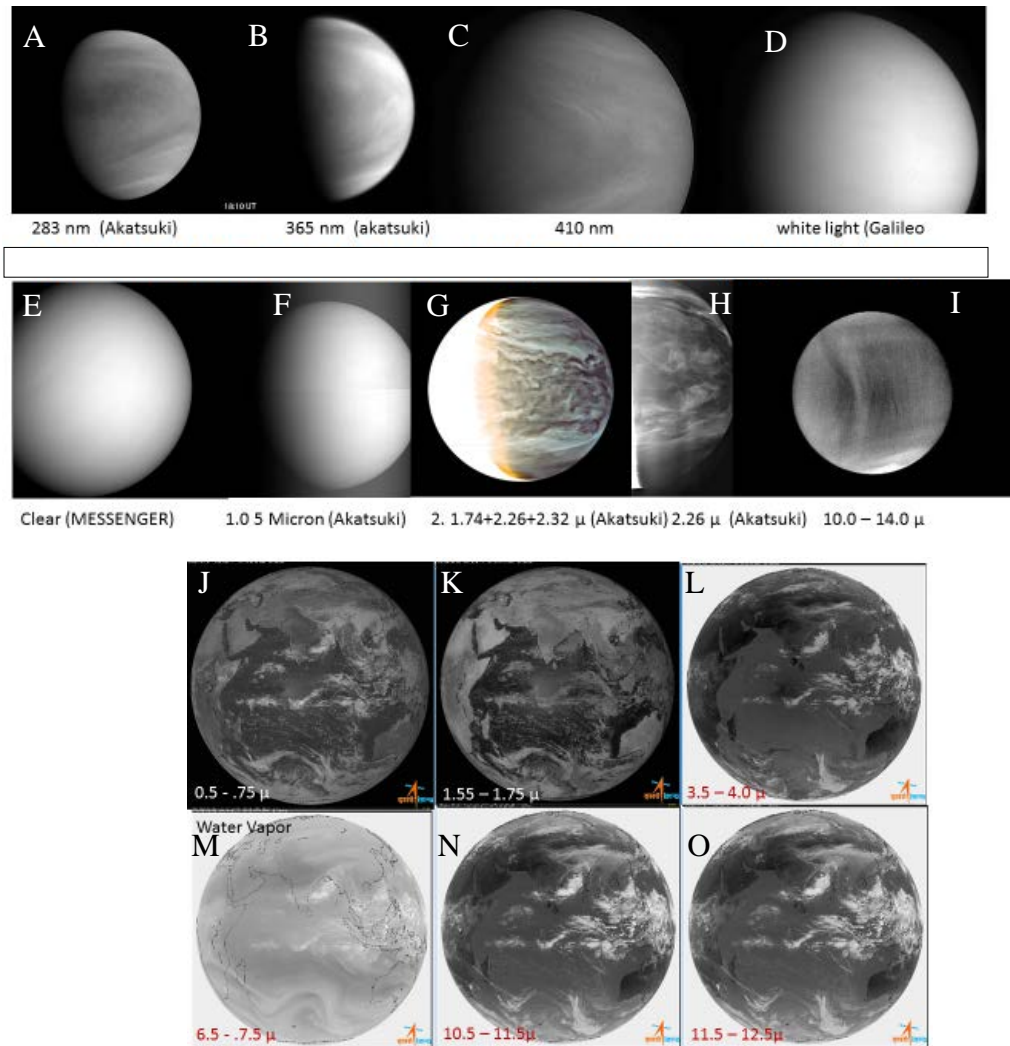
80 Comparisons of spectral measurements (**Figure 1**) obtained from the
81 Pioneer Venus, Magellan, Galileo, and Akatsuki missions show several
82 differences in albedo across the spectrum from the UV (**Figures 1A-C**) and the
83 visible (**Figures 1D-F**) to near infrared wavelengths (**Figures 1G-I**). Venus is
84 globally covered in clouds and devoid of contrasts in the visible and infrared
85 wavelengths in day side images (**Figures 1D-G**). Rather, contrasts in the cloud
86 cover are observed only at wavelengths shorter than blue in reflected sun light
87 (**Figures 1A-C**), and at near infrared wavelengths (1.7-2.4 μ m) on the nightside
88 (**Figures 1G & 1H**). Despite spacecraft investigations from orbit and entry
89 probes, the chemical and physical properties of these contrasts are still unknown,
90 including the lack of mixing, the identities of the contrasting substances, the
91 sources of these substances, and any potential sinks. Thermal infrared images (10-

92 15 μm) show small scale (~ 50 km) contrasts of less than 2 K in brightness
93 temperature on the day and night hemispheres at all latitudes, except poleward of
94 $\sim 65^\circ$ latitude in both hemispheres. At these latitudes, Hadley circulation is
95 presumed to suppress the cloud tops due to down-welling in polar regions, as
96 observed near the top and bottom of the Venus images (**Figure 1I**). In contrast,
97 clouds on Earth are often observed in satellite images as discrete features with
98 clear air in between at visible and short to thermal infrared wavelengths (**Figures**
99 **1 J-O**). Unlike on Earth, the observed contrasts in Venus' global cloud cover
100 vary with wavelength from visible to infrared (Limaye et al., 2017) in
101 morphology as well as magnitude as shown in **Figures 1A-C, 1G, and 1H**, Venus
102 and **Figures 1 J-O**, Earth.

103

104 The Venus UV contrasts were first observed in Earth based photographs
105 (Ross, 1928) and subsequently characterized by ground based polarimetry
106 (Hansen & Hovenier, 1974), spectroscopy (Barker, 1978; Barker, 1993), remote
107 spacecraft observations (Kawabata et al., 1980; Titov et al., 2008) and entry
108 probes (Esposito et al., 1983); Knollenberg et al. (1980); (Knollenberg, 1984;
109 Knollenberg & Hunten, 1980). Together, these studies indicate that the global
110 cloud cover is composed of sulfuric acid droplets (~ 1.1 μm equivalent radius) in a
111 mixture consisting mostly of small particles (~ 0.2 - 0.3 μm equivalent radius), with
112 larger particles (~ 2 - 8 μm diameter) present at lower altitudes (Knollenberg &
113 Hunten, 1979). In addition, slight differences in cloud particle properties at the
114 polar regions have been inferred from the Venus Express data (Wilson et al.,
115 2008).

116



117

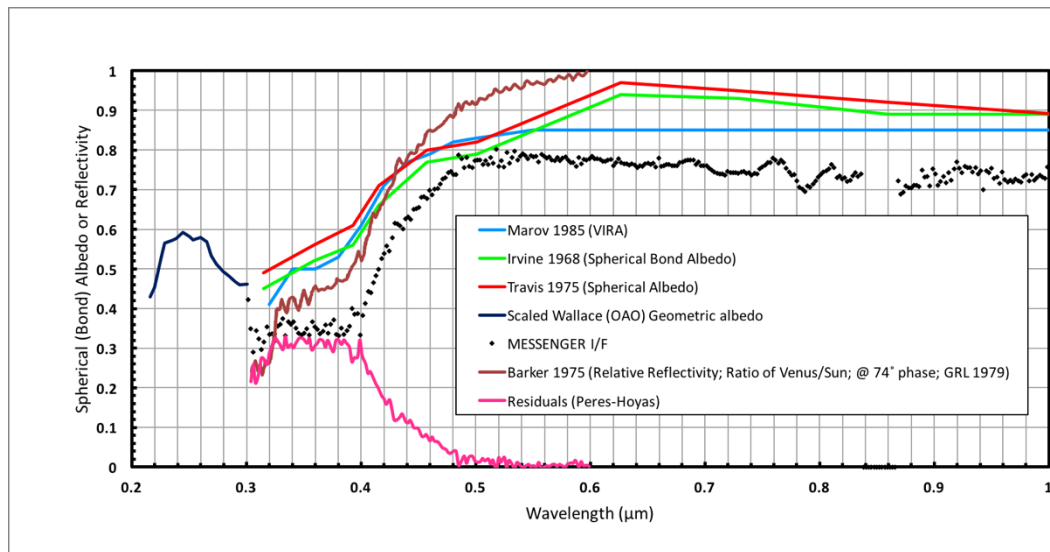
118

119 **Figure 1.** Difference in spectral contrasts of Venus at the wavelengths of (A)283
 120 nm and , (B) 365 nm (Akatsuki,), (C) 410 nm, (D) white light (Galileo, Belton et al.
 121 (1991)), (E) clear (MESSENGER, Hawkins et al. (2009)), (F) 0.5 μm (Akatsuki),
 122 (G) 1.74+2.26+2.32 μm (Akatsuki), (H) 2.26 μm (Akatsuki), and (I) 10.0-14.0
 123 μm; and spectral contrasts of Earth at the wavelengths of (J) 0.5-0.75 μm, (K)
 124 1.55-1.75 μm, (L) 3.5-4.0 μm, (M) 6.5-7.5 μm, (N) 10.5-11.5 μm, and (O)
 125 11.5-12.5 μm (ISRO, R. Katti et al. (2006)). Akatsuki data are available from:
 126 <https://www.darts.isas.jaxa.jp/planet/project/akatsuki/>
 127

128

129 Provided in **Figure 2** is a collective summary of Venus spectra between
130 200-1000 nm, including global geometric or spherical albedo estimates (Irvine,
131 1968; Moroz et al., 1985; Travis, 1975) and measurements from ground based
132 telescopes (Barker et al., 1975), and MESSENGER spacecraft during the second
133 Venus fly-by (Perez-Hoyos et al., 2013). Also shown is the calculated difference
134 between the VIRA cloud model and the MESSENGER spectra (updated from
135 Perez-Hoyas, 2013), which gives an indication of the spectral absorption by the
136 unknown materials in the clouds of Venus. We note here that the original
137 identification of the sulfuric acid composition of the Venus cloud particles was
138 derived by matching the index of refraction, required for matching the phase
139 dependence of disk integrated polarization at different optical wavelengths
140 (Hansen & Hovenier, 1974), and not by spectral identification. Interpretation of
141 Venus' UV and IR spectra, along with questions about the cloud composition and
142 ultraviolet absorbers, are summarized by (Krasnopolsky, 2006) and in chapters
143 within the review books on Venus (Hunten et al., 1983) and Venus II (Bougher
144 et al., 1989). Herein, we summarize briefly the pertinent cloud properties which
145 must play a part in the absorption of incident sunlight and the observed contrasts.
146 Travis (1975) pointed out that the spectral dependence of albedo and cloud
147 contrasts are different, and thus indicate at least two different absorbers. Pollack
148 et al. (1980) identified gaseous sulfur dioxide as a potential absorber, and ruled
149 out many other suggested candidates due to insufficient spectral overlap.
150 Esposito and Travis (1982) suggested from analysis of the polarization data
151 obtained from the Pioneer Venus Orbiter that the differential polarization between
152 bright and dark UV features could not be explained by haze abundance variations,
153 and favored a chemical model where water vapor and molecular oxygen are
154 depleted at the cloud tops.
155

156 Zasova et al. (1981) built upon Kuiper (1969) proposed presence of
157 incompletely hydrated FeCl_2 in the clouds, and offered that sulfur dioxide (below
158 330 nm) along with ferric chloride (FeCl_3) (above 330 nm) could explain the
159 observed lowered albedo below 500 nm. The partial contribution of sulfur dioxide
160 to UV absorption of incident solar radiation has been observed from Venus
161 Express observations (Lee et al., 2015b), as well as those from Hubble Space
162 Telescope (Jessup et al., 2015), and can also be discerned from differences in the
163 spectra of Venus at 283 nm (where there is some absorption by SO_2) and 365 nm
164 (where the contrast peaks and SO_2 does not absorb) taken by Akatsuki (**Figures**
165 **1A & 1B**). Based on Venus Express measurements, analysis of the glory feature
166 observed in unpolarized (Markiewicz et al., 2014) and polarized light (Rossi et al.,
167 2015) have yielded values for index of refraction larger than the those inferred by
168 Hansen and Hovenier (1974). Markiewicz et al. (2014) suggested that presence of
169 FeCl_3 attached to the sulfuric acid droplets, which may also act as cloud
170 condensation nuclei, could explain the higher indices of refraction. Krasnopolsky
171 (2017) concluded that sulfur aerosols cannot be the UV absorber since the
172 required abundance and vertical profile were incompatible with Venera 14
173 observations; however, the presence of FeCl_3 was compatible with contributions
174 towards the higher values of indices of refraction inferred by Markiewicz et al.
175 (2014). Nevertheless, some doubt remains whether analysis of glory features can
176 lead to an accurate inference of the index of refraction (Laven, 2008) values
177 between 1.07 and 1.7, as is the case for Venus.
178



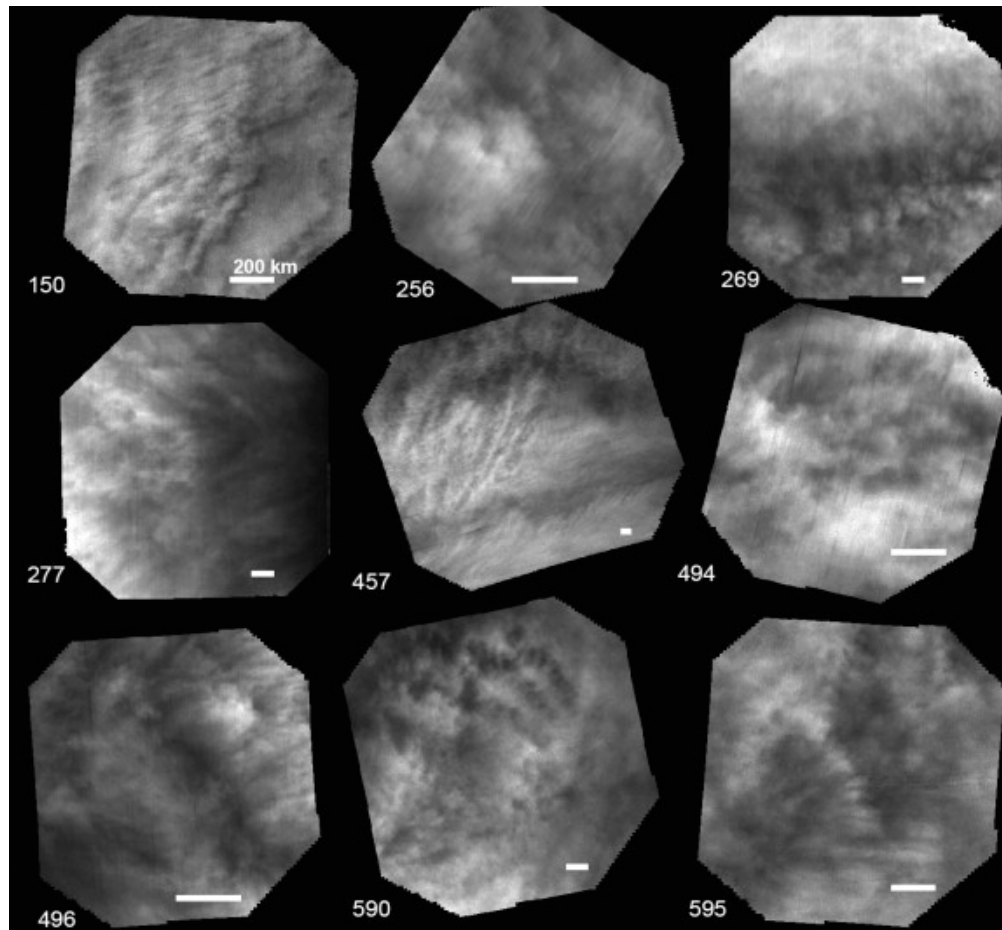
179

180 **Figure 2.** Venus spectra as measured by Moroz (VIRA, 1985), Irvine (1968),
 181 Travis (1975), Wallace (scaled geometric albedo), MESSENGER, and Barker
 182 (1975), including residuals.

183

184 Spatial Contrasts in the Ultraviolet Spectrum

185 From ground-based and spacecraft observations, it is widely accepted that
 186 Venus' clouds contain micron-sized particles (Hansen & Hovenier, 1974;
 187 Knollenberg et al., 1980) consisting of sulfuric acid solutions (75-98%). In fact,
 188 all UV and blue images of Venus show small scale (10-100 km) contrasts at 270
 189 nm (Pioneer Venus OCPP, polarimetry mode), 283 nm (Akatsuki), 365 nm
 190 (Mariner 10, Venus Monitoring Camera on Venus Express), 410 nm (Galileo),
 191 and 430 nm (MESSENGER MDIS), which evolve over time scales ranging from
 192 minutes (~50 km spatial scales) to days (~1000 km). Rapid changes in
 193 atmospheric appearances have also noted by Ross (1928), and have been observed
 194 in spacecraft images (Murray et al., 1974; Rossow et al., 1980; Titov et al., 2012).
 195



196

197 **Figure 3.** Views of the equatorial region of Venus from the Venus Monitoring
198 Camera obtained through the 365 nm filter. The numbers in the lower left of each
199 view indicate the orbit number of Venus express (nominal period of 24 hours)
200 while the white bar in the lower right of each image indicates 200 km scale.

201

202

203

204

205

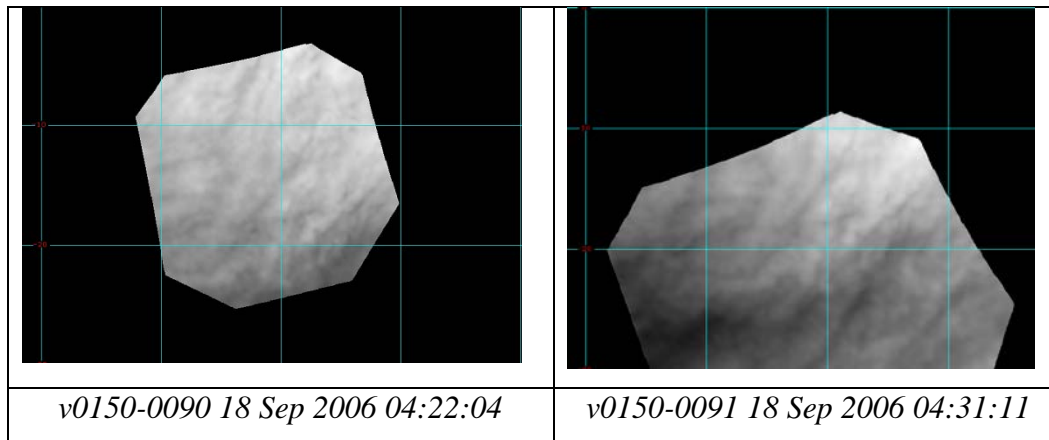
206

207

208

Figure 3 provides some views of the equatorial region of Venus that demonstrate the variability of the UV contrasts, over a variety of scales, as captured by the Venus Monitoring Camera (VMC) images on the Venus Express orbiter (Titov et al., 2012). Similarly, **Figure 4** provides two mapped UV images, from the Venus Monitoring Camera on Venus Express, taken only 9 minutes apart. The short-term evolution (growth and decay in terms of areal extent and contrast) of these features has been challenging to explain in terms of cloud

209 structure, cloud top altitude differences (Ignatiev et al., 2009), and/or purely
 210 dynamical processes.



211 *Figure 4. Rapid changes in the shape, size and magnitude of the ultraviolet*
 212 *contrasts are common on Venus, particularly at low latitudes where the*
 213 *absorption of incident solar radiation is greater. These two mapped Venus*
 214 *Monitoring Camera images taken through the 365 nm filter are only about 9*
 215 *minutes apart. The grid lines represent latitude and longitude lines, ten degrees*
 216 *apart.*
 217

218 Absorption below 330 nm is possible by sulfur dioxide (SO₂) and sulfur
 219 monoxide (SO), which have been detected on Venus from ground based
 220 observations (Barker, 1979), spacecraft (Conway et al., 1979; Stewart et al.,
 221 1979), and entry probe measurements (Oyama et al., 1980; Surkov et al., 1978).
 222 Proposed candidates (besides SO₂) for absorption in the 200-500 nm range
 223 include fine graphite grains (Shimizu, 1977), elementary sulfur polymers (Hapke
 224 & Nelson, 1975; Toon et al., 1982; Young, 1973), octasulfur (S₈) (Schulze-
 225 Makuch & Irwin, 2006), nitric oxide (Shaya & Caldwell, 1976), croconic acid
 226 (Hartley et al., 1989), hydrated ferric chloride (Kuiper, 1969), hydrobromic acid
 227 (Sill, 1975), and chlorine (Pollack et al., 1980). Besides SO₂ and SO, others such
 228 as carbon sulfide (CS₂) (Barker, 1978; Young, 1978) and carbonyl sulfide (COS)
 229 (Bezard et al., 1990) have been detected and also absorb below 330 nm, but not

230 between 330-600 nm (Mills et al. (2007). Esposito et al. (1983) and
231 (Krasnopolsky, 2006) have also published discussions regarding the unknown
232 ultraviolet absorber. The plausibility of sulfur aerosols as absorbers has been
233 postulated (Krasnopolsky, 2016; 2017), where analysis of the (limited) data from
234 in-situ measurements has suggested that the additional ultraviolet absorber was
235 likely FeCl_3 . Additionally, a sulfur oxide isomer (OSSO) has recently been
236 proposed as an alternative UV absorber (between 320-400 nm) and a potential
237 sulfur reservoir – however, the lifetimes of the two isomers of OSSO are very
238 short (a few seconds) and the estimates of opacity are uncertain (Frandsen et al.,
239 2016).

240

241 Spectroscopic measurements from VeGa 1 and VeGa 2, using a Xenon
242 lamp, as the probes descended on the night side, established that the UV absorbers
243 are present from the highest altitudes measureable (64 km) to the base of the
244 clouds at 47 km (Bertaux et al., 1996). On the day side, much of the incident
245 sunlight at UV wavelengths is absorbed at an altitude of 57 km, preventing
246 detection of the absorber using sunlight. To date, there are very few
247 measurements providing spatial and temporal variability of the absorbers. Spatial
248 and temporal variability has been detected in the case of SO_2 above the cloud tops
249 (Encrenaz et al., 2016), but the reasons or causes of the variations remain
250 unknown. Near simultaneous Akatsuki observations of Venus at 283 and 365 nm
251 have indicated (Lee et al., 2017) that SO_2 variations can explain some of the
252 differences in the contrasts, but as noted earlier, there are other trace species
253 which may also contribute to the observed variations.

254

255 Based on observations of the glory effect, FeCl_3 has also been proposed as
256 a candidate (Markiewicz et al., 2014), and remains the most likely contender as a
257 UV contrasting agent (Krasnopolsky, 2017). However, Zasova et al. (1981) note

258 that FeCl_3 is not stable in the presence of sulfuric acid, presumably due to
259 formation of $\text{Fe}_2(\text{SO}_4)_3$. As such, a continuous resupply of FeCl_3 would be
260 required (presumably from the surface) to support the observed contrasts. This
261 assessment, in turn, poses several questions regarding the mechanism of FeCl_3
262 particle transport to 50 km above the Venus surface, and the potential for FeCl_3
263 particles to act as cloud condensation nuclei (on observed timescales).

264

265 Thus, the identities of the UV absorber/s (330-600 nm) remains uncertain,
266 and the accuracy of current cloud models do not yield adequate explanations for
267 the lack of mixing (for the substance(s) responsible for the UV contrasts), or the
268 spatial and temporal changes in opacity. In this absence of cohesive physical and
269 chemical explanations, we present a discussion of Venus' clouds as a favorable
270 habitat for life, where biological sources may serve as contributing factors to the
271 observed spectral contrasts.

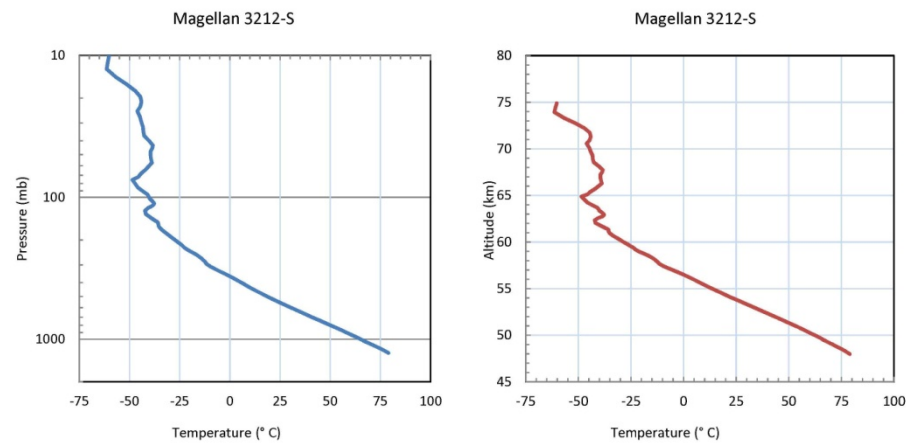
272

273 **Can Biology Contribute to Venus' Spectral Signatures?**

274 The possibility of airborne Venus life was discussed by Morowitz and
275 Sagan (Morowitz, 1967) and followed up by Cockell (Cockell, 1999), Schulze-
276 Makuch et al, and Shulze-Makuch and Irwin (Schulze-Makuch et al., 2004;
277 Schulze-Makuch & Irwin, 2002; 2006). These reports introduced the premise that
278 acid resistant terrestrial bacteria could potentially tolerate the Venus cloud
279 environment, and metabolize through phototrophic and chemotrophic means. As
280 is the case for any extremotolerant biology discussion, parameters such as
281 temperatures, radiation levels, and the presence of available water serve as major
282 limitations for habitability. However, in the context of Venus' clouds, these
283 specific issues are likely non-limiting.

284

285



286

287

288 **Figure 5.** Representative atmospheric temperature variation with pressure (left)
289 and with altitude (right) in the Venus atmosphere. The profile shows Magellan
290 radio occultation profile (Jenkins et al., 1998).

291

292 As displayed in **Figure 5**, the bottom cloud layer at ~48-50 km possesses
293 rather favorable conditions, with temperatures of ~60 °C and pressures of ~1000
294 mbar, or ~1 atm. Further, as described by Cockell (1999), UV radiation in the
295 Venus' cloud layer is likely not prohibitive to life, since the UV flux in the upper
296 levels of the atmosphere of Venus are comparable to the surface flux of Archaen
297 Earth, when life on Earth was thought to emerge, and substantially attenuated
298 within Venus' cloud layer due to atmospheric CO₂ and the aforementioned UV
299 absorbers. In terms of water availability, water vapor values at altitudes of 40 km
300 and higher are thought to vary widely from 20-50 ppm at latitudes of 60°, to >500
301 ppm near the equator, with global averages suggesting mixing ratios of 40-200
302 ppm. However, desiccation in the Venus atmosphere may be avoidable despite
303 these low water abundances, due to the hygroscopic nature of sulfuric acid (which
304 would likely yield droplets or aerosols containing liquid water, even at high
305 altitudes due to freezing point depression). Nonetheless, any inferences regarding
306 the cloud particles, either near the cloud tops or at high altitudes, are the result of

307 remotely sensed observations, and are not conclusive with respect to
308 characterizing particle states as liquid or solid. However, if the Venus cloud
309 particles are spherical, then the prevailing theory is that the droplets must be
310 liquid (Hansen & Hovenier, 1974).

311

312 Across the cloud layers, the sulfuric acid aerosols are described in roughly
313 three size modes ranging in diameter from $\sim 0.4 \mu\text{m}$ (mode 1), $\sim 2 \mu\text{m}$ (mode 2),
314 and $\sim 8 \mu\text{m}$ (mode 3), with a small number of particles as large as $\sim 18 \mu\text{m}$, as
315 measured by the Venera missions (Knollenberg et al. (1980). For the total cloud
316 layer (lower, middle, and upper clouds), $\sim 70\%$ of the columnar mass loading (~ 32
317 $\text{mg}\cdot\text{m}^{-3}$, assuming a total 12.5 km column) arises from particles in the lower
318 clouds ($\sim 21 \text{mg}\cdot\text{m}^{-3}$), where $\sim 94\%$ of this mass is associated with the mode 3
319 particles ($\sim 20 \text{mg}\cdot\text{m}^{-3}$), ranging in diameter from $8.0 \pm 2.5 \mu\text{m}$. Assuming that
320 these particles are indeed suspensions (or possibly heterogenous mixtures similar
321 to terrestrial aerosols), then the majority of the observed UV contrasting materials
322 and/or the major biomass are likely to be found in the lower clouds. In
323 comparison, the middle cloud layer comprises only 24% of the total cloud
324 columnar mass loading (assuming a 6 km column), despite the potential
325 habitability of this region, where temperatures and pressures range from 10-50 °C
326 and 400-800 mb.

327

328 For the lower cloud layer (47.5-50.5 km), particle densities are reported to
329 be $\sim 50 \text{particles}\cdot\text{cm}^{-3}$ for the larger sizes ($\sim 2\text{-}8 \mu\text{m}$ diameter) and 600
330 $\text{particles}\cdot\text{cm}^{-3}$ for the smallest sizes ($0.4 \mu\text{m}$ diameter), where in the middle and
331 upper cloud layers ($\sim 50\text{-}70 \text{km}$) the respective particle densities are 10-50
332 $\text{particles}\cdot\text{cm}^{-3}$ ($\sim 2\text{-}8 \mu\text{m}$ diameter) and 300-800 $\text{particles}\cdot\text{cm}^{-3}$ ($\sim 0.3\text{-}0.4 \mu\text{m}$
333 diameter), with the largest particle densities of $\sim 800 \text{particles}\cdot\text{cm}^{-3}$ ($\sim 0.4 \mu\text{m}$
334 diameter) being detected at the highest altitudes. Among these particle

335 distributions, the largest masses are associated with the $\sim 5\text{-}15\ \mu\text{m}$ sized particles
336 in the lower clouds, and $\sim 2\text{-}15\ \mu\text{m}$ particles in the middle clouds; with mass
337 loading estimates ranging from $\sim 0.1\text{-}100$ and $\sim 0.01\text{-}10\ \text{mg}\cdot\text{m}^{-3}$ for the lower and
338 middle cloud regions (50.5-56.5 km), respectively, as reported by Knollenberg et
339 al. (1980).

340

341 In comparison, the primary biological aerosols in Earth's atmosphere
342 range in particle size from nanometer to sub-millimeter, and are composed of
343 differing biological materials including bacteria, fungal spores, fungal hyphen
344 fragments, pollen, plant spores, plant debris, algae, and viral particles (Fröhlich-
345 Nowoisky et al., 2016; Morris et al., 2011). Global estimates of the total primary
346 biological aerosols indicate $\sim 10^4\ \text{particles}\cdot\text{m}^{-3}$, where the median diameters of
347 particles containing cultivable bacteria are reported to be $\sim 4\ \mu\text{m}$ at continental
348 sites, and $\sim 2\ \mu\text{m}$ at coastal sites (Després et al., 2012). Global measurements
349 show that these bioaerosols are dominated by bacteria at $\sim 10^4\ \text{cells}\cdot\text{m}^{-3}$ (Fröhlich-
350 Nowoisky et al., 2016), thus amounting to a biomass of $\sim 5\ \text{ng}\cdot\text{m}^{-3}$ when assuming
351 a buoyant cell density of $1.041\ \text{g}\cdot\text{cm}^{-3}$ (Bakken & Olsen, 1983). However,
352 localized measurements in the cloud-forming regions in the lower troposphere
353 reveal much higher abundances of $8.1 \times 10^4\ \text{cells}\cdot\text{mL}^{-1}$, or $\sim 10^{11}\ \text{cells}\cdot\text{m}^{-3}$
354 (Amato et al., 2007), amounting to a theoretical cloud biomass of $\sim 44\ \text{mg}\cdot\text{m}^{-3}$.

355

356 For Venus' lower clouds, therefore, the mass loading estimates ($\sim 0.1\text{-}100$
357 $\text{mg}\cdot\text{m}^{-3}$) are comparable to the upper biomass value for terrestrial bioaerosols (~ 44
358 $\text{mg}\cdot\text{m}^{-3}$), while the particle size regime ($\leq 8\ \mu\text{m}$) opens the possibility that the
359 clouds may similarly harbor suspensions of single cells or aggregated microbial
360 communities. In theory, the 2 and 8 μm sized particles (modes 2 and 3) could
361 harbor a maximum of $\sim 10^8$ and $10^{10}\ \text{cells}\cdot\text{m}^{-3}$, respectively; these estimates
362 assume spherical cloud particles, spherical microorganisms with a mean diameter

363 of 1 μm , and particle densities of $50 \text{ particles}\cdot\text{cm}^{-3}$ ($5\times 10^7 \text{ particles}\cdot\text{m}^{-3}$). Using
364 these assumptions (including buoyant cell density), the theoretical and maximum
365 biomass loadings for these particles amount to 0.2 and $14 \text{ mg}\cdot\text{m}^{-3}$, respectively.
366 Again, these values are comparable to the upper biomass levels of bacterial
367 aerosols on Earth ($\sim 44 \text{ mg}\cdot\text{m}^{-3}$). Moreover, when compared to Venus, these
368 values are respectively ~ 6 and ~ 1.5 -fold lower than the columnar mass loadings
369 for the mode 2 and 3 particles (1.3 and $20 \text{ mg}\cdot\text{m}^{-3}$) from the lower cloud region
370 (when assuming a 3 km column depth), and well within the aforementioned range
371 of total mass loading estimates. These calculations and comparisons suggest that
372 the mode 2 and 3 particles, from Venus' lower cloud layer, could possess
373 sufficient mass balance to harbor water, solutes, and microorganisms.

374

375 To date, there are no in-depth studies focusing on the spectroscopy of
376 aerosolized microorganisms or biomolecules under Venus conditions. Under
377 terrestrial conditions, there are limited reports on the passive detection of
378 aerosolized *Bacillus* spores using infrared spectroscopy (FT-IR), with
379 measurements on $\sim 10^4$ - $10^9 \text{ cells}\cdot\text{m}^{-3}$ providing mass extinction coefficients (at
380 $\sim 1100 \text{ cm}^{-1}$) in the range of ~ 720 - $1400 \text{ cm}^2\cdot\text{g}^{-1}$ (Ben-David, 2003; Ben-David et
381 al., 2003; Blecka et al., 2012; Gurton, 2001). Further, turbidity (or optical
382 density) measurements (at 540 nm) on concentrated aqueous suspensions of
383 bacteria ($\sim 10^{15} \text{ cells}\cdot\text{m}^{-3}$) provide mass extinction coefficients of $\sim 4000 \text{ cm}^2\cdot\text{g}^{-1}$
384 (Spaun, 1962). Additionally, there are multiple reports on the remote sensing of
385 microbial blooms in fresh and ocean waters, where the intense absorption and/or
386 fluorescence properties of photosynthetic pigments (eg., chlorophyll *a* and
387 phycocyanin) yield very large mass extinction coefficients, with $\sim 2\times 10^5 \text{ cm}^2\cdot\text{g}^{-1}$
388 (at $\sim 640 \text{ nm}$) representing the terrestrial global average of chlorophyll *a* in the
389 oceans (Bidigare et al., 1990; Hunter et al., 2010; Schalles, 2006).

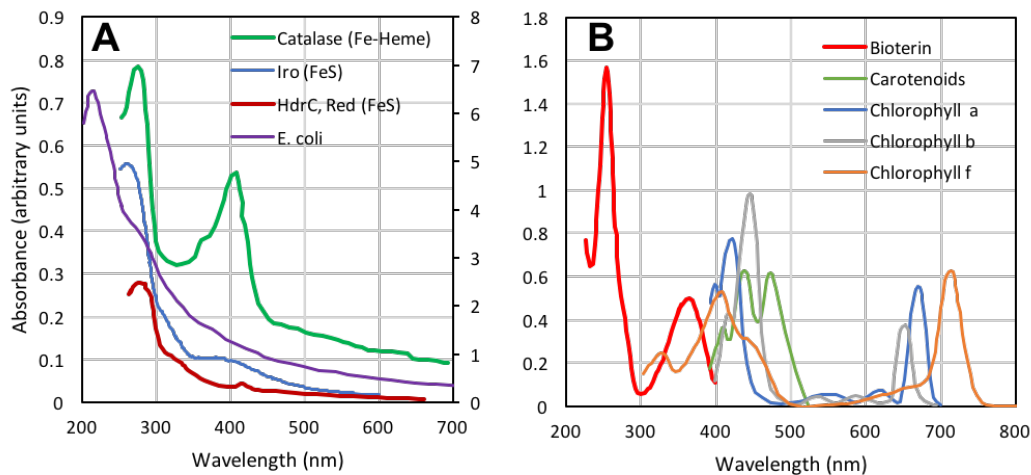
390

391 The lower clouds of Venus exhibit comparable mass extinction
392 coefficients ranging from $\sim 500\text{-}5000 \text{ cm}^2 \cdot \text{g}^{-1}$, as estimated from size particle
393 spectrometer (LCPS) measurements at 600 nm, and calculated using a density of
394 $2 \text{ mg} \cdot \text{cm}^{-3}$, as indicated by Knollenberg and Hunten (1980). These total values
395 suggest that Venus' lower cloud region could harbor sufficient biomass to be
396 characterizable and quantifiable through optical techniques. Moreover,
397 comparison of Venus and Earth mass extinction coefficients are suggestive of the
398 presence of high cell densities and/or appreciable concentrations of chromogenic
399 pigments in Venus' lower clouds (as inferred from measurements at 600 nm).

400

401 If Venus' clouds indeed harbor biology, then these biotic materials could
402 potentially exhibit spectral signatures that overlap with those of Venus' clouds.
403 For example, the observed contrasts at 270, 283, 365, 410, and 430 nm (Pioneer,
404 Akatsuki, Galileo, and MESSENGER) are tantalizing similar to the absorption
405 properties of terrestrial biological molecules, which have maximum wavelengths
406 of absorption across the UV and visible spectra. Examples include nucleic acids
407 and proteins which have respective λ_{max} values of 260 and 280 nm, where
408 absorbances at these wavelengths often overlap, as is shown in **Figure 6A** for
409 cellular extracts of *Escherichia coli* (*E.coli*). Typical absorbances of iron-
410 containing proteins (which would presumably be high in abundance in an Fe-rich
411 environment) are also shown in **Figure 6A**, with Fe-heme and iron-sulfur (Fe-S)
412 cluster proteins displaying λ_{max} values between 350-450 nm (for the coordinated
413 iron complex within the protein) and at ~ 280 nm (for the aromatic amino acids
414 within the protein). Across the visible spectrum, many organic cofactors and
415 biochemicals such as pterins, carotenoids, and chlorophylls also strongly absorb
416 between 300-500 nm (**Figure 6B**), with the photosynthetic pigments additionally
417 absorbing in the far visible and near infrared regions (**Figure 6B**).

418



419

420 **Figure 6.** Absorbance spectra for (A) whole cells of *E. coli* and purified iron-containing
 421 proteins of Iro and HdrC, which are FeS proteins from *A. ferrooxidans*, and catalase, a
 422 Fe-heme protein from *Acinetobacter gyllenbergii* 2P01AA; and (B) various cofactors and
 423 biochemicals, including bioterin, carotenoids, and chlorophylls a, b, and f; plots are
 424 adapted from (A) Derecho 2012 (doi:[10.1089/ast.2014.1193](https://doi.org/10.1089/ast.2014.1193)), Ossa 2011
 425 (doi:[10.1016/j.procbio.2011.03.001](https://doi.org/10.1016/j.procbio.2011.03.001)), and Zeng 2007 (doi:[10.1016/j.pep.2006.09.018](https://doi.org/10.1016/j.pep.2006.09.018));
 426 and (B) Airs 2014 (doi:[10.1016/j.febslet.2014.08.026](https://doi.org/10.1016/j.febslet.2014.08.026)) and [http://hyperphysics.phy-](http://hyperphysics.phy-astr.gsu.edu/hbase/Biology/ligabs.html)
 427 [astr.gsu.edu/hbase/Biology/ligabs.html](http://hyperphysics.phy-astr.gsu.edu/hbase/Biology/ligabs.html).
 428

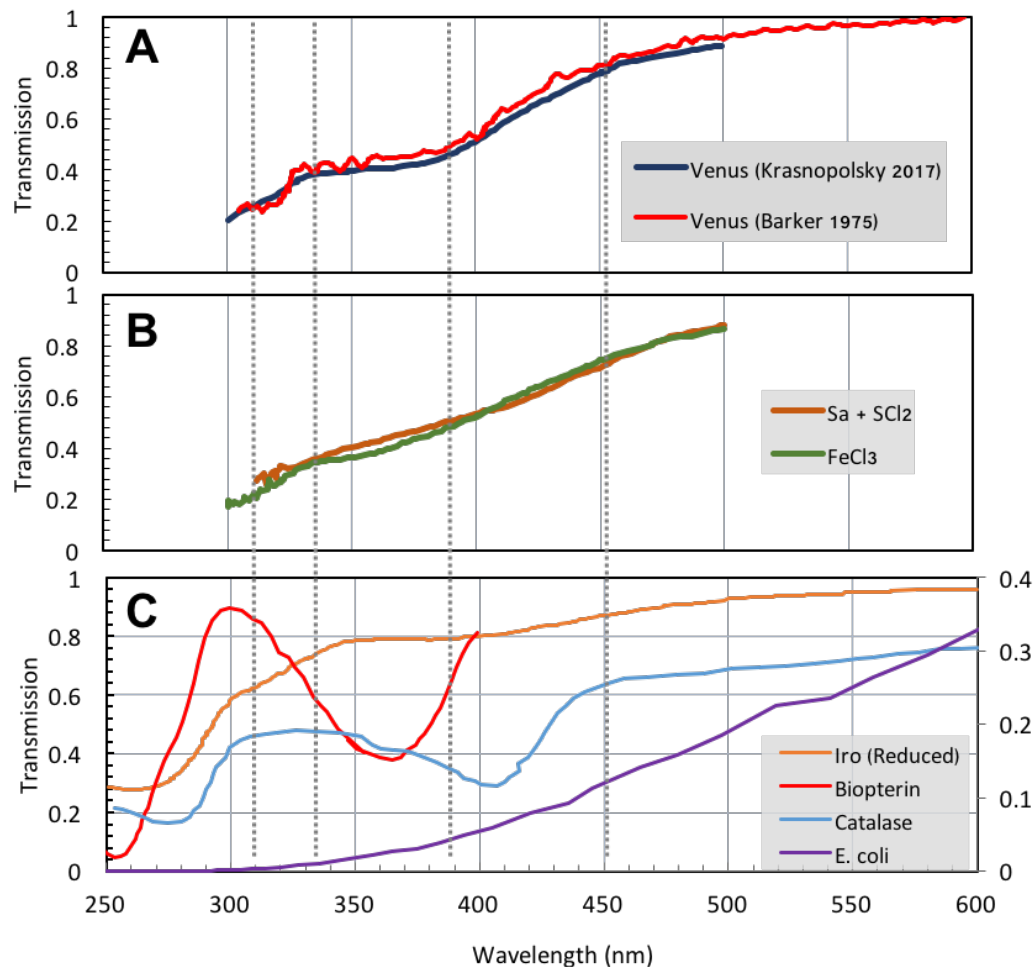
429 As described in the preceding section, however, there are several abiotic
 430 candidates that show reasonable spectral overlap with Venus, including
 431 aerosolized elemental sulfur and ferric chloride. Comparisons of transmission
 432 spectra for these compounds and the dayside Venus albedo, as displayed in
 433 **Figures 7A** and **7B**, show that the changes in transmission > 300 nm are
 434 relatively similar. For comparative purposes, the transmission spectra of whole
 435 cells of *E. coli* and differing biological molecules are displayed in **Figure 7C**,
 436 including two iron-containing proteins and bioterin. Interestingly, the spectrum
 437 for the Iro protein (but less so for catalase) shares several similarities to the Venus
 438 albedo, as denoted by the gray dotted lines in **Figure 7**. In the context of Venus
 439 survival, these similarities could perhaps be important, as Iro is a Fe-S protein
 440 believed to be involved in iron respiration (in the acidophilic and sulfur-

441 metabolizing bacterium, *Acidithiobacillus ferrooxidans*, Zeng et al. (2007)).
442 While purely speculative, the lack of significant spectral similarities between the
443 Venus and *E. coli* spectra suggest that any cloud-based microorganisms may
444 contain high abundances of Fe-S proteins, such as Iro, in order to exhibit the
445 observed transmission properties between 300-450 nm.

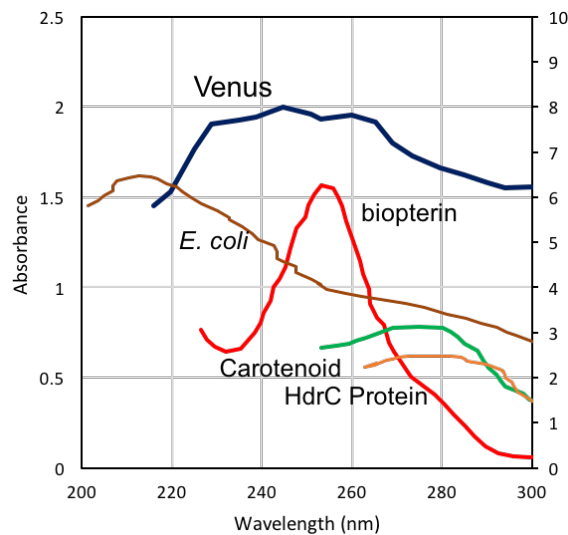
446

447 Additionally, comparisons to biopterin serve to illustrate the impact of
448 relative abundance, as lower concentrations of this cofactor would also yield
449 regions of spectral overlap with the observed Venus albedo. Again, in terms of
450 speculation, this is interesting, as bacterial pterin cofactors are involved in the
451 metabolism of sulfur compounds such as sulfite and dimethyl sulfoxide. Finally,
452 as displayed in **Figure 8**, the UV albedo of Venus (220-300 nm) shares
453 similarities with several UV-active biological materials (especially when
454 considering differing relative abundances), including whole cells of *E. coli*,
455 biopterin, carotenoids, and HdrC (an additional Fe-S protein from *A.*
456 *ferrooxidans*). These preliminary comparisons demonstrate that spectral overlaps
457 may be obtained from either abiotic or biotic sources. Hence, these spectral
458 overlaps perhaps warrant the need for deeper investigations into possibility of
459 biosignatures on Venus.

460



461
 462 **Figure 7.** Comparison of transmission spectra for (A) visible Venus albedo, as obtained
 463 from Barker 1975 (red) and Krasnopolsky 2017 (blue), and (B) aerosolized elemental
 464 sulfur (S_a) + sulfur dichloride (SCL_2) (orange) and ferric chloride ($FeCl_3$) (green), and
 465 (C) the Fe-S-containing Iro protein isolated from *A. ferrooxidans* (green), Fe-heme-
 466 containing catalase protein from *Acinetobacter gyllenbergii* 2P01AA (blue), biopterin
 467 (red), a whole cell preparation of *E. coli* (purple); plots adapted from (A) Barker 1975
 468 and Krasnopolsky 2017, (B) Krasnopolsky 2017, and (C) Alupoaei 2003
 469 (doi:10.1002/bit.20001), Derecho 2012 (doi:10.1089/ast.2014.1193), Nisshanthini 2015
 470 (doi:10.1007/s12275-015-4138-0), and Zeng (doi:10.1016/j.pep.2006.09.018).
 471



472

473 **Figure 8.** Comparison of UV spectra for Venus albedo, as obtained from Wallace (scaled
 474 geometric albedo), whole cell preparation of *E. coli*, biopterin, carotenoids, and HdrC
 475 (and FeS protein from *A. ferrooxidans*); plots adapted from Alupoaei 2003
 476 (doi:10.1002/bit.20001), Nisshanthini 2015 (doi:10.1007/s12275-015-4138-0), and Ossa
 477 2011 (doi:[10.1016/j.procbio.2011.03.001](https://doi.org/10.1016/j.procbio.2011.03.001)).

478

479 Of course, these discussions must also consider the nightside opacity
 480 contrasts, which are observed vividly at 2.3 μm (**Figures 1G & 1H**). Similar to
 481 the UV contrasts, the 2.3 μm contrasts are not well understood, with potential
 482 causes including the presence of CO, and the effects of differential opacities in the
 483 upper cloud, which may impede the transmission of radiation emitted by the
 484 lower atmosphere and the surface of Venus. However, IR studies on biological
 485 and organic molecules show that reflectance and absorption at $\sim 2.3 \mu\text{m}$ is clearly
 486 associated with C-H groups (C-H stretch) (Clark et al., 2009; Dalton et al., 2003),
 487 which is found in high abundance in lipid molecules (the primary constituent of
 488 cellular membranes). Given that the cloud layer of Venus has zonal flows which
 489 circle the planet in 4 to 6 days in the cloud layer ($\sim 50\text{-}65 \text{ km}$), these winds may
 490 potentially carry indigenous microorganisms around the planet, ultimately
 491 yielding contrasts on both night and day sides.

492 Survival in Venus' Clouds

493 Several terrestrial microorganisms could serve as relevant analogs for life
494 in Venus' clouds, which are sulfuric acid-enriched, anaerobic (CO₂ dominated),
495 and iron-rich environments. On Earth, airborne and cultivable microorganisms are
496 routinely collected with specialized aircraft and balloons at altitudes ranging from
497 15-42 km (Narlikar et al., 2003; Smith et al., 2013). As mentioned, cell counts of
498 terrestrial primary biological aerosols range from 10⁴-10¹¹ cells·m⁻³, with active
499 spectral techniques, such as laser-induced fluorescence, providing comparable
500 measures of 6x10⁷ cells·m⁻³.

501 For Venus' clouds, however, any potential biomass would clearly be
502 dependent upon available water, carbon, and other biogenic nutrients (*e.g.*, sulfur,
503 nitrogen, phosphorous, boron, and transition metals). The phototropic reduction of
504 atmospheric CO₂ would likely be a major source for carbon acquisition, with an
505 attenuated UV flux within the cloud layer providing the driving energy source.
506 Further, both phosphorus and sulfur (along with iron) have been detected by the
507 X-ray fluorescent radiometer on VeGa 1 and VeGa 2 landers (Andreychikov,
508 1987), with the most abundant phosphorus compound in the lower cloud layer
509 possibly being partially hydrated phosphoric anhydride P₂O₅+H₃PO₄
510 (Krasnopolsky, 2006). For water availability, the low vapor pressure in the clouds
511 is likely offset by the aerosols composed of aqueous sulfuric acid (75-98%),
512 where the aforementioned 2 and 8 μm spherical particles (mode 2 & 3) equate to
513 suspension volumes of ~4 and 260 pL, respectively.

514

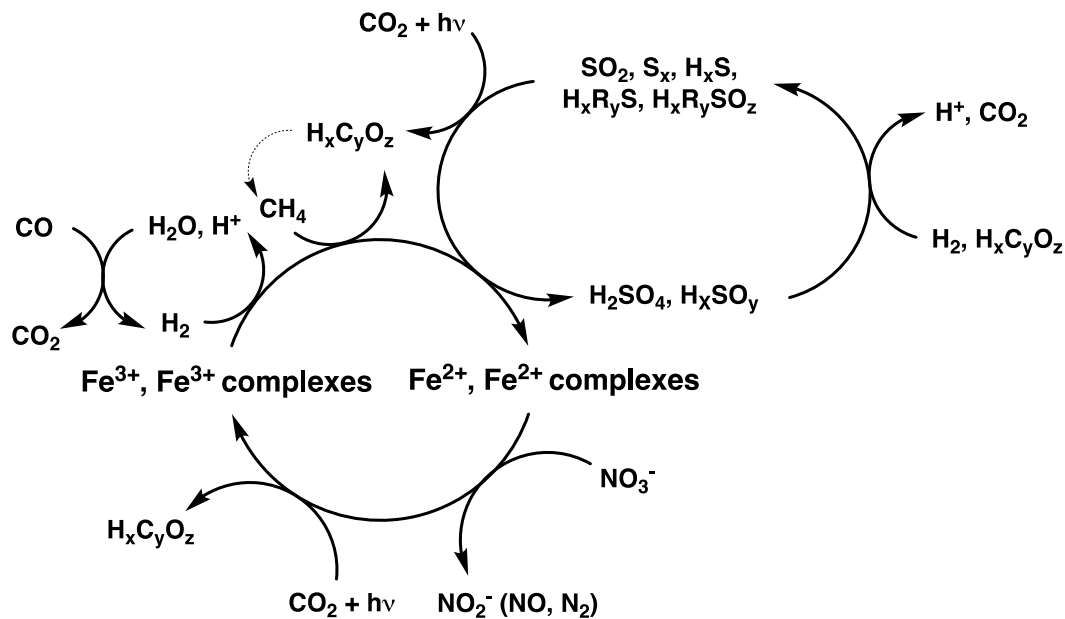
515 In terms of survival in sulfur-rich and low pH environments,
516 *Acidithiobacillus ferrooxidans* serves as an exemplar terrestrial analog for life in
517 Venus' clouds, as this bacterium thrives at extremely low pH values (pH 1–2),
518 fixes both carbon dioxide and nitrogen gas from the atmosphere (Valdes et al.,

519 2008), and obtains its energy for growth from the oxidation of hydrogen, ferrous
520 iron, elemental sulfur, or partially oxidized sulfur compounds (Vera et al., 2008).
521 This chemolithoautotrophic and acidophilic γ -proteobacterium also thrives at
522 temperatures of 50-60 °C, similar to those found in the lower clouds of Venus
523 (**Figure 3**). Moreover, under low pH and anaerobic conditions, this bacterium
524 produces sulfuric acid, and possibly other oxidized forms of sulfur by
525 metabolically oxidizing elemental sulfur and using Fe^{3+} as a terminal electron
526 acceptor (Pronk et al., 1992). Members of the archaeal *Stygiolobus* genus of the
527 Order Sulfolobales also anaerobically oxidize elemental sulfur to yield sulfuric
528 acid under acidic conditions, and optimal growth temperatures of ~80 °C, and also
529 utilize Fe^{3+} as a terminal electron acceptor (Seeger et al., 1991). Additional
530 terrestrial analogs include green sulfur bacteria, which couple the oxidation of
531 elemental sulfur to the anoxygenic phototrophic reduction of CO_2 (Frigaard &
532 Dahl, 2009), and the sulfate-reducing bacteria, which couple the oxidation of low
533 molecular weight organics and hydrogen gas to the reduction of sulfuric acid (and
534 other oxidized forms of sulfur) to form compounds including sulfite and hydrogen
535 sulfide (Muyzer & Stams, 2008).

536 Together, these terrestrial analogs assist in framing the biochemical
537 potential for an iron and sulfur-centered metabolism in Venus' clouds, where
538 oxidation of Fe^{2+} and sulfur compounds would be intrinsically coupled to the
539 anoxic photosynthetic reduction of CO_2 . As summarized in **Figure 9**, these
540 respective iron and sulfur redox cycles could hypothetically be sustained by
541 coupling to the redox-reactive constituents within Venus' clouds and atmosphere.
542 For instance, nitrate reduction could additionally be coupled to the oxidation of
543 Fe^{2+} , while completion of the $\text{Fe}^{3+}/\text{Fe}^{2+}$ redox cycle could be afforded by coupling
544 the reduction of Fe^{3+} to the oxidation of hydrogen, methane, and/or differing low
545 oxidation state sulfur compounds (*e.g.*, S_x , HS^- , SO_x , $\text{H}_x\text{R}_y\text{S}$, & $\text{H}_x\text{R}_y\text{SO}_z$). In

546 parallel, redox cycling between the differing sulfur oxidation states could be
 547 afforded by coupling the reduction of polyatomic sulfur compounds to the
 548 oxidation of hydrogen and/or low molecular weight organics.

549



550

551

552 **Figure 9.** Diagram of iron and sulfur-focused metabolic redox reactions that
 553 could occur in the Venus clouds, where $\text{Fe}^{3+/2+}$ complexes refer to inorganic and
 554 organic ligands and dotted arrows refer to possible redox cycles.

555

556 Transport from the Surface to the Clouds

557 Numerical simulations have suggested that Venus had a habitable climate
 558 for at least 750 million years, with liquid water on its surface for perhaps as long
 559 as two billion years (Way et al., 2016). Presence of past liquid water was first
 560 reported from comparisons of atmospheric deuterium/hydrogen ratios between
 561 Venus and Earth (Donahue & Hodges, 1992; Donahue et al., 1982). In context,
 562 this suggests a geological timeframe that is sufficient for life to have evolved in
 563 the Venus environment, especially when the time estimates required for the

564 evolution of life on Earth are considered (Des Marais, 1998; Lazcano & Miller,
565 1994; Nisbet & Sleep, 2001). As conditions on Venus' surface warmed and
566 became increasingly inhospitable for life, surface water could have evaporated to
567 the clouds, with multiple possible mechanisms transporting microorganisms in the
568 atmosphere to the clouds. Ultimately, these microorganisms could have adapted
569 to the cloud environments due to selective pressures arising from surface
570 transport, aerosolization, limited water availability, and low pH environments.

571

572 Within the context of terrestrial biology, surface-to-atmosphere transport
573 of microorganisms is reasonably well accepted, as is the atmospheric transport of
574 biologically relevant elements and low molecular weight metabolites (Burrows et
575 al., 2009; Fröhlich-Nowoisky et al., 2016; Morris et al., 2011). The movement of
576 water, organics, and other life-essential nutrients in the upper atmosphere on
577 Venus are likely similarly regulated by surface topography, diurnal cycles, strong
578 storms, or a variety of other conceivable physical weathering forces. On Earth, all
579 evidence to date indicates that airborne microbes do not remain perpetually aloft.
580 Instead, bioaerosols are continuously swept into the atmosphere through strong
581 convections that emanate from diverse marine and surface sources, and eventually
582 fall out of the atmosphere through gravitational settling or precipitation.

583

584 However, for Venus, the persistent spectral contrasts indicate that any
585 cloud-based microbial population would have to remain aloft for long periods, or
586 be replenished on relatively fast timescales as needed. Plausible atmospheric
587 transport mechanisms can be inferred from the VeGa 1 and VeGa 2 balloons,
588 which occasionally experienced very strong updrafts and downdrafts (some
589 triggered by underlying topography) at their nominal float level (~54 km).
590 Blamont et al. (1986) reported that the typical vertical motions (up and down)
591 encountered by the two balloons were 1 to 2 m·s⁻¹. The recent discovery, from

592 Akatsuki measurements (Fukuhara et al., 2017), of stationary gravity waves at the
593 cloud tops, which are considered to be the result of surface topography, indicate
594 that vertical motions are possible even within the very stable cloud layer. These
595 measurements suggest that ambient winds blowing over mountains and hills on
596 the surface appears to trigger vertical motions, which can reach the bottom of the
597 clouds without any impediment, and extend up to the middle cloud layer. The
598 very stable lapse rates in the Venus clouds, due to deposition of solar energy,
599 could also maintain airborne populations aloft for long periods. To a large extent,
600 the atmosphere below the clouds down to the surface is close to being neutrally
601 stable, with at least two layers with superadiabatic lapse rates, one near 4 km
602 above the surface, and another at about 15-17 km, as based on the VeGa 2 lander
603 data (Pioneer Venus probe sensors did not provide any data below 12 km due to
604 an electrical problem and published values are extrapolated using an adiabatic
605 lapse rate for pure CO₂, Seiff et al. (1995).

606

607 By extension, therefore, the observed UV contrasts of Venus are perhaps
608 best compared to bacterial blooms, which sustain high microbial abundances and
609 experience both temporal and spatial variability. For instance, periodic bursts in
610 nutrients (such iron and phosphorous) can promote broad fluctuations in
611 metabolite composition, cell aggregation, and/or cellular abundances, which
612 ultimately result in measurable optical changes in color, opacity, and/or turbidity
613 (Blondeau-Patissier et al., 2014; Egli et al., 2004). In Venus' clouds, such blooms
614 may also occur on timescales that match atmospheric cycling, while changes in
615 the metabolism of sulfur compounds (e.g., dimethyl sulfide, polyatomic sulfur
616 compounds, and alkyl sulfoxides) could impact the degree of UV contrasts on a
617 slower timescale. In sum, evaporation and atmospheric circulation could account
618 for the initial and current transport of biomass from the surface, and vertically
619 through the cloud layer, with recycling between the bottom and the top layers.

620 Biological material at the higher altitudes would then likely be partly or fully
621 degraded through photochemical means, where the resulting organic products
622 would be recycled through the cloud layer, potentially serving as carbon sources
623 for any cloud-based biology. Such a scenario would be consistent with the
624 conclusions of Knollenberg and Hunten (1980), that there is a source for the
625 smaller particles in the upper cloud layer. Alternatively, large impacts could have
626 resulted in the interplanetary exchange of rocks between Earth and Venus over the
627 course of planetary histories, potentially seeding viable terrestrial bacteria into the
628 Venus atmosphere.

629

630 **Future Studies and Potential Challenges**

631 Further exploration of Venus' cloud layer offers several attractive features,
632 as the need to build lander or rover spacecraft are not necessary. Indeed, if
633 microbes are actively metabolizing or reproducing in Earth's atmosphere, then the
634 search for habitable zones beyond our planet should be broadened to include
635 planetary atmospheres. As highlighted in this report, Venus' clouds are
636 exceptional targets for astrobiology, where ground-based studies on the physical,
637 chemical, and spectral properties (200-3000 nm) of microorganisms under Venus
638 cloud conditions would assist in the identification of potential atmospheric
639 biosignatures. These future studies will need to address the many sources of
640 variation associated with the spectroscopy of bioaerosols including: (1) cell
641 morphology (either cocci, bacilli, or spirilla); (2) cell state (vegetative or
642 sporulated); (3) cell viability; (4) cell aggregation and biofilm formation; (5)
643 presence of abiotic materials (e.g., dust, salts, polymer matrices); (6) state of
644 hydration; (7) environmental and atmospheric conditions (*e.g.*, sunlight,
645 atmospheric composition, and carrier gasses); and (8) variations based on
646 emission source (type) and location.

647 In conclusion, to thoroughly investigate the habitability (or even the
648 presence or absence of life) of the Venus clouds, a long lived aerial platform
649 capable of observing the temporal changes in the spectral, physical, and chemical
650 properties of the cloud layer aerosols would be ideal. Example platforms for
651 passive and active optical strategies (e.g., IR or LIDAR based methods) include
652 Aerobots (van den Berg et al., 2006) and VAMP, a concept being developed by
653 Northrop Grumman Aerospace (Lee et al., 2015a), which could be deployed on a
654 future NASA flagship mission to Venus, or on Russia's Venera-D mission
655 currently being studied for launch (Senske et al., 2017).

656

657 **Acknowledgements**

658 Funding from NASA Grants NNX09AE85G and NNX16AC79G supported the
659 development of the ideas presented in this paper. We acknowledge editing
660 contributions from Amanda Evans and Rosalyn Pertzborn, and motivating
661 discussions with many in the Venus research community. This paper was in part
662 inspired by the Spaceward Bound: India expedition in Ladakh, India (August
663 2016), where the continuous lifting of sulfur salt deposits from the shores of the
664 high altitude lake of Tso kar (~4500 m) invoked comparisons to early Venus,
665 when life may have been swept from the surface into the clouds.

666

667 **Author Disclosure Statement**

668 No competing financial interests exist for any of the authors.

669

670 **References:**

671

- 672 Barker, E. S. (1978). *Detection of CS₂ in the UV Spectrum of Venus*. Paper
673 presented at the Bulletin of the American Astronomical Society.
674 <http://adsabs.harvard.edu/abs/1978BAAS...10Q.548B>
675 Hawkins, S. E., III, Murchie, S. L., Becker, K. J., Selby, C. M., Turner, F. S.,
676 Noble, M. W., Chabot, N. L., Choo, T. H., Darlington, E. H., Denevi, B.

- 677 W., Domingue, D. L., Ernst, C. M., Holsclaw, G. M., Laslo, N. R.,
678 McClintock, W. E., Prockter, L. M., Robinson, M. S., Solomon, S. C., &
679 Sterner, R. E., II. (2009). *In-flight performance of MESSENGER's*
680 *Mercury Dual Imaging System*. Paper presented at the Instruments and
681 Methods for Astrobiology and Planetary Missions XII.
682 <http://adsabs.harvard.edu/abs/2009SPIE.7441E..0ZH>
- 683 Senske, D., Zasova, L., Economou, T., Eismont, N., Esposito, L., Gerasimov, M.,
684 Ignatiev, N., Ivanov, M., Lea Jessup, K., Khatuntsev, I., Korablev, O.,
685 Kremic, T., Limaye, S., Lomakin, I., Martynov, M., & Ocampo, A.
686 (2017). *Venera-D, A Mission Concept for the Comprehensive Scientific*
687 *Exploration of Venus*. Paper presented at the Lunar and Planetary Science
688 Conference. <http://adsabs.harvard.edu/abs/2017LPI....48.1155S>
- 689 Titov, D. V., Markiewicz, W. J., Moissl, R., Ignatiev, N., Limaye, S., Khatuntsev,
690 I., Roatsch, T., & Almeida, M. (2008). *Morphology of the Venus clouds*
691 *from the imaging by Venus Monitoring Camera onboard Venus Express*.
692 Paper presented at the European Planetary Science Congress 2008.
693 <http://adsabs.harvard.edu/abs/2008epsc.conf..225T>
- 694 Young, A. T. (1978). *Carbon Disulfide on Venus*. Paper presented at the Bulletin
695 of the American Astronomical Society.
696 <http://adsabs.harvard.edu/abs/1978BAAS...10..548Y>

697 **Uncategorized References**

- 698 Amato, P., Parazols, M., Sancelme, M., Mailhot, G., Laj, P., & Delort, A.-M.
699 (2007). An important oceanic source of micro-organisms for cloud water
700 at the Puy de Dôme (France). *Atmospheric Environment*, 41(37), 8253-
701 8263. doi:<http://doi.org/10.1016/j.atmosenv.2007.06.022>
- 702 Andreychikov, B. M., I. K. Akhmetshin, B. N. Korchuganov, L. M. Mukhin, B. I.
703 Ogorodnikov, I. V. Petryanov, and V. I. Skitovich (1987). X-ray
704 radiometric analysis of the cloud aerosol of Venus by the Vega 1 and 2
705 probes. *Cosmic Research, English Translation*, 25, 16.
- 706 Bakken, L. R., & Olsen, R. A. (1983). Buoyant densities and dry-matter contents
707 of microorganisms: conversion of a measured biovolume into biomass.
708 *Appl Environ Microbiol*, 45(4), 1188-1195.
- 709 Barker, E. S. (1979). Detection of SO₂ in the UV spectrum of Venus.
710 *Geophysical Research Letters*, 6, 117-120.
- 711 Barker, E. S. (1993). *SO-2 Abundance on Venus: After Pioneer Venus*.
- 712 Barker, E. S., Woodman, J. H., Perry, M. A., Hapke, B. A., & Nelson, R. (1975).
713 Relative spectrophotometry of Venus from 3067 to 5960 Å. *Journal of*
714 *Atmospheric Sciences*, 32, 1205-1211.
- 715 Belton, M. J. S., Gierasch, P. J., Smith, M. D., Helfenstein, P., Schinder, P. J.,
716 Pollack, J. B., Rages, K. A., Morrison, D., Klaasen, K. P., & Pilcher, C. B.

- 717 (1991). Images from Galileo of the Venus cloud deck. *Science*, 253, 1531-
718 1536.
- 719 Ben-David, A. (2003). Remote detection of biological aerosols at a distance of 3
720 km with a passive Fourier transform infrared (FTIR) sensor. *Optics*
721 *Express*, 11(5), 418-429.
- 722 Ben-David, A., M. D'Amico, F., Ren, H., Emge, D., C. Samuels, A., O. Jensen, J.,
723 & R. Loerop, W. (2003). *Identification and Detection of Bacterial Spores*
724 *With a Passive FTIR in an Open Air Point Release*.
- 725 Bertaux, J.-L., Widemann, T., Hauchecorne, A., Moroz, V. I., & Ekonomov, A. P.
726 (1996). VEGA 1 and VEGA 2 entry probes: An investigation of local UV
727 absorption (220-400 nm) in the atmosphere of Venus (SO₂, aerosols,
728 cloud structure). *Journal of Geophysical Research*, 101, 12709-12746.
- 729 Bezard, B., de Bergh, C., Crisp, D., & Maillard, J.-P. (1990). The deep
730 atmosphere of Venus revealed by high-resolution nightside spectra.
731 *Nature*, 345(6275), 508-511.
- 732 Bidigare, R. R., Kennicutt, M. C., Ondrusek, M. E., Keller, M. D., & Guillard, R.
733 R. L. (1990). Novel chlorophyll-related compounds in marine
734 phytoplankton: distributions and geochemical implications. *Energy &*
735 *Fuels*, 4(6), 653-657. doi:10.1021/ef00024a006
- 736 Blamont, J. E., Young, R. E., Seiff, A., Ragent, B., Sagdeev, R., Linkin, V. M.,
737 Kerzhanovich, V. V., Ingersoll, A. P., Crisp, D., Elson, L. S., Preston, R.
738 A., Golitsyn, G. S., & Ivanov, V. N. (1986). Implications of the VEGA
739 balloon results for Venus atmospheric dynamics. *Science*, 231, 1422-1425.
- 740 Blecka, M. I., Rataj, M., & Szymanski, G. (2012). Passive detection of biological
741 aerosols in the atmosphere with a Fourier Transform Instrument (FTIR)--
742 the results of the measurements in the laboratory and in the field. *Orig Life*
743 *Evol Biosph*, 42(2-3), 101-111. doi:10.1007/s11084-012-9288-z
- 744 Blondeau-Patissier, D., Gower, J. F., Dekker, A. G., Phinn, S. R., & Brando, V. E.
745 (2014). A review of ocean color remote sensing methods and statistical
746 techniques for the detection, mapping and analysis of phytoplankton
747 blooms in coastal and open oceans. *Progress in Oceanography*, 123, 123-
748 144.
- 749 Bougher, S. W., Hunten, D. M., Phillips, R. J., Hunten, D. M., & Phillips, R. J.
750 (1989). *Venus II*.
- 751 Burrows, S. M., Butler, T., Jöckel, P., Tost, H., Kerkweg, A., Pöschl, U., &
752 Lawrence, M. G. (2009). Bacteria in the global atmosphere - Part 2:
753 Modeling of emissions and transport between different ecosystems.
754 *Atmospheric Chemistry & Physics*, 9, 9281-9297.
- 755 Clark, R. N., Curchin, J. M., Hoefen, T. M., & Swayze, G. A. (2009). Reflectance
756 spectroscopy of organic compounds: 1. Alkanes. *Journal of Geophysical*
757 *Research: Planets*, 114(E3), n/a-n/a. doi:10.1029/2008JE003150

- 758 Cockell, C. S. (1999). Life on venus. *Planetary and Space Science*, 47(12), 1487-
759 1501. doi:Doi 10.1016/S0032-0633(99)00036-7
- 760 Conway, R. R., McCoy, R. P., Barth, C. A., & Lane, A. L. (1979). IUE detection
761 of sulfur dioxide in the atmosphere of Venus. *Geophysical Research*
762 *Letters*, 6, 629-631.
- 763 Dalton, J. B., Mogul, R., Kagawa, H. K., Chan, S. L., & Jamieson, C. S. (2003).
764 Near-infrared detection of potential evidence for microscopic organisms
765 on Europa. *Astrobiology*, 3(3), 505-529.
766 doi:10.1089/153110703322610618
- 767 Des Marais, D. J. (1998). Earth's early biosphere. *Gravit Space Biol Bull*, 11(2),
768 23-30.
- 769 Després, V., Huffman, J. A., Burrows, S. M., Hoose, C., Safatov, A., Buryak, G.,
770 Fröhlich-Nowoisky, J., Elbert, W., Andreae, M., Pöschl, U., & Jaenicke,
771 R. (2012). Primary biological aerosol particles in the atmosphere: a
772 review. *Tellus B: Chemical and Physical Meteorology*, 64(1), 15598.
773 doi:10.3402/tellusb.v64i0.15598
- 774 Donahue, T. M., & Hodges, R. R., Jr. (1992). Past and present water budget of
775 Venus. *Journal of Geophysical Research*, 97, 6083-6091.
- 776 Donahue, T. M., Hoffman, J. H., Hodges, R. R., & Watson, A. J. (1982). Venus
777 was wet - A measurement of the ratio of deuterium to hydrogen. *Science*,
778 216, 630-633.
- 779 Egli, K., Wiggli, M., Fritz, M., Klug, J., Gerss, J., & Bachofen, R. (2004). Spatial
780 and temporal dynamics of a plume of phototrophic microorganisms in a
781 meromictic alpine lake using turbidity as a measure of cell density.
782 *Aquatic microbial ecology*, 35(2), 105-113.
- 783 Encrenaz, T., Greathouse, T. K., Richter, M. J., DeWitt, C., Widemann, T.,
784 Bézard, B., Fouchet, T., Atreya, S. K., & Sagawa, H. (2016). HDO and
785 SO₂ thermal mapping on Venus. III. Short-term and long-term variations
786 between 2012 and 2016. *Astronomy and Astrophysics*, 595.
- 787 Esposito, L. W., Knollenberg, R. G., Marov, M. I., Toon, O. B., Turco, R. P.,
788 Colin, L., Donahue, T. M., & Moroz, V. I. (1983). The clouds are hazes of
789 Venus. In D. M. Hunten (Ed.), *Venus* (pp. 484-564).
- 790 Esposito, L. W., & Travis, L. D. (1982). Polarization studies of the Venus UV
791 contrasts - Cloud height and haze variability. *Icarus*, 51, 374-390.
- 792 Frandsen, B. N., Wennberg, P. O., & Kjaergaard, H. G. (2016). Identification of
793 OSSO as a near-UV absorber in the Venusian atmosphere. *Geophysical*
794 *Research Letters*, 43(21), 11146-11155. doi:10.1002/2016gl070916
- 795 Frigaard, N. U., & Dahl, C. (2009). Sulfur metabolism in phototrophic sulfur
796 bacteria. *Adv Microb Physiol*, 54, 103-200. doi:10.1016/s0065-
797 2911(08)00002-7

- 798 Fröhlich-Nowoisky, J., Kampf, C. J., Weber, B., Huffman, J. A., Pöhlker, C.,
799 Andreae, M. O., Lang-Yona, N., Burrows, S. M., Gunthe, S. S., Elbert,
800 W., Su, H., Hoor, P., Thines, E., Hoffmann, T., Després, V. R., & Pöschl,
801 U. (2016). Bioaerosols in the Earth system: Climate, health, and
802 ecosystem interactions. *Atmospheric Research*, 182, 346-376.
803 doi:<http://doi.org/10.1016/j.atmosres.2016.07.018>
- 804 Fukuhara, T., Futaguchi, M., Hashimoto, G. L., Horinouchi, T., Imamura, T.,
805 Iwagami, N., Kouyama, T., Murakami, S. Y., Nakamura, M., Ogohara,
806 K., Sato, M., Sato, T. M., Suzuki, M., Taguchi, M., Takagi, S., Ueno, M.,
807 Watanabe, S., Yamada, M., & Yamazaki, A. (2017). Large stationary
808 gravity wave in the atmosphere of Venus. *Nature Geoscience*, 10(2), 85-+.
809 doi:10.1038/Ngeo2873
- 810 Gurton, K. P. L., David; Kvavilashvili, Ramaz. (2001). Extinction, Absorption,
811 Scattering, and Backscatter for Aerosolized Bacillus Subtilis Var. Niger
812 Endospores from 3 to 13 Micrometers. 23.
- 813 Hansen, J. E., & Hovenier, J. W. (1974). Interpretation of the polarization of
814 Venus. *Journal of Atmospheric Sciences*, 31, 1137-1160.
- 815 Hapke, B., & Nelson, R. (1975). Evidence for an elemental sulfur component of
816 the clouds from Venus spectrophotometry. *Journal of Atmospheric
817 Sciences*, 32, 1212-1218.
- 818 Hartley, K. K., Wolff, A. R., & Travis, L. D. (1989). Croconic acid: An absorber
819 in the Venus clouds? *Icarus*, 77(2), 382-390.
820 doi:[http://dx.doi.org/10.1016/0019-1035\(89\)90095-X](http://dx.doi.org/10.1016/0019-1035(89)90095-X)
- 821 Hunten, D. M., Colin, L., Donahue, T. M., Moroz, V. I., Colin, L., Donahue, T.
822 M., & Moroz, V. I. (1983). *Venus*.
- 823 Hunter, P. D., Tyler, A. N., Carvalho, L., Codd, G. A., & Maberly, S. C. (2010).
824 Hyperspectral remote sensing of cyanobacterial pigments as indicators for
825 cell populations and toxins in eutrophic lakes. *Remote Sensing of
826 Environment*, 114(11), 2705-2718.
827 doi:<https://doi.org/10.1016/j.rse.2010.06.006>
- 828 Ignatiev, N. I., Titov, D. V., Piccioni, G., Drossart, P., Markiewicz, W. J., Cottini,
829 V., Roatsch, T., Almeida, M., & Manoel, N. (2009). Altimetry of the
830 Venus cloud tops from the Venus Express observations. *Journal of
831 Geophysical Research (Planets)*, 114.
- 832 Irvine, W. M. (1968). Monochromatic phase curves and albedos for Venus.
833 *Journal of Atmospheric Sciences*, 25, 610-616.
- 834 Jessup, K. L., Marcq, E., Mills, F., Mahieux, A., Limaye, S., Wilson, C., Allen,
835 M., Bertaux, J.-L., Markiewicz, W., Roman, T., Vandaele, A.-C., Wilquet,
836 V., & Yung, Y. (2015). Coordinated Hubble Space Telescope and Venus
837 Express Observations of Venus' upper cloud deck. *Icarus*, 258, 309-336.

- 838 Kawabata, K., Coffeen, D. L., Hansen, J. E., Lane, W. A., Sato, M., & Travis, L.
839 D. (1980). Cloud and haze properties from Pioneer Venus polarimetry.
840 *Journal of Geophysical Research*, 85, 8129-8140.
- 841 Knollenberg, R., Travis, L., Tomasko, M., Smith, P., Ragent, B., Esposito, L.,
842 McCleese, D., Martonchik, J., & Beer, R. (1980). The clouds of Venus - A
843 synthesis report. *Journal of Geophysical Research*, 85, 8059-8081.
- 844 Knollenberg, R. G. (1984). A reexamination of the evidence for large, solid
845 particles in the clouds of Venus. *Icarus*, 57, 161-183.
- 846 Knollenberg, R. G., & Hunten, D. M. (1979). Clouds of Venus - A preliminary
847 assessment of microstructure. *Science*, 205, 70-74.
- 848 Knollenberg, R. G., & Hunten, D. M. (1980). The microphysics of the clouds of
849 Venus - Results of the Pioneer Venus particle size spectrometer
850 experiment. *Journal of Geophysical Research*, 85, 8039-8058.
- 851 Krasnopolsky, V. A. (2006). Chemical composition of Venus atmosphere and
852 clouds: Some unsolved problems. *Planetary and Space Science*, 54, 1352-
853 1359.
- 854 Krasnopolsky, V. A. (2016). Sulfur aerosol in the clouds of Venus. *Icarus*, 274,
855 33-36.
- 856 Krasnopolsky, V. A. (2017). On the iron chloride aerosol in the clouds of Venus.
857 *Icarus*, 286, 134-137.
- 858 Kuiper, G. P. (1969). Identification of the Venus cloud layers. *Communications of*
859 *the Lunar and Planetary Laboratory*, 6, 229-245.
- 860 Laven, P. (2008). Effects of refractive index on glories. *Applied Optics*, 47, H133.
- 861 Lazcano, A., & Miller, S. L. (1994). How long did it take for life to begin and
862 evolve to cyanobacteria? *J Mol Evol*, 39(6), 546-554.
- 863 Lee, G., Polidan, R. S., & Ross, F. (2015a). Venus Atmospheric Maneuverable
864 Platform (VAMP) - A Low Cost Venus Exploration Concept. *AGU Fall*
865 *Meeting Abstracts*, 23.
- 866 Lee, Y. J., Imamura, T., Schröder, S. E., & Marcq, E. (2015b). Long-term
867 variations of the UV contrast on Venus observed by the Venus Monitoring
868 Camera on board Venus Express. *Icarus*, 253, 1-15.
- 869 Lee, Y. J., Yamazaki, A., Imamura, T., Yamada, M., Watanabe, S., Sato, T. M.,
870 Ogohara, K., Hashimoto, G. L., & Murakami, S. (2017). Scattering
871 Properties of the Venusian Clouds Observed by the UV Imager on board
872 Akatsuki. *The Astronomical Journal*, 154(2), 44.
- 873 Markiewicz, W. J., Petrova, E., Shalygina, O., Almeida, M., Titov, D. V., Limaye,
874 S. S., Ignatiev, N., Roatsch, T., & Matz, K. D. (2014). Glory on Venus
875 cloud tops and the unknown UV absorber. *Icarus*, 234, 200-203.
- 876 Mills, F. P., Esposito, L. W., & Yung, Y. L. (2007). Atmospheric composition,
877 chemistry, and clouds. *Exploring Venus As A Terrestrial Planet*, 176, 73-
878 100.

- 879 Morowitz, H. a. C. S. (1967). Life in the Clouds of Venus? *Nature*, 215, 1259-
880 1260.
- 881 Moroz, V. I., Ekonomov, A. P., Moshkin, B. E., Revercomb, H. E., Sromovsky,
882 L. A., & Schofield, J. T. (1985). Solar and thermal radiation in the Venus
883 atmosphere. *Advances in Space Research*, 5, 197-232.
- 884 Morris, C. E., Sands, D. C., Bardin, M., Jaenicke, R., Vogel, B., Leyronas, C.,
885 Ariya, P. A., & Psenner, R. (2011). Microbiology and atmospheric
886 processes: research challenges concerning the impact of airborne micro-
887 organisms on the atmosphere and climate. *Biogeosciences*, 8(1), 17-25.
888 doi:10.5194/bg-8-17-2011
- 889 Murray, B. C., Belton, M. J. S., Danielson, G. E., Davies, M. E., Gault, D.,
890 Hapke, B., O'Leary, B., Strom, R. G., Suomi, V., & Trask, N. (1974).
891 Venus: Atmospheric Motion and Structure from Mariner 10 Pictures.
892 *Science*, 183, 1307-1315.
- 893 Muyzer, G., & Stams, A. J. M. (2008). The ecology and biotechnology of
894 sulphate-reducing bacteria. *Nat Rev Micro*, 6(6), 441-454.
- 895 Narlikar, J. V., Lloyd, D., Wickramasinghe, N. C., Harris, M. J., Turner, M. P.,
896 Al-Mufti, S., Wallis, M. K., Wainwright, M., Rajaratnam, P., Shivaji, S.,
897 Reddy, G. S. N., Ramadurai, S., & Hoyle, F. (2003). A Balloon
898 Experiment to detect Microorganisms in the Outer Space. *Astrophysics
899 and Space Science*, 285, 555-562.
- 900 Nisbet, E. G., & Sleep, N. H. (2001). The habitat and nature of early life. *Nature*,
901 409(6823), 1083-1091. doi:10.1038/35059210
- 902 Oyama, V. I., Carle, G. C., Woeller, F., Pollack, J. B., Reynolds, R. T., & Craig,
903 R. A. (1980). Pioneer Venus gas chromatography of the lower atmosphere
904 of Venus. *Journal of Geophysical Research*, 85, 7891-7902.
- 905 Perez-Hoyos, S., Garcia-Muñoz, A., Sánchez-Lavega, A., & McClintock, W. M.
906 (2013). Analysis of MESSENGER/MASCS data during second Venus
907 flyby. *European Planetary Science Congress 2013, held 8-13 September
908 in London, UK. Online at: <A
909 href="http://meetings.copernicus.org/epsc2013">
910 http://meetings.copernicus.org/epsc2013, id.EPSC2013-156, 8.*
- 911 Pollack, J. B., Toon, O. B., Whitten, R. C., Boese, R., Ragent, B., Tomasko, M.,
912 Eposito, L., Travis, L., & Wiedman, D. (1980). Distribution and source of
913 the UV absorption in Venus' atmosphere. *Journal of Geophysical
914 Research*, 85, 8141-8150.
- 915 Pronk, J. T., de Bruyn, J. C., Bos, P., & Kuenen, J. G. (1992). Anaerobic Growth
916 of *Thiobacillus ferrooxidans*. *Applied and Environmental Microbiology*,
917 58(7), 2227-2230.
- 918 R. Katti, V., R. Pratap, V., K. Dave, R., & Mankad, K. (2006). *INSAT-3D: an
919 advanced meteorological mission over Indian Ocean.*

- 920 Ross, F. E. (1928). Photographs of Venus. *The Astrophysical Journal*, 68, 57.
- 921 Rossow, W. B., del Genio, A. D., Limaye, S. S., & Travis, L. D. (1980). Cloud
922 morphology and motions from Pioneer Venus images. *Journal of*
923 *Geophysical Research*, 85, 8107-8128.
- 924 Schalles, J. F. (2006). Optical remote sensing techniques to estimate
925 phytoplankton chlorophyll and concentrations in coastal waters with
926 varying suspended matter and CDOM concentrations. In L. L. Richardson
927 & E. F. LeDrew (Eds.), *Remote sensing of aquatic coastal ecosystem*
928 *processes* (pp. 27-79). Dordrecht: Springer Netherlands.
- 929 Schulze-Makuch, D., Grinspoon, D. H., Abbas, O., Irwin, L. N., & Bullock, M. A.
930 (2004). A sulfur-based survival strategy for putative phototrophic life in
931 the venusian atmosphere. *Astrobiology*, 4(1), 11-18.
932 doi:10.1089/153110704773600203
- 933 Schulze-Makuch, D., & Irwin, L. N. (2002). Reassessing the possibility of life on
934 venus: proposal for an astrobiology mission. *Astrobiology*, 2(2), 197-202.
935 doi:10.1089/15311070260192264
- 936 Schulze-Makuch, D., & Irwin, L. N. (2006). The prospect of alien life in exotic
937 forms on other worlds. *Naturwissenschaften*, 93(4), 155-172.
938 doi:10.1007/s00114-005-0078-6
- 939 Segerer, A. H., Trincone, A., Gahrtz, M., & Stetter, K. O. (1991). *Stygiolobus*
940 *azoricus* gen. nov., sp. nov. Represents a Novel Genus of Anaerobic,
941 Extremely Thermoacidophilic Archaeobacteria of the Order Sulfolobales.
942 *International Journal of Systematic and Evolutionary Microbiology*,
943 41(4), 495-501. doi:10.1099/00207713-41-4-495
- 944 Seiff, A., Sromovsky, L., Borucki, W., Craig, R., Juergens, D., Young, R. E., &
945 Ragent, B. (1995). Pioneer Venus 12.5 KM Anomaly Workshop Report,
946 volume 1. *NASA STI/Recon Technical Report N*, 95.
- 947 Shaya, E., & Caldwell, J. (1976). Photometry of Venus below 2200 Å from the
948 Orbiting Astronomical Observatory-2. *Icarus*, 27, 255-264.
- 949 Shimizu, M. (1977). Ultraviolet absorbers in the Venus clouds. *Astrophysics and*
950 *Space Science*, 51, 497-499.
- 951 Sill, G. T. (1975). The composition of the ultraviolet dark markings on Venus.
952 *Journal of Atmospheric Sciences*, 32, 1201-1204.
- 953 Smith, D., Timonen, H., Jaffe, D., Griffin, D. W., Birmele, M., Perry, K. D.,
954 Ward, P. D., & Roberts, M. (2013). Intercontinental dispersal of bacteria
955 and archaea by transpacific winds. *Applied and Environmental*
956 *Microbiology*, 79(4), 1134-1139. doi:10.1128/AEM.03029-12
- 957 Spaun, J. (1962). Problems in standardization of turbidity determinations on
958 bacterial suspensions. *Bulletin of the World Health Organization*, 26(2),
959 219-225.

- 960 Stewart, A. I., Anderson, D. E., Esposito, L. W., & Barth, C. A. (1979).
961 Ultraviolet spectroscopy of Venus - Initial results from the Pioneer Venus
962 orbiter. *Science*, *203*, 777-779.
- 963 Surkov, Y. A., Ivanova, V. F., Pudov, A. N., Verkin, B. I., Bagrov, N. N., &
964 Philipenko, A. P. (1978). Mass-spectral study of the chemical composition
965 of the Venus atmosphere by Venera 9 and Venera 10 space probes.
966 *Geokhimiia*, *4*, 506-513.
- 967 Titov, D. V., Markiewicz, W. J., Ignatiev, N. I., Song, L., Limaye, S. S., Sanchez-
968 Lavega, A., Hesemann, J., Almeida, M., Roatsch, T., Matz, K.-D.,
969 Scholten, F., Crisp, D., Esposito, L. W., Hviid, S. F., Jaumann, R., Keller,
970 H. U., & Moissl, R. (2012). Morphology of the cloud tops as observed by
971 the Venus Express Monitoring Camera. *Icarus*, *217*, 682-701.
- 972 Toon, O. B., Pollack, J. B., & Turco, R. P. (1982). The ultraviolet absorber on
973 Venus - Amorphous sulfur. *Icarus*, *51*, 358-373.
- 974 Travis, L. D. (1975). On the origin of ultraviolet contrasts on Venus. *Journal of*
975 *Atmospheric Sciences*, *32*, 1190-1200.
- 976 Valdes, J., Pedroso, I., Quatrini, R., Dodson, R. J., Tettelin, H., Blake, R., 2nd,
977 Eisen, J. A., & Holmes, D. S. (2008). Acidithiobacillus ferrooxidans
978 metabolism: from genome sequence to industrial applications. *BMC*
979 *Genomics*, *9*, 597. doi:10.1186/1471-2164-9-597
- 980 van den Berg, M. L., Falkner, P., Atzei, A. C., & Peacock, A. (2006). Venus
981 microsat explorer programme, an ESA technology reference study. *Acta*
982 *Astronautica*, *59*, 593-597.
- 983 Vera, M., Pagliai, F., Guiliani, N., & Jerez, C. A. (2008). The
984 chemolithoautotroph Acidithiobacillus ferrooxidans can survive under
985 phosphate-limiting conditions by expressing a C-P lyase operon that
986 allows it to grow on phosphonates. *Appl Environ Microbiol*, *74*(6), 1829-
987 1835. doi:10.1128/aem.02101-07
- 988 Way, M. J., Del Genio, A. D., Kiang, N. Y., Sohl, L. E., Grinspoon, D. H.,
989 Aleinov, I., Kelley, M., & Clune, T. (2016). Was Venus the first habitable
990 world of our solar system? *Geophysical Research Letters*, *43*, 8376-8383.
- 991 Wilson, C. F., Guerlet, S., Irwin, P. G. J., Tsang, C. C. C., Taylor, F. W., Carlson,
992 R. W., Drossart, P., & Piccioni, G. (2008). Evidence for anomalous cloud
993 particles at the poles of Venus. *Journal of Geophysical Research*
994 *(Planets)*, *113*.
- 995 Young, A. T. (1973). Are the Clouds of Venus Sulfuric Acid? *Icarus*, *18*, 564-
996 582.
- 997 Zasova, L. V., Krasnopolskii, V. A., & Moroz, V. I. (1981). Vertical distribution
998 of SO₂ in upper cloud layer of Venus and origin of U.V.-absorption.
999 *Advances in Space Research*, *1*, 13-16.

- 1000 Zeng, J., Geng, M., Liu, Y., Zhao, W., Xia, L., Liu, J., & Qiu, G. (2007).
1001 Expression, purification and molecular modelling of the Iro protein from
1002 Acidithiobacillus ferrooxidans Fe-1. *Protein Expression and Purification*,
1003 52(1), 146-152. doi:<http://dx.doi.org/10.1016/j.pep.2006.09.018>
1004